Summer 2017

Synthesis and Characterization of a Novel Ligand and Its Silver(I) and Palladium(II) Complexes: An Incidental Discovery of Halogen Bonding in Three Structures of Iodoimidazoles

Chideraa Iheanyi Nwachukwu
Missouri State University, nwachukwu123@live.missouristate.edu

Recommended Citation
Nwachukwu, Chideraa Iheanyi, "Synthesis and Characterization of a Novel Ligand and Its Silver(I) and Palladium(II) Complexes: An Incidental Discovery of Halogen Bonding in Three Structures of Iodoimidazoles" (2017). *MSU Graduate Theses*. 3112.
https://bearworks.missouristate.edu/theses/3112

SYNTHESIS AND CHARACTERIZATION OF A NOVEL LIGAND AND ITS SILVER(I) AND PALLADIUM(II) COMPLEXES: AN INCIDENTAL DISCOVERY OF HALOGEN BONDING IN THREE STRUCTURES OF IODOIMIDAZOLES

A Masters Thesis

Presented to

The Graduate College of

Missouri State University

In Partial Fulfillment

Of the Requirements for the Degree

Master of Science, Chemistry

By

Chideraa I. Nwachukwu

August 2017

SYNTHESIS AND CHARACTERIZATION OF A NOVEL LIGAND AND ITS SILVER(I) AND PALLADIUM(II) COMPLEXES: AN INCIDENTAL DISCOVERY OF HALOGEN BONDING IN THREE STRUCTURES OF IODOIMIDAZOLES

Chemistry

Missouri State University, August 2017

Master of Science

Chideraa I. Nwachukwu

ABSTRACT

Ligand design is a vital component of coordination chemistry, and the use of ligands for complexation of metal cations have been explored for many years. Several metal complexes of silver and palladium have been reported in literature and these complexes have been fully studied. I chose to study silver and palladium, because these metals are precious and are used in several industries such as electronics and jewelry industry and also in catalysis. In addition to economic incentives to recover these metals, it should be noted that these heavy metals often pose both environmental and health hazards. For example, low levels of silver have been found to lead to the death of aquatic animals. Herein, I describe the synthesis of a novel ligand, 4-[(2-imidazylethynyl)]-5-(2-pyridylethynyl) veratrole and its silver(I) and palladium(II) complexes. The ligand was characterized by ^{1}H, ^{13}C NMR, and by elemental analysis. The single X-ray structure of the ligand and the palladium complex were also determined. ^{1}H NMR titration revealed a 1:1 complex formation between the ligand and silver, and the ligand and palladium cations. Long range plans involve the attachment of this ligands to a polymer support for the extraction of these cations from waste. Furthermore, I also described the X-ray structure of three iodoimidazole derivatives; 1-benzyl-2-iodo-1H-imidazole, 1-benzyl-4-iodo-1H-imidazole and 1-benzyl-2-iodo-1H-benzimidazole and the halogen bonds that dominate the intermolecular interactions in each of these three structures.

KEYWORDS: ligand, NMR titration, complexes, halogen bonding, x-ray structure.

This abstract is approved as to form and content

____

Dr. Eric Bosch
Chairperson, Advisory Committee
Missouri State University

SYNTHESIS AND CHARACTERIZATION OF A NOVEL LIGAND AND ITS SILVER(I) AND PALLADIUM(II) COMPLEXES: AN INCIDENTAL DISCOVERY OF HALOGEN BONDING IN THREE STRUCTURES OF IODOIMIDAZOLES

By

Chideraa I. Nwachukwu

A Masters Thesis
Submitted to the Graduate College
Of Missouri State University
In Partial Fulfillment of the Requirements
For the Degree of Master of Science, Chemistry

August 2017

Approved:

Dr. Eric Bosch

Dr. Reza Sedaghat-Herati

Dr. Nikolay Gerasimchuk

Dr. Jerry Easdon

Dr. Julie Masterson, Dean, Graduate College

ACKNOWLEDGEMENTS

First, I would like to thank my advisor, Dr. Eric Bosch, for being a great teacher and a splendid mentor. I really appreciate how he taught me with patience and would also go to lab with me whenever I encountered a problem in my research. His words of encouragement and motivation kept me going, he never wrote me off for a day even when I thought I was not good enough. I admired how he put in so much work in doing his own research and teaching. Also, I would like to thank him for how he made me fall in love with organic chemistry after I had the advanced organic chemistry class with him. Thank you very much Dr. Bosch, I will really miss working with you.

Secondly, I would like to thank all my professors, those that taught me and those that helped me all these years. I would like to specially thank the members of my thesis committee Dr. Nikolay Gerasimschuk, Dr. Reza Sedaghat-Herati and Dr. Jerry Easdon for taking their time to read through my thesis and making sure all the information was correct. I would also like to thank my parents Callistus and Angelina Nwachukwu for all their support and encouragement all these years. I also appreciate all my siblings support.

I would like to thank the Missouri State Chemistry department, the Graduate College and the National Science Foundation research funding that made this thesis possible. I would like to thank Linda Allen for her words of encouragement and guidance all through my program. Finally, I would like to thank all my friends and classmates for their support in the last two years, in particular Margaret Adelani and Otega Ejegbavwo who were always there for me.

I dedicate this thesis to God.

TABLE OF CONTENTS

LIST OF FIGURES

INTRODUCTION

Ligand design and synthesis continues to lead the line in modern coordination chemistry, due to its importance in many diverse areas of chemistry. These areas include catalysis,[1,2] metallo-pharmaceuticals,[3,4] metallo-suprachemistry[5] metal cations sensors,[6,7] to name a few. Indeed, the importance of ligand design is underscored by the recent American Chemical Science Selects Virtual Issue focused on ligand design.[8] A ligand is defined as an ion or molecule that binds to a metal atom to form a coordination complex. The bond between the metal and the ligand is formed from the donation of one or more electron pairs from the ligand to the metal, and this bond is referred to as a coordinate covalent bond. Since the advent of coordination complexes by Alfred Warner, many ligands have been designed to specifically complex metals. Silver and palladium have received great attention over the years due to their unique properties. These properties have led to the utilization of these metals in electronic industry, jewelry industry, catalysis, to name a few.

My project was to devise a ligand with the potential to form neutral complexes with silver and palladium cations. The design plan was to modify a known *trans*-coordinating ditopic pyridyl ligand. The known *trans*-ligand was designed with a 1,2-diethynylbenzene core and the *trans*-coordination of silver and palladium cations was demonstrated.[9] In the design of this ditopic ligand, I planned to incorporate an imidazoyl moiety in place of one of the pyridyl groups with the expectation that neutral silver and palladium complexes could be formed in solution. To evaluate the potential application of the ligand, the long-term goal would involve the attachment of the ligand to a polymer support for the extraction of silver and palladium cations from waste.

Silver

It is a soft, white lustrous transition metal belonging to group 11 on the periodic table, below copper and above gold. It has an atomic number of 47, with three main oxidation states (0, +1, and +2) and two naturally occurring isotopes, ^{107}Ag and ^{109}Ag, with relative abundances of 51.84% and 48.16% respectively. Silver has the highest thermal conductivity, electrical conductivity, as well as reflectivity of all metals on the periodic table. It is also a soft Lewis acid with affinity for Lewis bases containing nitrogen, sulfur and oxygen atoms. Most of the world supply of silver is produced as a by-product of copper, gold, lead and zinc refining. These unique properties of silver led to numerous application of this metal in different areas

Uses and toxicity of silver. Silver is traditionally used in photography, money/coins, electronics, medicine, jewelry, silverware, clothing and in other areas. However, amongst all other uses of silver, its most recent use in synthesis of nanowires has attracted much attention because of their potentials application in electronic devices.[10,11] These include their use as flexible transparent conductors in flat screens, solar cells and transparent heaters.[11] Silver is used to make smart fabrics for aesthetics and various other purposes. The antimicrobial and antibacterial properties of silver has been exploited in medicine, where it is used for treatment of wounds and also for water purification.

Silver ion is one of the most toxic heavy metal ions, surpassed only by mercury, and has therefore been assigned to the highest toxicity class, together with cadmium, chromium (VI), copper, and mercury.[12,13] Surprisingly, the toxicity of this metal was not investigated until the mid-70's.[14] In subsequent years, research towards understanding the environmental toxicity of silver has been carried out, and its various adverse effects are now known. Most silver released in the environment do remain in the soil or waste water sludge[15] and are lethal to both plants and sea animals.[16,17] Low levels of silver in the environment have been found to lead to death of aquatic animals,[18] which might have an extended consequence on humans, hence, the need for a recovery process or technique for removal of this metal from the environment.

Coordination chemistry of silver(I). The coordination chemistry of silver with nitrogen donors, particularly with polypyridyl ligands, is very rich because of the flexible coordination sphere of this cation and its ability to form, both in solution[19] and in solid state. The coordination flexibility of this cation allows for coordination with a variety of ligands designed for different coordination geometries.[20] Silver(I) is a soft metal center with high affinity for soft nitrogen ligands.[21] Over the years, silver(I) has been thought to have strong preference for linear coordination,[22] but a study by Young et al., reveals that out of 3319 solid structures of silver(I) complexes, 24 % were two coordinate, 23 % three coordinate, 44 % four coordinate and the remaining 9 % showed coordination geometries greater than four.[23] The coordination geometry flexibility of this cation has been attributed to its lack of stereochemical directionality as a result of its filled d-shell which makes it difficult to predict the geometry of a silver complex beforehand.[20] An example of each of the three common geometries formed with pyridyl ligands are shown in Figure 1. These geometries show the flexibility of this metal, and its ability to form both in solution and it solid state, which makes the study of the complexes formed by this metal even more interesting.

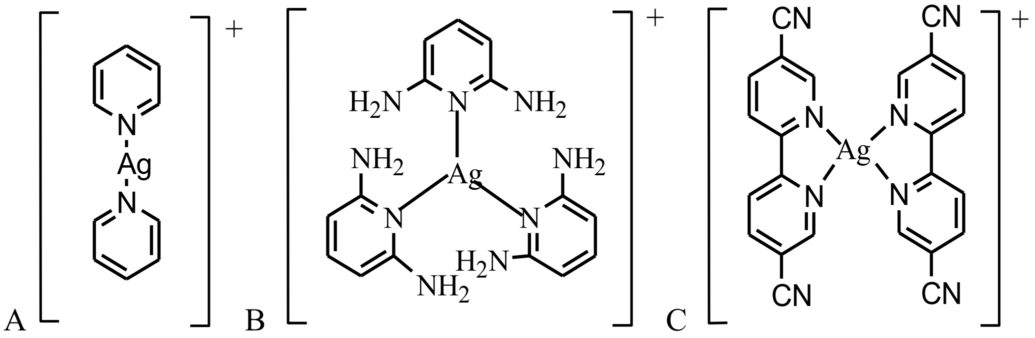

Figure 1. Representative pyridine complexes with silver(I). (A) Linear complex.[24] (B) Trigonal complex.[25] (C) Tetragonal complex.[26]

Palladium

Palladium is a soft silver-white metal belonging to group 10 on the periodic table, below nickel and above platinum, with atomic number of 46. Palladium commonly exists in three oxidation states: 0 (metallic), +2 and +4. Palladium is composed of seven isotopes, of which six of them are stable, ^{102}Pd, ^{104}Pd, ^{105}Pd, ^{106}Pd, ^{108}Pd and ^{110}Pd. The most stable radioisotope is ^{107}Pd with a half-life of 6.5 million years. Palladium is mostly obtained from ores along with copper, gold, nickel and platinum.

Uses and toxicity of palladium. Palladium is an important metal majorly used as a catalytic converter in automobiles to convert harmful hydrocarbons, carbon monoxide and oxides of nitrogen emitted from automobiles to less harmful carbon dioxide, water vapor, and nitrogen. It is arguably the most used transition metal in organic synthesis. Notable mention, is its use as a catalyst in virtually all carbon-carbon cross coupling reactions.[27] It is used to make jewelries, used in electronic industry as ceramic capacitors, found in laptops and phones. It is also used in dental alloys for dental fillers.

Palladium has low toxicity and little recorded impact in the environmental. However, the sensitization risk of this metal is its major source of health concern in humans. Low doses of this metal causes allergic reactions such as skin and eye irritations in humans.[28] High doses of palladium could be malicious. Test on mice exposed to this metal shows that it could be carcinogenic,[29] although no clear case of this risk has been reported in humans. Some plants are killed from low levels of palladium salts in the environment, although most plants tolerate it.[28] Given the use of heavy metals like palladium in automobile catalytic converters, there is concern that this is a potential entry point for palladium in the environment.

Coordination chemistry of palladium(II). Palladium(II) complexes are one of the commonly used catalyst in chemical transformations. The geometry of these complexes play an important role in catalysis.[30] The most favorable geometry adopted by palladium(II) complexes, is the square planar geometry. Two square planar palladium(II) complexes are shown in Figure 2.[9,31]

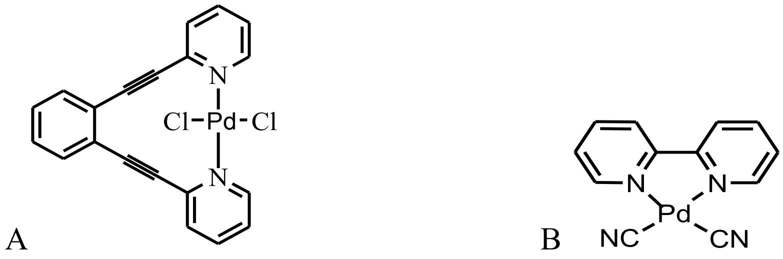

Figure 2. Two square planar palladium(II) complexes.[9,31]

It is pertinent to note that the spatial position of the pyridyl groups in complex A, are ideal to complex palladium as evidenced by the fact that the bond angles about the palladium are essentially perpendicular, with an N-Pd-Cl bond angles of 89.96° and 89.85° (Fig 2A).[9] In contrast to the second complex in Figure 2B, the angles about the palladium deviate from orthogonality (with N-Pd-CN bond angles of 95.92° and 96.58°) [31] due to the narrow bite angle of the 2,2'-dipyridyl ligand.

Dipyridyl ligands

Among dipyridyl ligands, 2,2′-bipyridine and 1,10-phenanthroline are especially common ligands used in the synthesis of wide variety of metal complexes.[32–35] Several *trans* and *cis*-coordinating ligands have been synthesized from bipyridyl moieties, and they have been shown to be important ligands in coordination chemistry. A *trans*-spanning 1,2-bis(2′ pyridylethynyl)benzene ligand was first reported by Bosch et al. He also reported the silver(I) and palladium(II) complexes of this ligand (Figures 3).

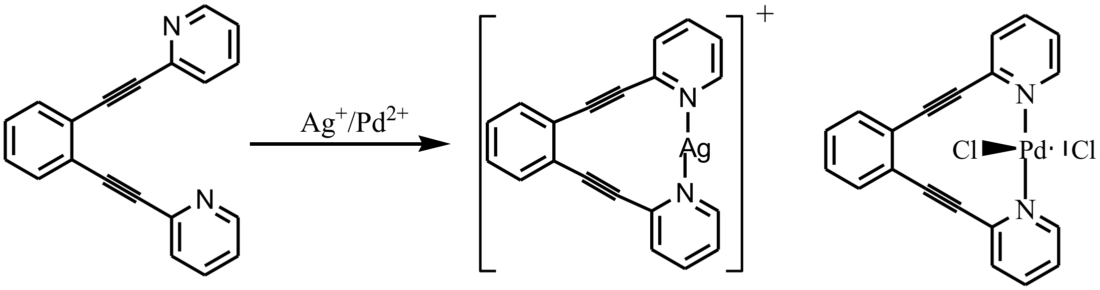

Figure 3. 1,2-bis(2′ pyridylethynyl)benzene and its silver(I) and palladium(II) complexes.[9]

However, Thummel independently reported two palladium(II) complexes of 1,2-bis(2′ pyridylethynyl)benzene.[36] The dimethoxy analogue of 1,2-bis(2′ pyridylethynyl)benzene ligand was independently prepared by Bunz, et al. He reported other conformations, apart from the *trans*-coordinating conformation that the ligand could adopt to accommodate larger cationic centers such a rhodium.[37] Even though *cis*-bidentate ligands are known to effect oxidative addition and reductive elimination steps in catalysis, which is believed to proceed at the *cis*-position of the metal center (Figure

4),[30] there are still few examples of transition-metal-catalyzed reactions with *trans*-bidentate ligands.

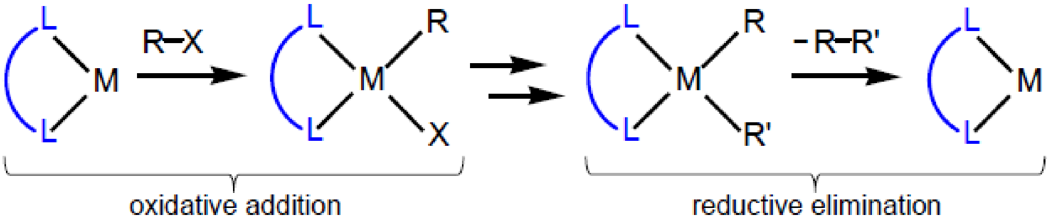

Figure 4. Oxidative addition and reductive elimination of *cis*-transition metal complex.

For example, Ueda et al. reported a palladium catalyzed Heck reaction using a rigid *trans*-bidendate ligand.[38] Also, Suzaki et al. in 2011 reported a *trans*-palladium complex of 1,2-bis(2-pyridylethynyl) benzene used to catalyze the Mizoroki–Heck cyclization of difunctionalized substrates.[39] Furthermore, Atobe reported an oxidative homocoupling of terminal acetylenes co-catalyzed by a *trans*-coordinating ligand,1-(2-pyridylethynyl)-2-(2-thienylethynyl) benzene.[40]

Ligand Design

Since silver is a soft acid, it has a high affinity for nitrogen containing ligands such as ligands containing imidazole and pyridine groups. While Figures 1, 2 and 3 show pyridine-based ligands, there are many silver complexes with imidazole based ligands.[41–43] Two examples of linear imidazole-silver complexes are shown in Figure 5. With the knowledge that imidazole and pyridine based ligands could be used to synthesize silver complexes, we reasoned we could design a related *trans*-coordinating ligand based on the combination of a pyridyl group with an imidazoyl moiety.

Figure 5. Imidazole-silver complexes.[41,43]

I reasoned that following coordination to the more basic imidazole, the intramolecular reorganization to the *trans*-complex could be followed by deprotonation in aqueous conditions resulting in the formation of a neutral complex as shown in Figure 6. After evaluating the effectiveness of this ligand, the long-term plan would involve the attachment of this ligands, or a variation, to a polymer support for the extraction of silver and palladium cations from waste.

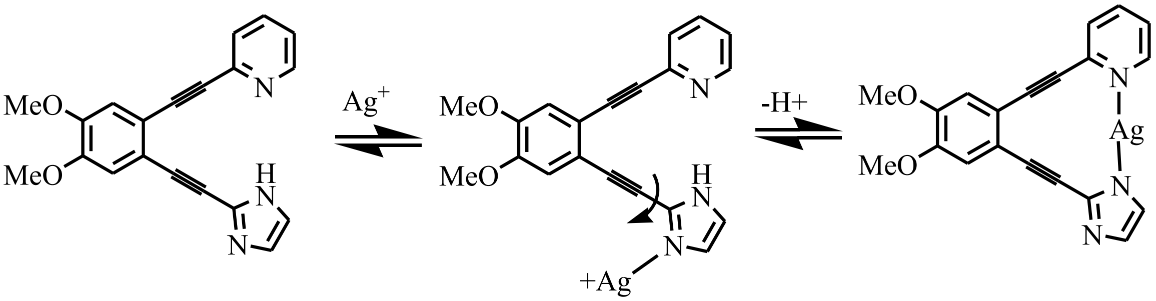

Figure 6. Formation of neutral silver(I) complex with the ligand.

RESULT AND DISCUSSION

I reasoned that the desired ligand could be synthesized by sequentially coupling 2-ethynylpyridine and 2-ethynylimidazole with an ortho-diiodobenzene. Given that 2-ethynylypyridine is available commercially at moderate cost, we planned to add the ethynylpyridine first as shown in the retro-synthetic scheme in Figure 7.

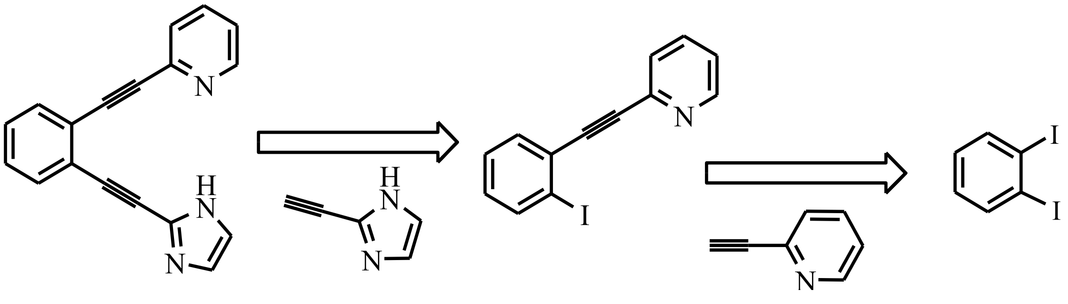

Figure 7. Retro-synthetic scheme for ligand design.

A brief literature search on Sonogashira coupling involving iodoimidazoles and terminal alkynes revealed that the coupling *only* proceeded with the imidazole N-H protected.[44–55] While the reason for this has not been elucidated, it could be due to the deprotonation of the slightly acidic imidazole hydrogen by the triethylamine (base) used in Sonogashira coupling. As a result, we developed a specific strategy to achieve the synthesis of our ligand (Figure 8). Thus, synthesis of 2-ethynylimidazole could be achieved via the synthetic route shown in reaction 1 in Figure 8. ‘P’ represents a protecting group and two different groups were employed in the synthesis of the target compound, which would be discussed later.

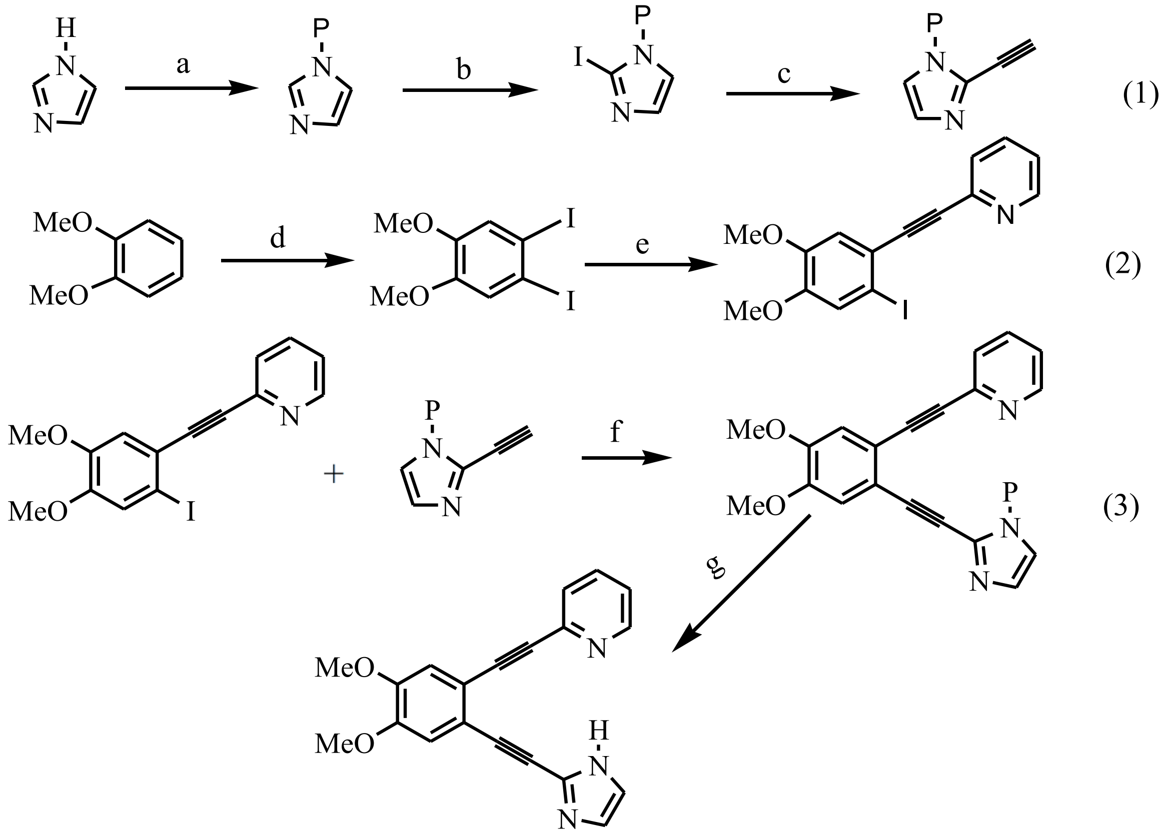

Figure 8. Synthetic route used for the synthesis of the desired imidazole-pyridine ligand.

Diiodoveratrole could be synthesized from commercially available dimethoxy-benzene. I decided to use veratrole because the methoxy groups are important for facile introduction of two ortho-iodine atoms. Also, protons on the two methoxy groups have unique NMR chemical shifts when the iodine atoms are replaced. Two chemical shifts are observed upon substitution of one of the iodine while a single chemical shift is observed upon substitution of the two iodine atoms. Thus, the methoxy group serve as an NMR signature for differentiating between the mono-substituted ethynylpyridyl product and its di-substituted counterpart. The mono-substituted 2-ethynylpyridine product can be synthesized via the route shown in reaction 2 in Figure 8. While the synthesis of the desired ligand was achieved via reaction 3 in Figure 8. For choice of 'P", I decided to use the benzyl group since it was relatively cheap and could be deprotected under mildly acidic conditions.

1-Benzyl-2-iodo-1H-imidazole, 2

To synthesize 2-ethynylimidazole, via the benzyl protecting group route, the first step involved the benzylation of imidazole followed by iodination to afford the precursor required to synthesize 2-ethynylimidazole as shown in Figure 9.

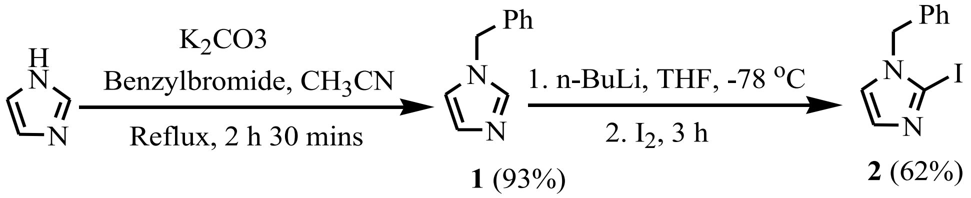

Figure 9. Synthesis of 1-benzyl-2-iodo-1H-imidazole, **2**.

Attempted synthesis of 1- (benzyl)-2-[2-(trimethylsilyl)ethynyl]imidazole, 2b

Several attempts to couple compound **2** with trimethylsilyl acetylene via a Sonogashira coupling failed (Figure 10). I tried to use different solvents such as dichloromethane and tetrahydrofuran. Also, I varied the temperature and also used a different palladium source(palladium tetrakis) but all these proved futile.

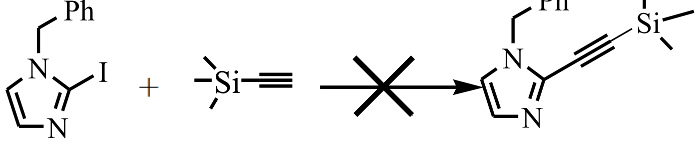

2b

Figure 10. Unsuccessful synthesis of 1-(benzyl)-2-[2-(trimethylsilyl)ethynyl]imidazole, **2b**.

Compound **2** was recrystallized from a mixture of 9/1 hexane-ethylacetate mixture to afford white needle like crystals. A good crystal for X-ray diffraction was selected and the X-ray structure was solved. Interestingly, the X-ray structure of **2** showed a strong C-I----N halogen bond which connects the molecules into a one-dimensional zigzag ribbon (Figure 12). The asymmetric unit of the X-ray structure of **2** contains a single molecule. The phenyl group is essentially orthogonal to the imidazole group with the dihedral angle between the planes defined by the phenyl C atoms and the imidazole nitrogen and carbon atoms of 84°. The phenyl proton H6 is positioned above imidazole nitrogen N1 with torsional angle N1-C4-C5-C6 = 13.0 (4)° and the H6···N1 distance of 2.58 Å compared to the sum of the van der Waals radii of 2.75 Å.[56] There is also a close contact between one of the benzyl protons and iodine atom with a H4B···I1 distance of 3.04 Å compared to the sum of the van der Waals radii of 3.18 Å.[56] The three dimensional structure of **2** features an imidazole N···I halogen bond as shown in Figure 11. The distance N2···I1 is 2.8765 (2) Å which is 81% of the sum of the van der Waals radii of 3.53 Å.[56]

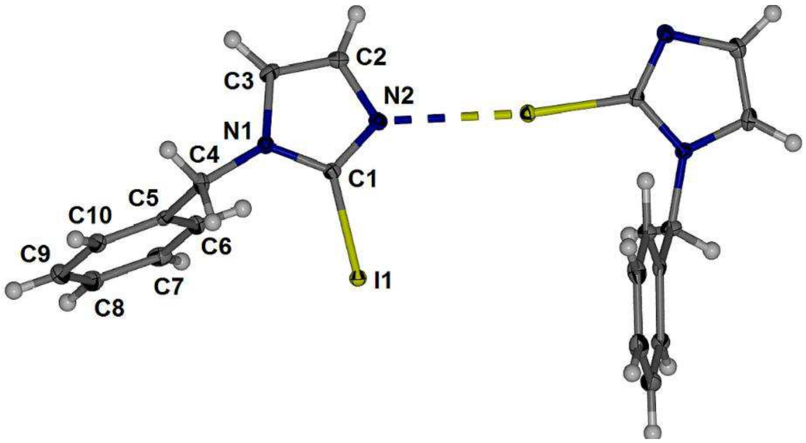

Figure 11. Structure of **2** showing the imidazole N···I halogen bond.

The halogen bond is almost linear with a C-I···N angle of 174.42 (9)°.[57] Linear one-dimensional ribbons of zig-zag halogen bonded molecules of **2** dominate the three-dimensional structure as shown in Figure 12. These one-dimensional ribbons run parallel to the a-axis and are close packed with no other significant intermolecular interactions. The CCDC # for compound **2** is 1518620.

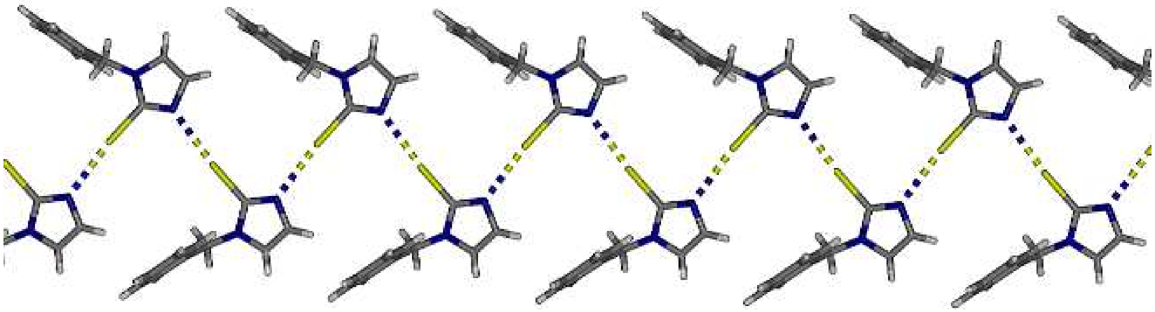

Figure 12. One-dimensional zig-zag halogen bonded ribbon in the X-ray structure of **2**.

Literature search revealed that very few studies have been done on halogen bonding involving iodoimidazoles. Therefore, this interesting result instigated the exploration of halogen bonding in two other 1-benzyl iodoimidazole derivatives.

1-Benzyl-2-iodo-1H-benzimidazole, 4

Compound **4** was synthesized from commercially available benzoimidazole using a slightly different procedure to that used to synthesize **2** (Figure 13). Compound **4** was recrystallized from a mixture of 3:2 hexane/ethylacetate to afford white rodlike crystals suitable for X-ray analysis. Several attempts to couple compound 4 with trimethysilylacetylene via a Sonogashira coupling were unsuccessful.

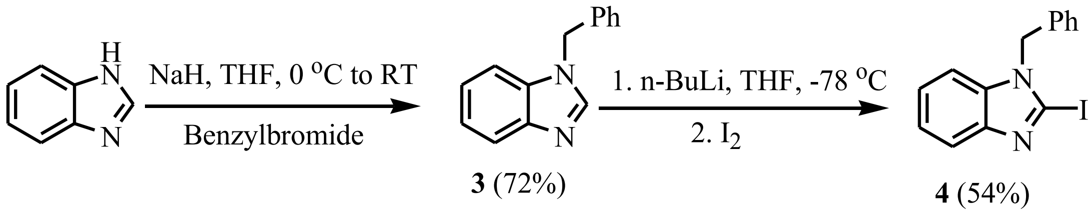

Figure 13. Synthesis of benzyl-2-iodo-1H-benzimidazole, **4**.

In contrast to compound **2**, the X-ray structure of **4** is dominated by a C-I···π interaction (Figure 14). The structure of **4** also contains a single molecule in the asymmetric unit with a dihedral angle between the imidazole and benzyl rings of 86°. In this structure, the phenyl proton H9 is positioned above N1 with dihedral angle N1-C8-C9-C14 equal to -13.4°. There is also a C-I···π interaction to the phenyl ring of an adjacent molecule resulting in a C-I···π bonded molecular dimeric motif.[57]

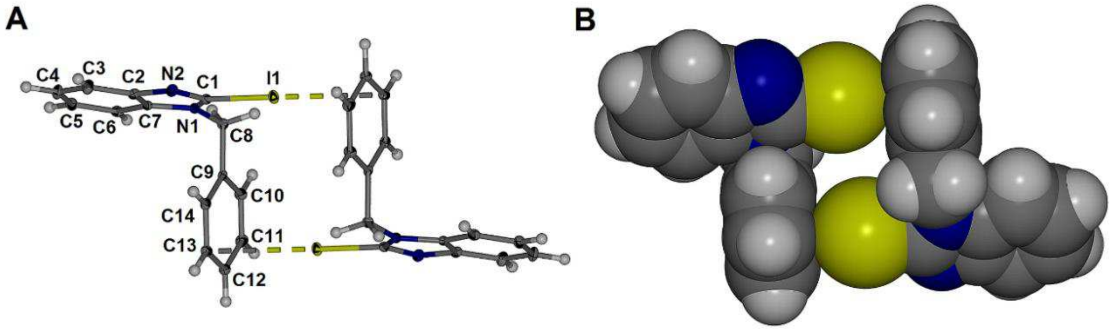

Figure 14. Structure of the C-I···π halogen bonded dimers formed in the structure of **4**, showing atom labelling and the C-I···π phenyl interaction with displacement ellipsoids drawn at the 50% level in **A** and as a space-filling model in **B**.

In the C-I···π bonded dimer of **4**, the C-I bond is directed towards the phenyl carbon, C13, of the adjacent molecule with a C1-I1 ···C13 angle of 178.66 (1)°and an I3···C13 distance of 3.3929 (4) Å. This distance is 92% of the sum of the van der Waals radii of 3.68 Å [41]. The C-I···Cg1 distance is 3.4562 (4) Å where Cg1 is the centroid of the phenyl ring C9-C14. The C-I···Cg1 angle is 156.94 (1)°. There is also an intramolecular C-H···π interaction since the benzyl proton H14 lies above the imidazole ring with a N1-C8-C9-C14 torsional angle of -13.4°. This interaction is labelled "x" in Figure 15. The H14-N1 distance is 2.51 Å and the C14-H14···N1 angle is 101.19°. The H14···Cg2 distance is 2.82Å, where Cg2 is the centroid of the imidazole ring (N1-C1-N2-C2-C7), and the C14-H14···Cg2 angle is 125°.

The three-dimensional packing of **4** involves multiple cohesive interactions: two intermolecular C-H···π interactions and two π---π interactions. Benzoimidazole hydrogen H5 has C-H···π interaction with the pendant phenyl ring labelled "y" in Figure 15. The H5···Cg1 distance is 2.78 Å and the C-H···Cg1 angle is 149° where Cg1 is the centroid of phenyl ring. Benzyl proton H13 has an interaction with the benzoimidazole benzene ring, labelled "z" in Figure 15 with a H13···Cg3 distance 2.94 Å and a C13-H13···Cg3 angle of 141°. Cg3 is the centroid of the benzoimidazole ring. The benzoimidazole groups are alternately π-stacked (ππ in Figure 15) with the benzene rings overlaid and slightly offset. The CCDC # for compound **4** is 1518622.

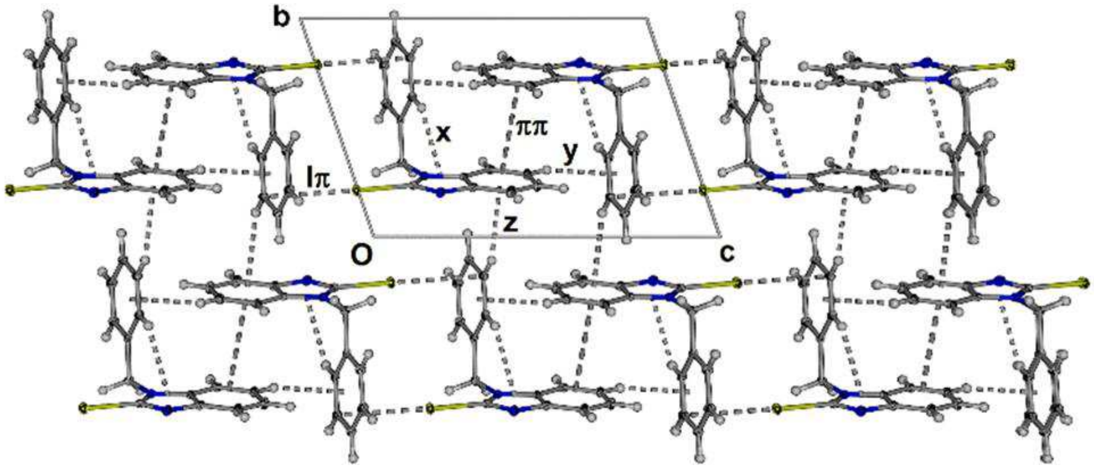

Figure 15. Partial view of the three dimensional packing of **4** viewed along the a-axis. The C-I···π interaction is labelled lπ and the C-H··· interactions labelled x, y and z and the π-stacking as ππ.

1-Benzyl-4-iodo-1H-imidazole, 5

Compound **5** was synthesized from commercially available 4(5)-iodo-1H-imidazole via a similar procedure to that used to synthesize **3** (Figure 16) and was recrystallized from a 1:2 mixture of acetonitrile and methanol to afford good crystals for X-ray diffraction.

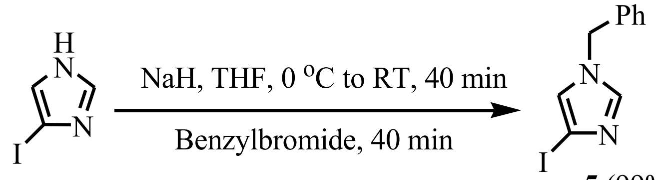

5 (99%)

Figure 16. Synthesis of 1-benzyl-4-iodo-1H-imidazole, **5**.

The X-ray structure of **5** contains a single molecule in the asymmetric unit with a bent shape. The phenyl group is also almost orthogonal to the imidazole group with the dihedral angle between the planes defined by the phenyl and imidazole rings of 84°. The phenyl ring is not oriented above the imidazole ring, with a torsional angle C6-C5-C4-N1 of -52.0 (2)°. The three-dimensional structure has a weak iodo···π-interaction with the pendant phenyl ring of an adjacent molecule that results in the formation of C-I···π halogen bonded dimers[57] as shown in figure 17.

In the C-I···π bonded dimer of **5**, the C-I bond is directed towards the phenyl carbons, C7 and C8, of the adjacent molecule with I1···C7 and I1···C8 distances of 3.551 (2) and 3.5534 (2) Å respectively both approximately 96% of the sum of the van der Waals radii of 3.68 Å[56]. The C2-I1···C7 and C2-I1···C8 angles are 152.99 (1) and 171.24 (1)° respectively. The C-I···Cg1 distance is 3.5861 (2) Å where Cg1 is the centroid of the phenyl ring, C5-C10. There are two other close contacts in the three-dimensional structure of **5**. One of these is a nonconventional C-H···N hydrogen bond between N2 and a benzylic hydrogen atom of an adjacent molecule with a N2···H4B distance of 2.55 Å, which is 93% of the sum of the van der Waals radii of 2.75 Å[56].

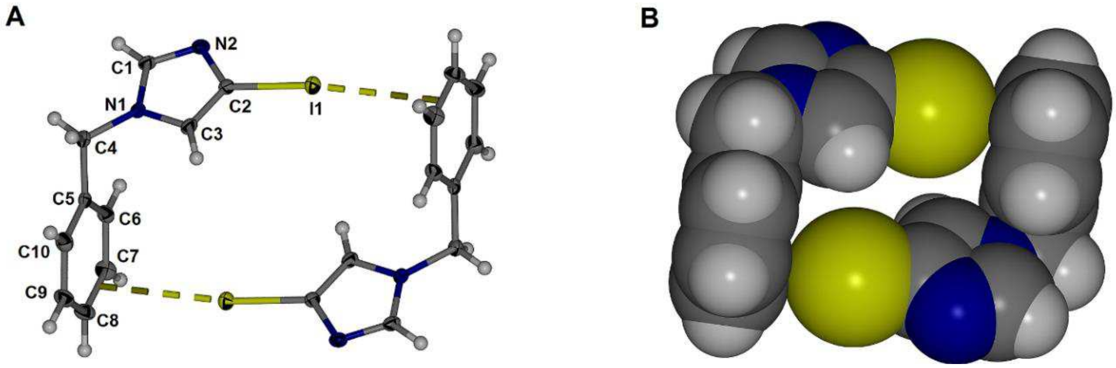

Figure 17. Structure of **5** showing atom labelling and the C-I···π phenyl interaction with displacement ellipsoids drawn at the 50% level in A and shown as a space-filling model in B.

The C-H···N angle is 157.52°. There is a close H···H contact of 2.26 Å between H4B and H7 of an adjacent molecule.61 The CCDC # for compound **5** is 1518621. Further search into literature revealed a better protecting group, 1-[[2-(trimethylsilyl)ethoxy]methyl] (SEM) for imidazoles involved in Sonogashira coupling. This group had previously been used to protect imidazoles used in Sonogashira couplings.[48,53]

1-[[2-(Trimethylsilyl)ethoxy]methyl]-2-ethynylimidazole, 9

The successful strategy involves protection of imidazole as the SEM ether followed by iodination, Sonogashira coupling with trimethylsilylacetylene and finally the deprotection of the trimethylsilyl group (Figure 18). In this sequence, imidazole was protected with SEM group as described by Dobowchik et al.[58] The crude SEM-imidazole was directly iodinated via a variation of the procedure by Knapp et al.[59]

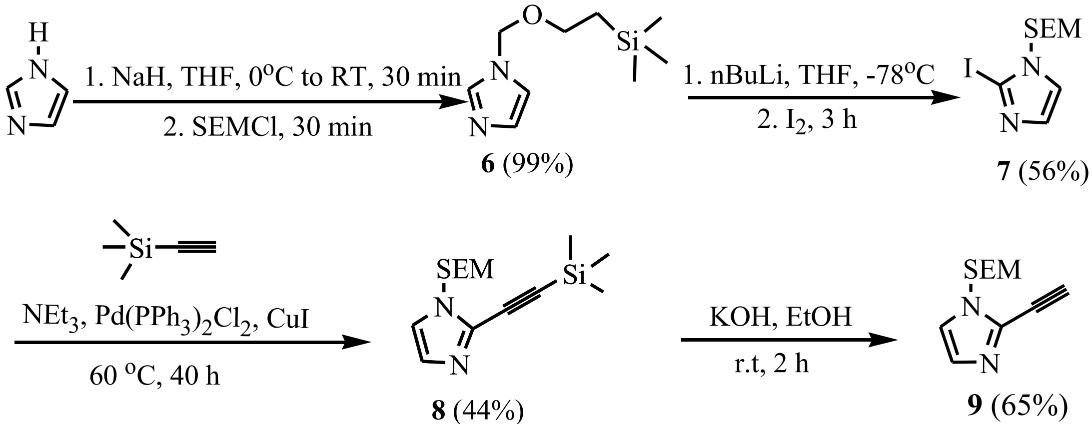

Figure 18. Synthesis of 1-{[2-(trimethysilyl)ethoxy]methyl}-2-ethynylimidazole, **9**.

After chromatographic purification, imidazole, **7** was coupled with trimethylsilylacetylene in low yield. Direct deprotection of **8** yielded the target ethynylimidazole in moderate yield. The overall yield of the SEM protected ethynylimidazole from imidazole was a meager 16%. Some reactions in this sequence posed some problems. For example, compound **6** could not be purified by column chromatography because it could not be seen on TLC plate under a UV lamp. It was also difficult to purify compound **8** by column chromatography due to very close Rf values between **8** and other impurities.

4-Iodo-5-(2-pyridylethynyl) veratrole, 11

This synthesis started with iodination of commercially available veratrole (1,2-dimethoxybenzene via a similar procedure to that reported by Lacour et al.[60] to yield 4,5-

diiodoveratrole, **10**, in excellent yield after recrystallization from a mixture of hexane and ethylacetate. The methoxy groups permitted the facile introduction of two ortho-iodine atoms. To optimize the yield of the target compound, **11**, relative to competitive disubstitution, we reacted excess diiodoveratrole (**10**), 2 equiv. with 2-ethynylpyridine. Sonogashira coupling under usual conditions followed by flash chromatography yielded **11** in moderate yield. The disubstituted product, 1,2-bis(2′ pyridylethynyl) veratrole, was also isolated as a brown solid, 26 %, along with recovered unreacted **10** (see Figure 19). The NMR data for **11** match those by Bunz et al.[61] and will therefore not be discussed in detail.

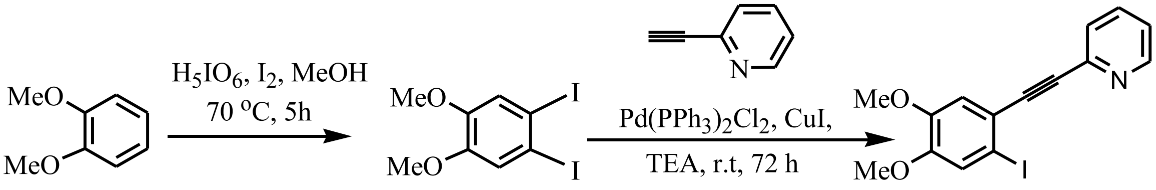

10 (91%)

11 (62%)

Figure 19. Synthesis of 4-iodo-5-(2-pyridylethynyl) veratrole, **11**.

4-[1-(2-Trimethylsilylethoxymethyl)]-1H-imidazylethynyl [5-(2-pyridylethynyl)] veratrole, 12

Having synthesized and characterized the following compounds, 4-iodo-5-(2-pyridylethynyl) veratrole and 1-[[2-(trimethylsilyl)ethoxy]methyl]-2-iodoimidazole**,** the next step was to combine the two components via a Sonogashira coupling to give **12**, the precursor to the desired ligand, **13** as shown in Figure 20. The Sonogashira coupling of 4-iodo-5-(2-pyridylethynyl) veratrole was performed in a mixture of THF and triethylamine due to the low solubility of **11** in trimethylamine. After flash chromatography, the compound was obtained as a red oil in poor yield. The compound was initially characterized by ^{1}H NMR. The ^{1}H NMR spectrum is shown in Figure 21.

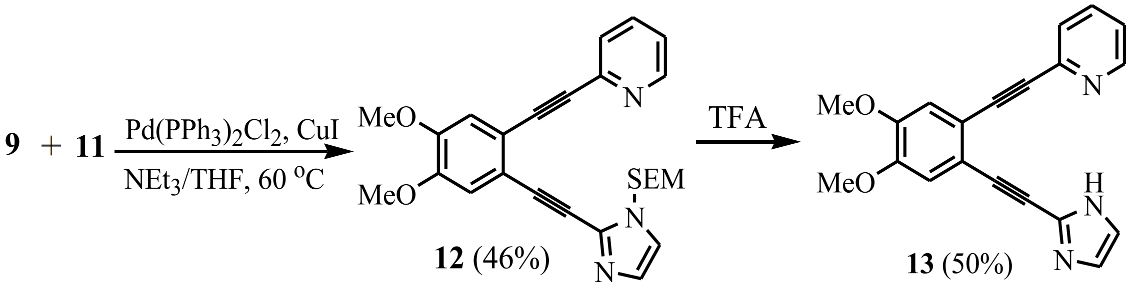

Figure 20. Synthesis of 4-[1-(2-trimethylsilylethoxymethyl)]-1H-imidazylethynyl [5-(2-pyridylethynyl)] veratrole, **12**.

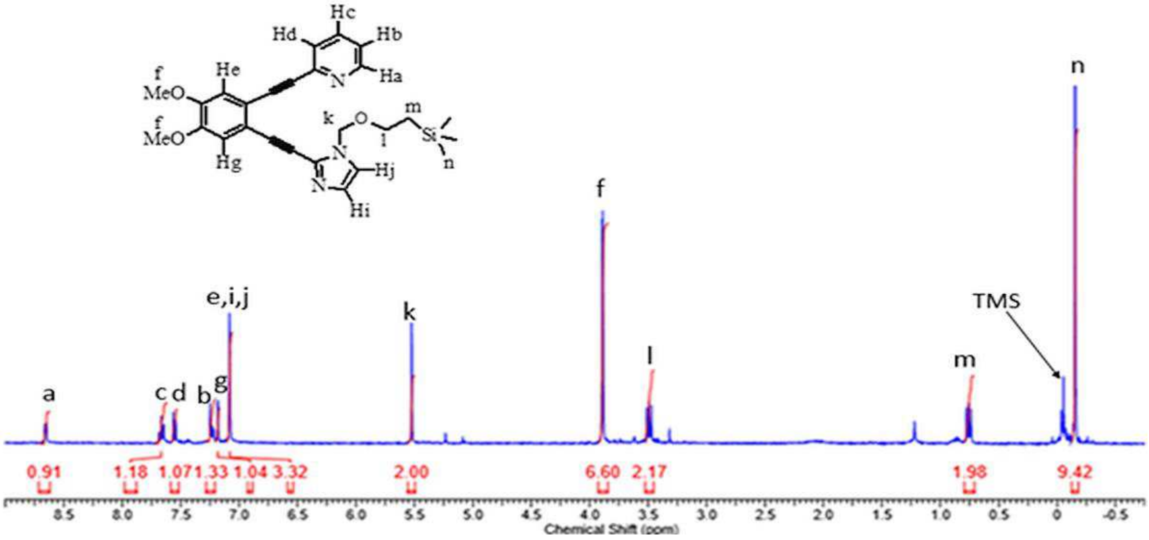

Figure 21. ^{1}H NMR 4-[1-(2-trimethylsilylethoxymethyl)]-1H-imidazylethynyl [5-(2-pyridylethynyl)] veratrole, **12** in 99.9 % $CDCl_3$.

The ^{1}H NMR spectrum has 11 sets of peaks as expected. Several of the peaks are distinctive and allow us to establish that each piece of the molecule is present. Thus, the 1H doublet at 8.65 ppm (a) corresponds to the H ortho to the pyridine N, the 6H singlet at 3.89 ppm (f) corresponds to the two methoxy groups on the central methoxy benzene ring, and the 2H singlet at 5.52 ppm (k) corresponds to the methylene group between O and N in the SEM protecting group. The relative integrations of these peaks are effectively 1:6:2 as expected for the SEM ligand, **12**. The spectrum is complex and will therefore be analyzed using two expanded spectral windows. The first spectral window shows only the aromatic protons (Figure 22).

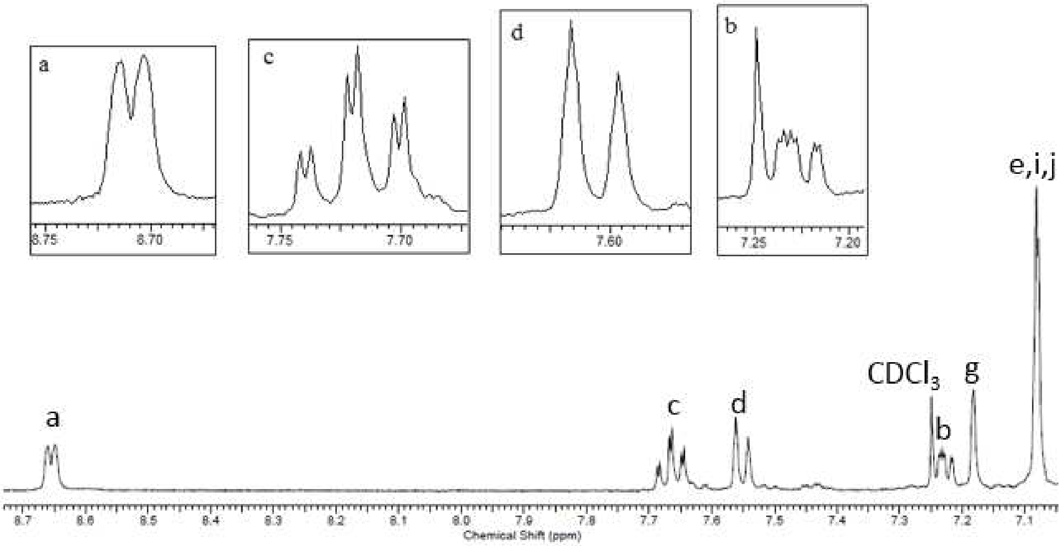

Figure 22. ^{1}H NMR of **12** in 99.9 % $CDCl_3$ showing only the aromatic proton peaks.

Proton ‘a’ is the most deshielded proton and therefore the signal for ‘a’ appears at 8.65 ppm as a doublet. It is split by proton ‘b’ with a coupling constant of $^3J = 4.8$ Hz. Hc (7.66 ppm) appears as a triplet of doublet. The proton Hc is split into a large triplet by coupling with ortho protons, Hb and Hd with $^3J = 7.8$ Hz and long-range coupling by Ha with $^4J = 2.0$ Hz. The signal for proton Hd appears at 7.55 ppm as a doublet and is coupled by ortho proton, Hc with $^3J = 7.8$ Hz. The proton signal Hb appears at 7.23 ppm as a doublet of doublet of doublet. Proton Hb has ortho coupling to Hc with a coupling constant of $^3J = 7.8$ Hz, and long range (meta) coupling with Ha ($^4J = 5.0$ Hz) and long range (para) coupling with Hd ($^4J = 1.2$ Hz). As expected, the signals for protons Ha, Hb, Hc and Hd have relative integrations of 1:1:1:1. The singlet at 7.18 ppm was assigned to Hg, while the other singlet at 7.08 ppm which integrates for three hydrogens corresponds to phenyl proton He, and imidazole protons Hi, Hj. The second spectral window shown in Figure 23, includes all the non-aromatic protons.

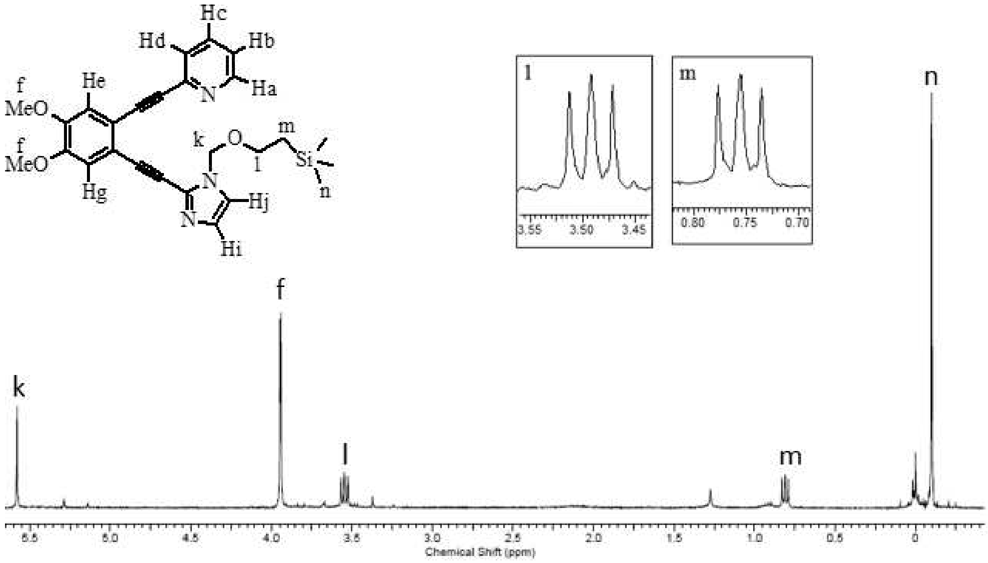

Figure 23. ^{1}H NMR of **12** in 99.9 % $CDCl_3$ showing only the non-aromatic protons.

The downfield signal labeled 'k' corresponds to the methylene protons flanked by two electronegative elements, O and N. This is a singlet that integrates for two hydrogens. The peak at 3.89 ppm (f) is a singlet that integrates for six hydrogens and corresponds to the methoxy hydrogens. The peak at 3.49 ppm is a triplet and it is assigned to the methylene protons (l) flanked by an oxygen atom. These protons are coupled by adjacent methylene protons, Hm with coupling constant $^3J = 8.4$ Hz. The triplet at 0.76 ppm then corresponds to the methylene protons, Hm with the same coupling constant. The relative integrations of the signals for Hk, Hl and Hm are 2:2:2 as expected. Finally, the singlet at -0.15 ppm integrates for 9 hydrogens and corresponds to the trimethylsilyl hydrogens from the SEM group (n). The ^{13}C NMR shown in Figure 24 also confirmed the presence of the entire piece of the molecule.

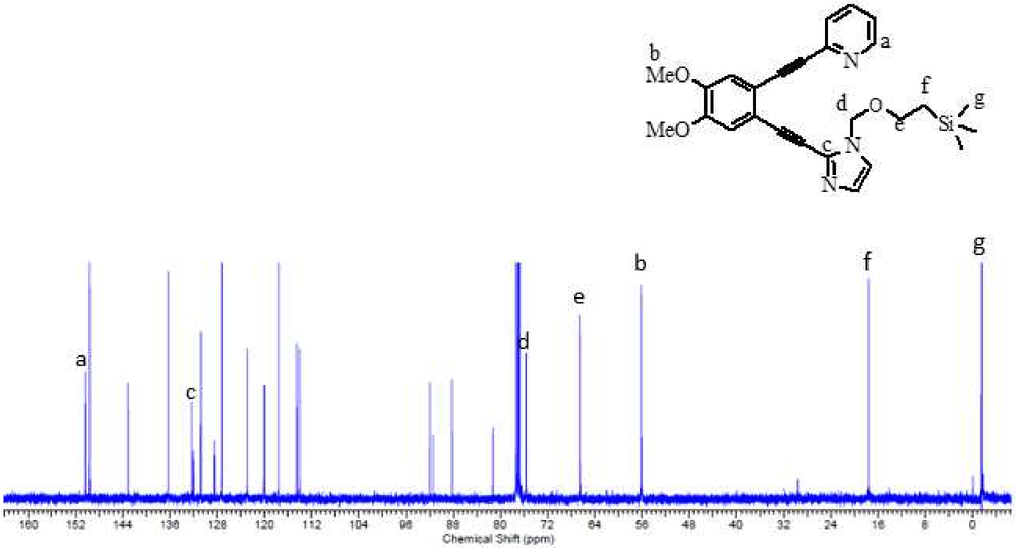

Figure 24. ^{13}C NMR of **12** in 99.9 % $CDCl_3$.

Several peaks could be assigned by the comparison to the NMR of the individual precursors. For example, the signal at 150.2 ppm corresponds to carbon ‘a’ on the pyridine ring. The corresponding chemical shift in precursor **11** was 150.5 ppm. The signal at 56.2 ppm corresponds to the carbon ‘b’ on the central benzene ring. The corresponding chemical shift observed for the methoxy groups in the precursor, **10** was 56.3 ppm and thesignal at 136.3 ppm corresponds to carbon ‘c’ on the imidazole ring with a corresponding chemical shift in the precursor, **9** of 131.1 ppm. In total, there are 14 peaks in the aromatic region between 150.2 and 114.7 ppm. These 14 peaks correspond to 6, 5 and 3 carbon atoms on the benzene, pyridyl and imidazoyl rings respectively. The four ethynyl carbon peaks are seen at 91.7, 91.6, 88.1 and 81.5 ppm respectively. The peaks at 75.6, 66.6, 17.7 and -1.4 ppm corresponds to the carbon atoms on the SEM group, while the peak at 56.2 corresponds to the methoxy carbon from the benzene ring.

4-[(2-Imidazylethynyl)]-5-(2-pyridylethynyl) Veratrole, 13

In contrast to other silyl based protecting groups, there are relatively few reported methods for deprotection of the SEM protecting group. Two of the milder methods uses either tetrabutylammonium fluoride or concentrated hydrochloric acid to effect deprotection. Unfortunately, Honda et al. reported that neither of these gave positive result with an alkyne present in the molecule.[53] The Honda group then reported a new procedure, which employed trifluoroacetic acid to effect deprotection of the SEM group.[53] Thus, **13** was obtained from **12** by treating it with trifluoroacetic acid. Flash chromatography, followed by recrystallized from a mixture of acetonitrile and dichloromethane gave crystals suitable for single X-ray structure determination.

Compound **13** was first characterized by ^{1}H and ^{13}C NMR spectroscopy. The ^{1}H NMR was recorded in both deuterated dimethylformamide (DMF-d_7) and Chlorofoam. The spectrum recorded in DMF-d_7 is shown in Figure 25. Additionally, the elemental analysis of **13** was performed and the observed compositions of C, H and N was within ± 0.4 % of the calculated values for **13**. From the spectrum above, we observed the disappearance of the SEM protecting group peaks, Hk (5.52 ppm), Hl (3.49 ppm), Hm (0.76 ppm) and Hn (-0.15 ppm) that were present in compound **12** and the appearance of imidazole hydrogen, Hp at 13.20 ppm. This confirms the complete replacement of the SEM group by hydrogen. The appearance of imidazole N-H proton (Hp) and the presence of Ha and Hf peaks at 13.20, 8.76 and 3.96 ppm respectively confirms that each piece of the molecule was present.

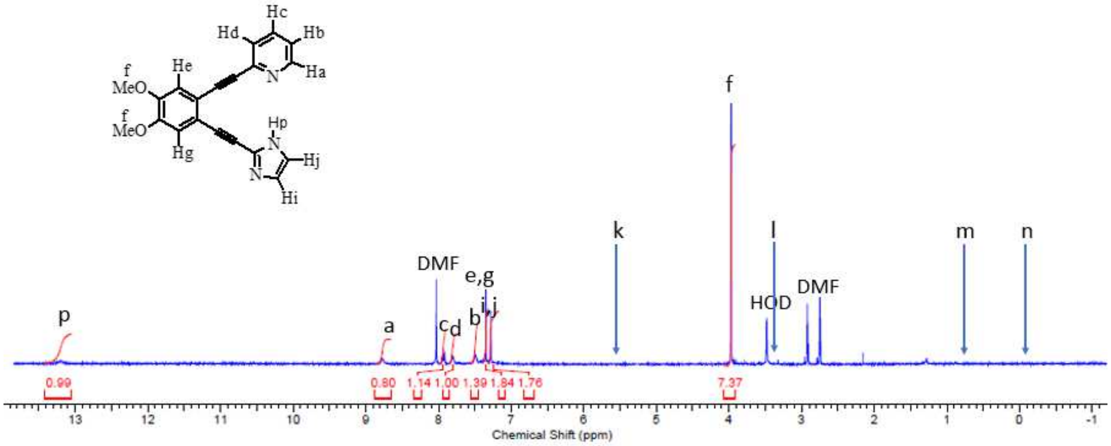

Figure 25. ^{1}H NMR of 4-[(2-Imidazylethynyl)]-5-(2-pyridylethynyl) veratrole, **13** in 99.9% DMF-d_7.

However, since ^{1}H NMR of **13** was recorded in DMF, it is reasonable to observe shifts in the peaks due to significant difference in polarity and solvation ability of the two solvents (chloroform and dimethylformamide). The spectral window showing only the aromatic region is shown in Figure 26. The imidazole N-H proton, Hp, was not observed when the NMR spectrum was recorded in $CDCl_3$. The pyridyl protons are Ha-Hd and the imidazole protons are Hi and Hj (on carbon) and Hp (on nitrogen). Proton 'p' is the most deshielded proton and therefore the signal for proton 'p' appears at 13.20 ppm which corresponds to imidazole N-H proton. The signal for Hp is broad because of the intramolecular hydrogen bonding of this proton with the pyridine nitrogen. The proton, Ha was observed at 8.76 ppm and appears as a doublet. Proton Ha is split by proton Hb with a coupling constant of $^3J = 4.4$ Hz. The signal for proton Hc appears at 7.93 ppm as a triplet of doublet. Proton Hc is split into a large triplet by coupling with ortho protons, Hb and Hd with $^3J = 7.8$ Hz and long-range coupling to Ha with $^4J = 1.6$ Hz.

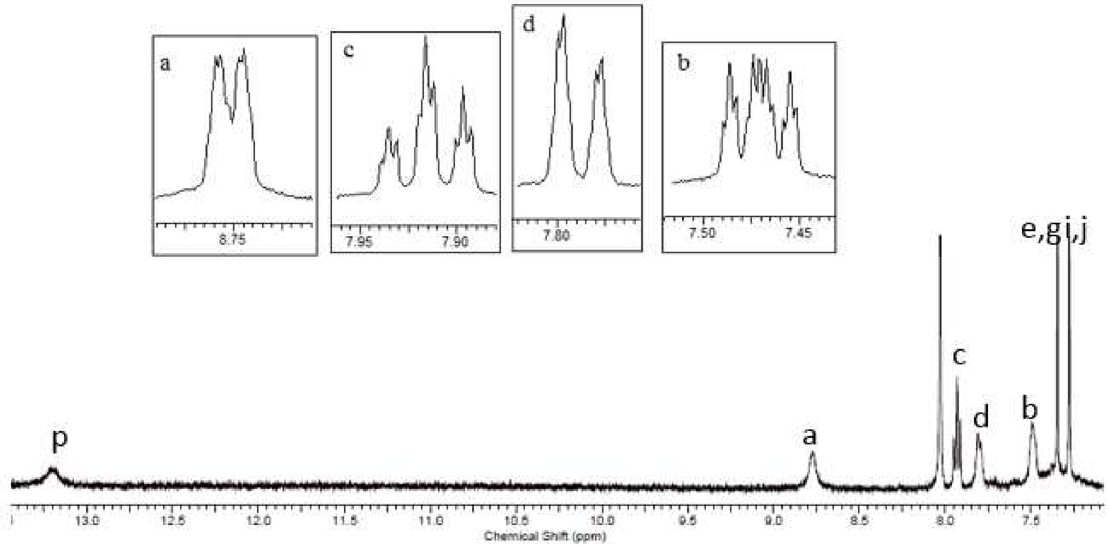

Figure 26. ^{1}H NMR of **13** recorded in dmf-d_7 showing only the aromatic peaks.

The signal for proton Hd appears at 7.79 ppm and is coupled to ortho proton, Hc with $^3J = 7.8$ Hz. The signal for proton Hb appears at 7.23 ppm as a doublet of doublet of doublet. Proton Hb has an ortho coupling to Hc with a coupling constant of $^3J = 7.6$ Hz, and long range (meta) coupling with Ha ($^4J = 4.8$ Hz) and long range (para) coupling with Hd ($^4J = 1.2$ Hz). As expected, the signal for protons Ha, Hb, Hc, Hd peaks had relative integrations of 1:1:1:1. The singlet at 7.34 ppm which integrates for two hydrogens correspond to the phenyl protons He and Hg while the other singlet at 7.27 ppm which also integrates for two protons corresponds to imidazole protons Hi and Hj. The ^{13}C NMR shown in Figure 27 also confirms the success of the deprotection. From the ^{13}C NMR spectrum, we observed the disappearance of the four carbon peaks associated with the SEM group (d,e,f, g) present in compound **12.** Overall, 11 peaks were observed in the aromatic region, ranging from 150.2 to 112.6 ppm. There is an overlap of two imidazole carbon peaks as well as two phenyl-carbon peaks. The four ethynyl carbon peaks were observed between 90.8 and 85.4 ppm and finally the methoxy peak at 56.3 ppm.

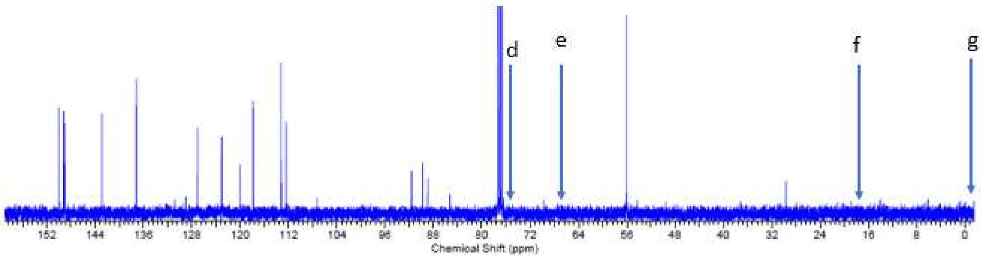

Figure 27. ^{13}C NMR spectrum of **13** in 99.9 % $CDCl_3$.

The single crystal X-ray structure of **13** contains a single molecule in its asymmetric unit and is shown in Figure 28. There is a significant deviation from planarity in the structure of the ligand. This deviation is evident as the interplanar dihedral angles formed between the benzene ring and the pyridyl and imidazole rings are 15.00 ^{o} and 15.09 ^{o} respectively. There is an intramolecular hydrogen bonding between N(1) and H(2) with N(1)---H(2) distance of 1.997 Å. The ethynyl bonds are slightly distorted from linearity with 1.3, 5.6, 7.2, and 7.1° for angles C(5)-C(6)-C(7), C(6)-C(7)-C(8), C(13)-C(14)-C(15), and C(14)-C(15)-C(16) respectively as shown in Figure 28. The distortion is more pronounced for angles C(13)-C(14)-C(15), and C(14)-C(15)-C(16). This distortion is due to the smaller size of the imidazole ring compared to the pyridyl ring as well as the intramolecular hydrogen bonding. There are several weak intermolecular interactions C-H---N, C-H---O and C-H---π hydrogen bonds) between molecules of compound **13** that help stabilize the formation of planar sheets of adjacent molecules as shown in Figure 29. The strong intramolecular N(1)-H(2) hydrogen bond, labelled 'a', has a N(1)---H(2) distance of 1.999 (13) Å, that corresponds to 73% of the sum of the van der Waals radii of 2.75 Å.

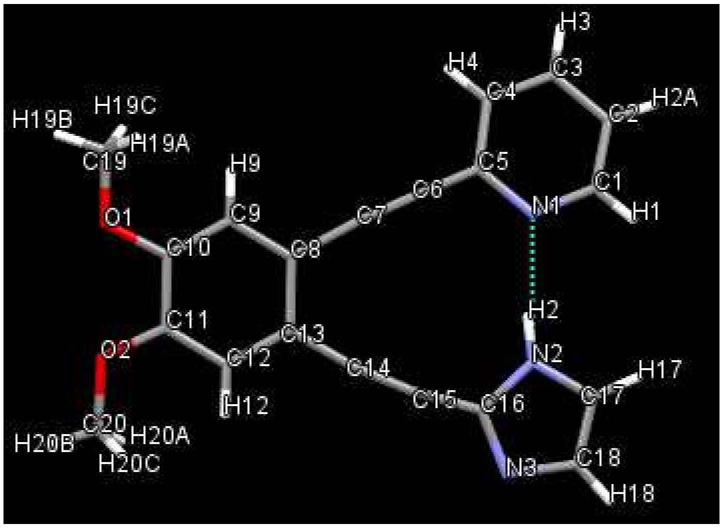

Figure 28. The labeled asymmetric unit of **13** showing intramolecular hydrogen bonding.

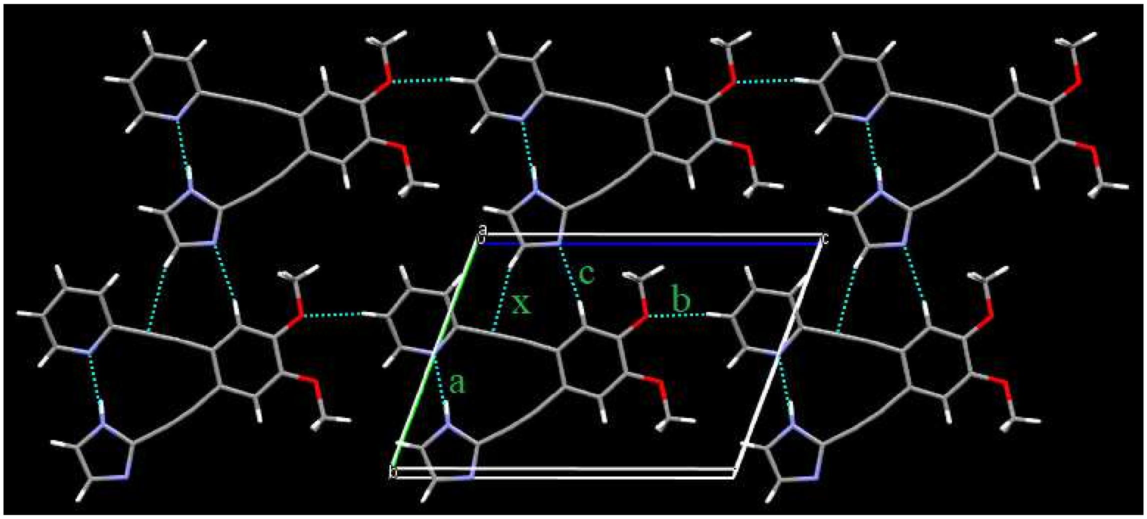

Figure 29. Side-by-side projection of molecules of **13** to form planar sheets.

A weak C-H---O hydrogen bond is also observed between the methoxy oxygen and the adjacent pyridine hydrogen, labelled 'b' in Fig. 29, with a H2A-O1 distance of 2.379

Å corresponding to approximately 87% of the sum of the van der Waals radii of 2.72 Å. There is also a nonconventional C-H---N hydrogen bond labelled 'c' in Fig. 29, with H9---N3 distance of 2.435 Å which corresponds 89% of the sum of the van der Waals radii of 2.75 Å. We also see a weak C-H---π(C≡C) interaction between an imidazole hydrogen and its neighbouring alkyne pie electrons, labelled 'x', with H18-C6 distance of 2.772 Å, corresponding to approximately 96% of the sum of the van der Waals radii of 2.9 Å. The crystal packing features cohesive π-π interactions as can be seen in Figure 30.

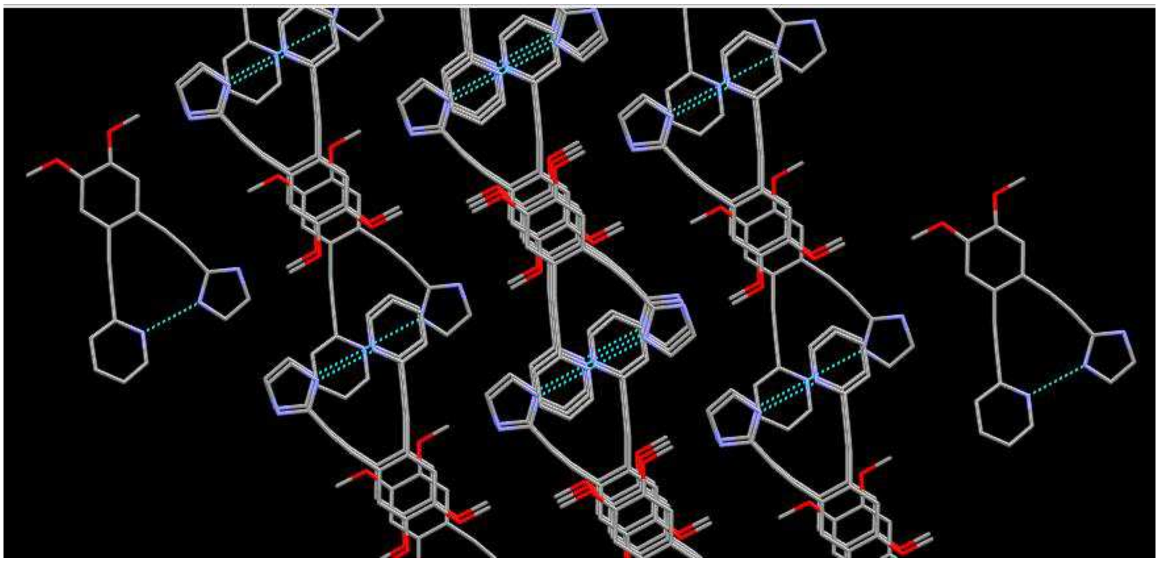

Figure 30. Three-dimensional projection of **13** showing π-π interactions, hydrogen atoms omitted for clarity.

The partial view of the three-dimensional packing of compound **13** clearly shows these π-π interactionsin (Figure 31). The overlay of the sheets is complex and the three-dimensional packing of **13** feature two cohesive π-π interactions. There is a π-π interaction between two central dimethoxybenzene, labelled 'd' with a C1g-C1g distance of 3.324 Å where C1g is the centroid of the benzene ring C9-C12. The other π-π interaction is between the imidazole ring and the pyridine ring, labelled ‘e’ with a C2g-C3g distance of 3.343 Å, C2g and C3g are centroids of pyridine ring N4-C1-C2-C3-C4-C5 and imidazole ring, N2-C16-N3-C17-C18 respectively.

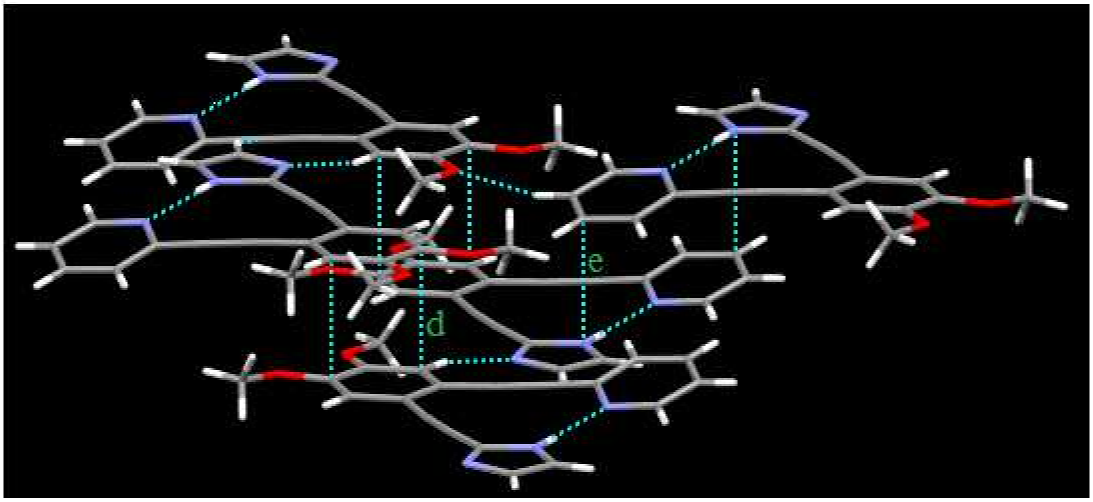

Figure 31. Partial view of the three-dimensional projection of **13** viewed along b-axis.

Complexation of silver(I) and palladium(II) salts by ligand 13

Ligand **13** was designed to complex silver(I) and palladium(II) cations and we chose to study this binding using NMR titration. In this method, small known increments of the metal salts are added into a solution of the ligand and the NMR spectrum recorded after mixing the solution. Previous NMR titration binding studies of Pd(II) by related *trans*-coordinating bipyridyl ligands revealed that binding of Pd(II) was slow on NMR time scale. Accordingly, proton signals for both the bound ligand and the unbound ligand are observed until one equivalent of Pd(II) was added.[62] Notably the pyridine protons signal of the complex were shifted downfield relative to the free ligand and the proton signal for the complex always appeared downfield.[62,63] This allows for quantification of bound to unbound ligand by simple relative integration of bound to unbound proton peaks. On the contrary, binding of silver(I) salts by related bipyridyl ligands is characterized by rapid exchange between complexed and un-complexed ligands. Thus, binding and release of silver(I) is faster than the NMR time scale. Therefore, an average spectrum of bound and unbound ligand is observed rather than distinct peaks corresponding to bound and unbound ligand. Thus, the proton chemical shift of the ligand protons gradually shifts downfield as the relative amount of Ag(I) is added until all the ligand is completely bound.[62] Under certain circumstances, the relative amounts of complexed and un-complexed ligand can be calculated and the binding constant determined.

The stoichiometry of complexation of Ag(I) by a ligand in solution can be determined using titration as described with a judicious, relatively high, choice of concentrations. The principle is that complexation of a metal cation by a ligand will result in a change in chemical shift of ligand protons in close proximity to the metal cation. When the ligand is fully bound, further addition of Ag(I) does not result in spectral changes. The spectra of the silver and palladium complexes were recorded in DMF-d_7. The full ^{1}H NMR spectra showing the ligand, the silver(I) and palladium(II) complexes are shown in Figure 32.

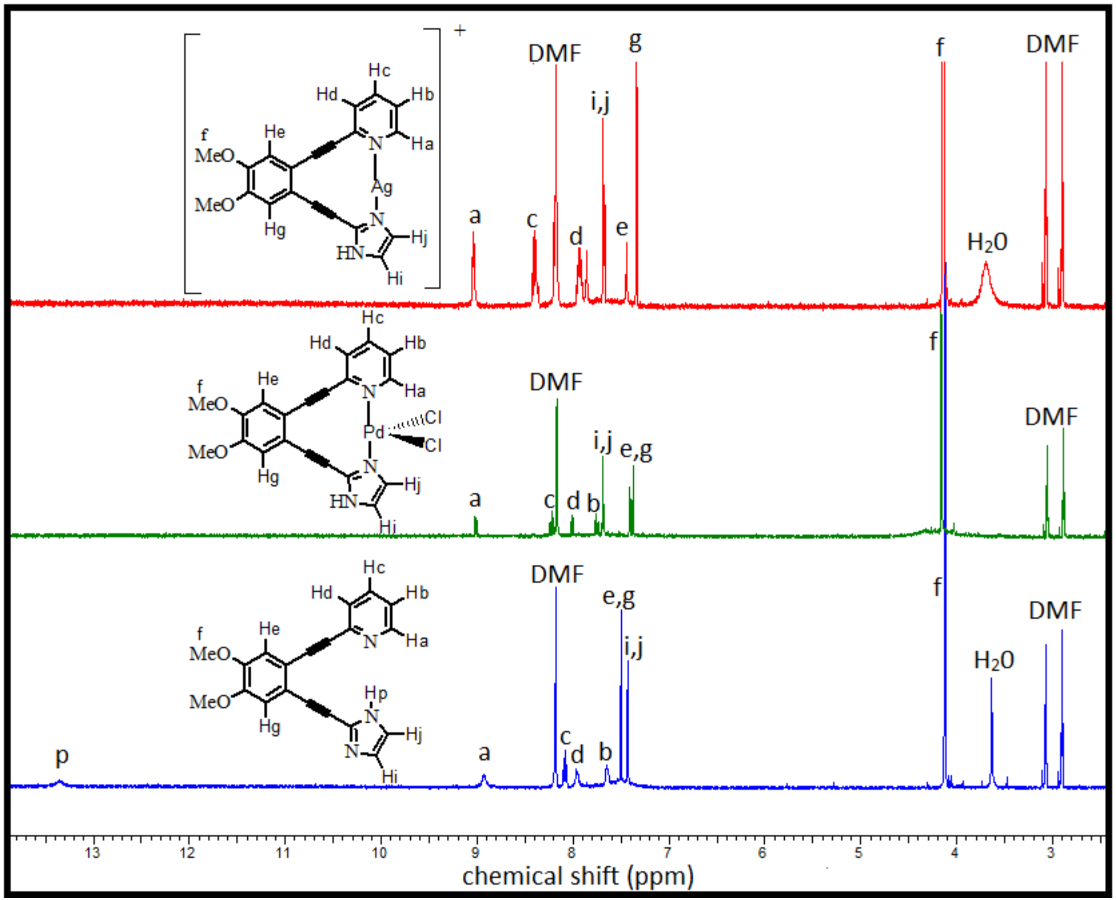

Figure 32. ^{1}H NMR spectrum of ligand, silver and palladium complex in DMF-d_7.

Titration of ligand, 13 with silver(I) salt

The stoichiometry of the ligand with silver was determined by gradually titrating a known concentration of AgOTf against a known concentration of the ligand (in an NMR tube). As the silver(I) concentration increased, the chemical shift of the pyridyl protons shifted steadily downfield until one equivalence of the silver salt was reached as shown in Fig. 33, indicating that a 1:1 complex was formed between the host and the guest molecule. A plot of the chemical shift (Δδ) against the mole ratio of host to guest also clearly shows a 1:1 stoichiometry (Figure 34). It is particularly noteworthy that there was no further change in chemical shift after a 1:1 ratio of ligand **13** to silver(I) was reached.

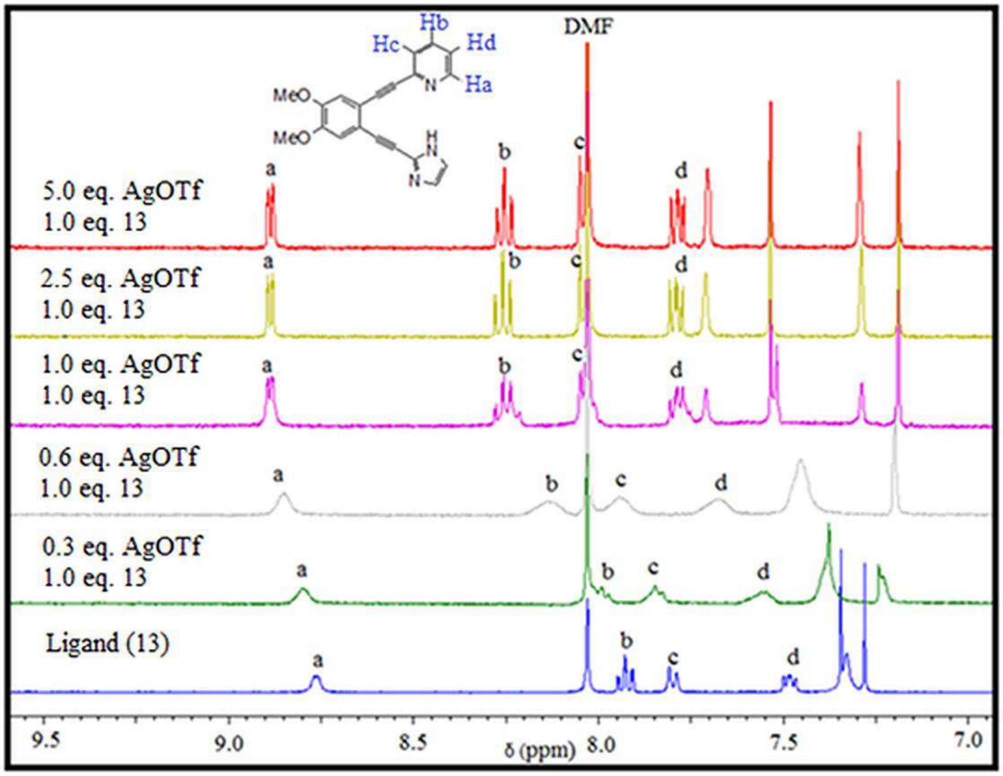

Figure 33. Spectral changes observed in incremental addition of silver(I) trifluoromethane sulfonate into a dmf solution of ligand **13** (30.36 nM).

The relative change in chemical shift (Δδ) for each pyridyl proton was plotted against the relative ratio of silver(I) to ligand **13**. This plot, Figure 34, emphasizes the 1:1 nature of the complex and the lack of secondary complexation at these concentrations of ligand and silver(I). These results are consistent with the reversible complexation of silver(I) cation that is faster than the NMR time scale. I believe that the formation of the silver complex takes place by initial complexation of the metal cation to the more basic external imidazole N of the ligand, **13** followed by rotation to afford linear complexation with the pyridyl nitrogen as shown in Figure 35.

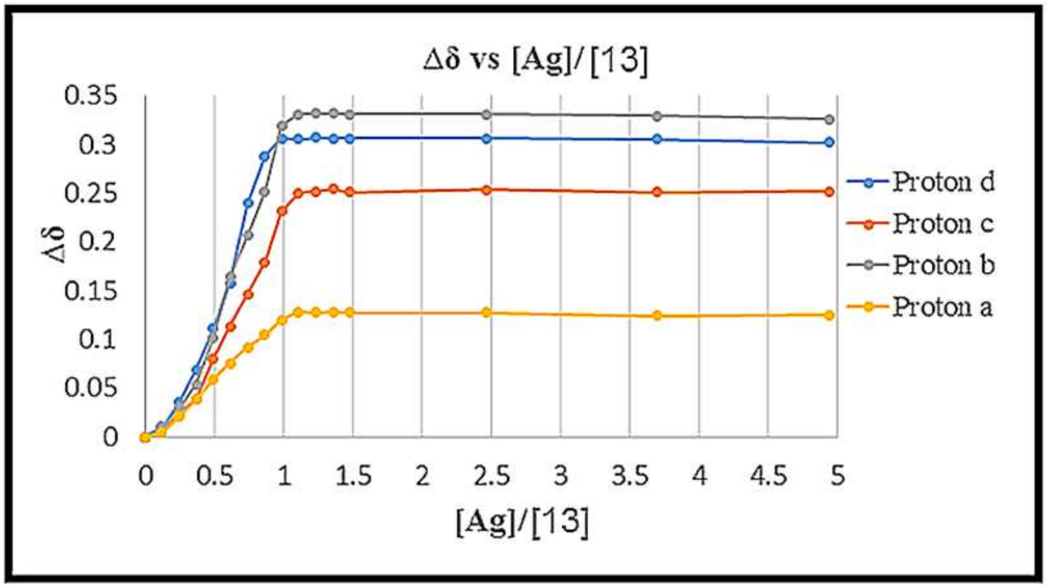

Figure 34. Plot of the change in chemical shift ((Δδ) of pyridyl protons of ligand **13**, on increamental addition of AgOTf.

I hypothesized that the complexation with a monovalent cation, would lead to the deprotonation of the imidazole hydrogen in the presence of a weak base, for example, water. At this stage, I do not have enough evidence to prove that this indeed happened in solution. This could be proven by either dissolving the complex in basic solution, which would possibly effect the deprotonation of the acidic imidazole hydrogen. Furthermore, I was unable to isolate crystals of the silver complex suitable for single crystal X-ray analysis.

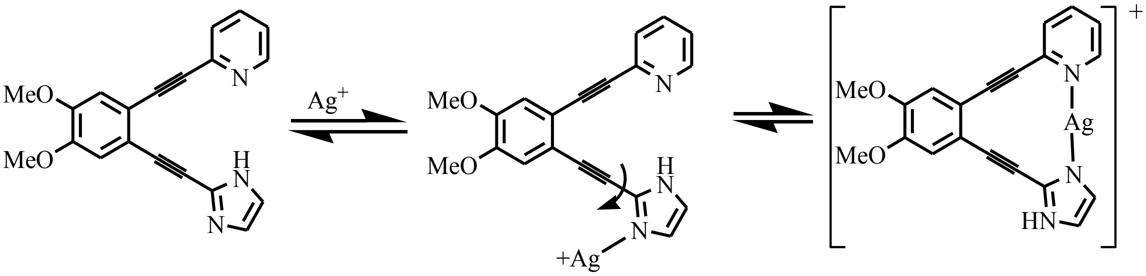

Figure 35. Proposed formation of silver complex of ligand **13.**

Complexation of ligand, 13 with palladium(II) salt

The titration of ligand, **13** with palladium(II) was performed using the same procedure as described for Ag(I). In this experiment, we used bis(acetonitrile)palladium(II) dichloride as a soluble source of Pd(II). Thus, aliquots of $PdCl_2(CH_3CN)_2$ were added into a known concentration of ligand **13** and the NMR spectrum recorded. On addition of 0.4 eq. of Pd(II) solution, proton signals for both Pd-complexed and un-complexed ligand were observed. The proton signals associated with the un-complexed ligand diminished with simultaneous increase in the intensity of the proton signals associated with the Pd-complexed ligand as shown in Figure 36. The signal for un-complexed ligand completely disappeared when 1.0 equiv. of Pd(II) was added. This confirmed that the expected 1:1 complex, **13.**Pd(II) was formed in solution. The formation of 1:1 complex, **13.**$PdCl_2$ in solution was confirmed by isolating and characterizing the solid from the solution obtained after NMR titration. Thus, the dmf-d7 solution of **13.**$PdCl_2$ obtained after the titration described above was transferred into a vial and carefully placed into a bigger vial containing ether. After 24 h, the solvents were removed, and the remaining precipitate recrystallized from a mixture of dichloromethane, ethanol and acetonitrile. A homogeneous mass of orange crystals were harvested after 5 days. The solid was taken for elemental analysis and the observed compositions of C, H and N was within ± 0.4 % of the calculated values. A single crystal suitable for X-ray analysis was selected and the structure determined.

The single crystal X-ray structure of **13.**$PdCl_2$ contains a single molecule in its asymmetric unit. The asymmetric unit of the complex contains the ligand coordinated to palladium and two chloride atoms.

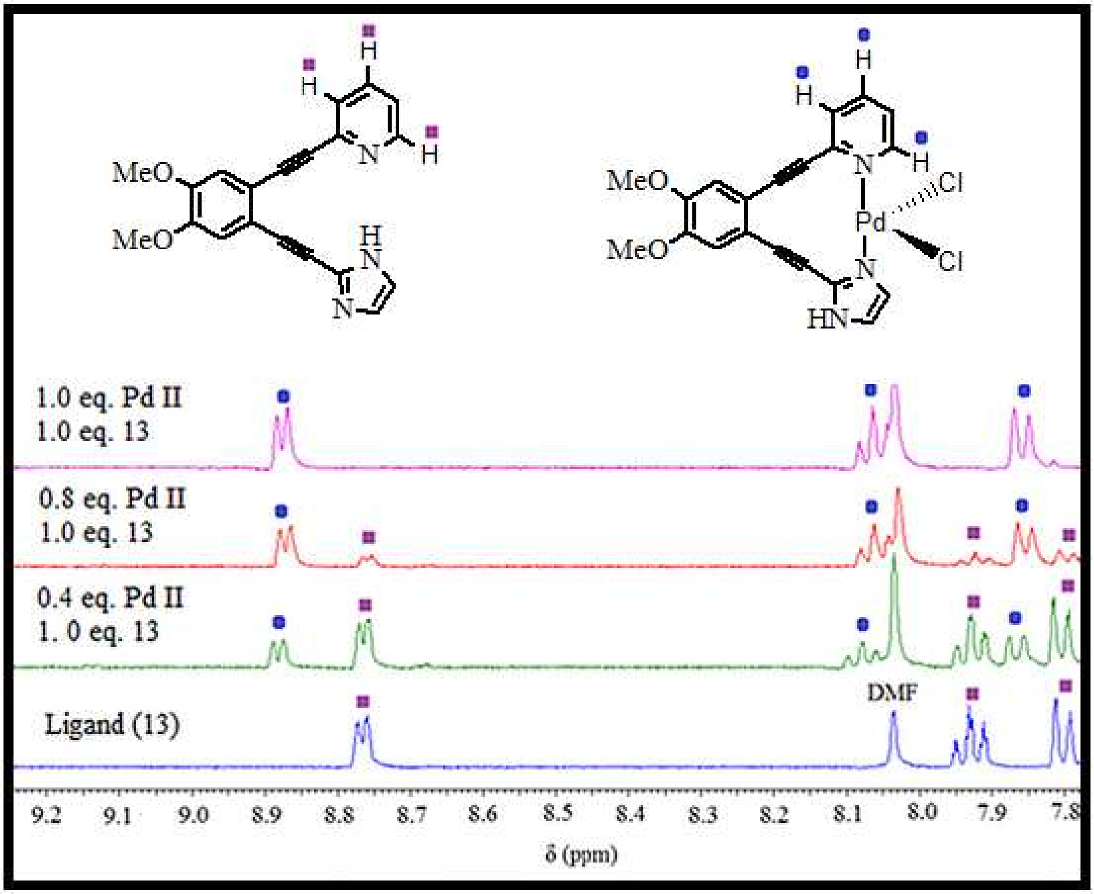

Figure 36. Stacked ^{1}H NMR spectra obtained on sequential addition of $PdCl_2(CH_3CN)_2$ into a 75.91 nM dmf-d7 solution of **13**.

The ligand is essentially planar as shown in Figure 37. Indeed the interplanar dihedral angles formed between the imidazole ring and the pyridyl and benzene rings are 2.690 (0.204)° and 1.695 (0.177)° respectively. The N(1)-Pd(1) and N(2)-Pd(1) distance are 2.018(3) and 2.006 (3) Å respectively while Pd(1)-Cl(1) and Pd(1)-Cl(2) distances are 2.319 (9) and 2.334 (10) Å respectively. The coordination about palladium is square planar with almost linear N(1)-Pd(1)-N(2) and Cl(1)-Pd(1)-Cl(2) angle of 176.87 (12) and 174.40(4)° respectively. The N-Pd-Cl angles are all virtually orthogonal with N(1)-Pd(1)-Cl(2), N(1)-Pd(1)-Cl(1), N(2)-Pd(1)-Cl(1), and N(2)-Pd(1)-Cl(2) at angles of 91.42 (9), 89.27 (9), 91.05(9), and 89.56 (9) respectively. The ethynyl bonds are slightly bent with distortions of 5.64, 4.3, 2.3, and 4.1° for bonds C(5)-C(6)-C(7), C(6)-C(7)-C(8), C(13)-C(14)-C(15), and C(14)-C(15)-C(16) respectively.

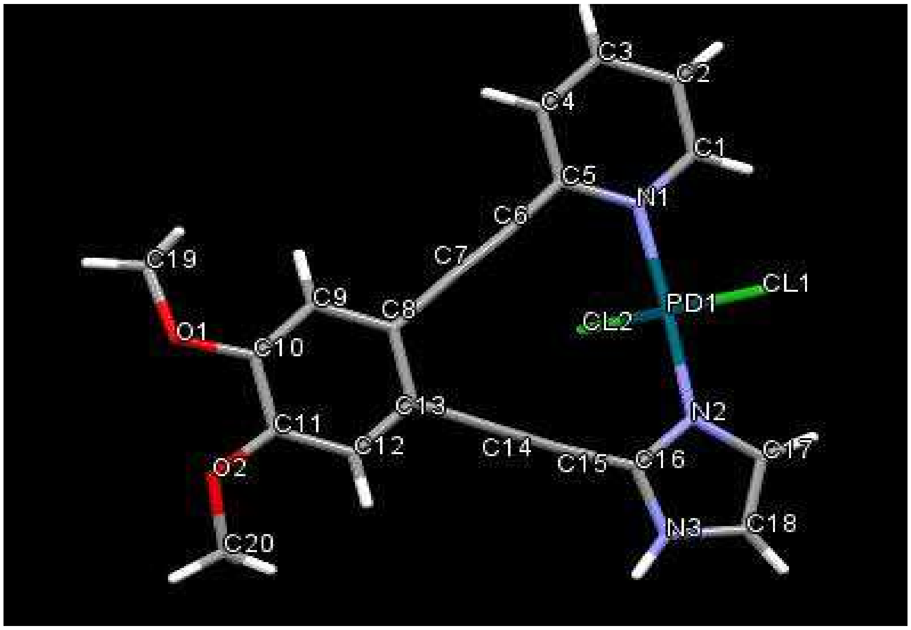

Figure 37. The labeled asymmetric unit of palladium complex of **13**.

The three dimensional packing of **13**.$PdCl_2$ also features multiple weak interaction: a C-H---Cl interaction labelled ‘a’ in Figure 38, with H-Cl distance of 2.918 Å which corresponds to 99% of the sum of the van der Waals radii of 3.3 Å There is a π-π interaction between two stacked imidazole rings, labeled ‘b’ if Figure 38, with C4g-C4g distance 3.363 Å, where C4g is the centroid of the imidazole ring. There is also a nonconventional N-H---Cl interaction labelled ‘c’ in Fig. 38. The H-Cl distance is 2.424 Å. A C-H---π interaction labelled ‘d’ in Figure 38, with H-Cg5 distance of 2.871 Å where Cg5 is the centroid of the benzene ring. Finally, a N-H---Cl interaction labelled ‘e’ in Figure 38, with H-Cl distance of 2.424 Å.

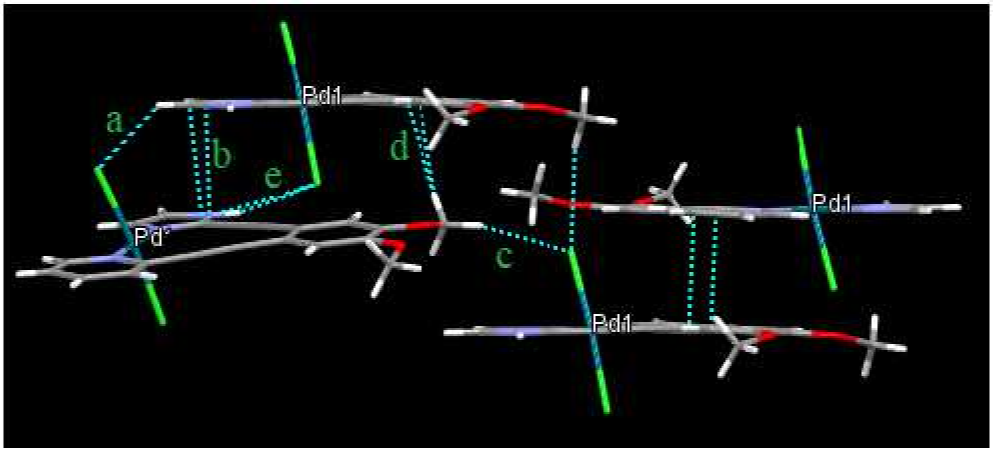

Figure 38. Partial view of the three-dimensional projection of **13**.PdCl$_2$ viewed along the b-axis.

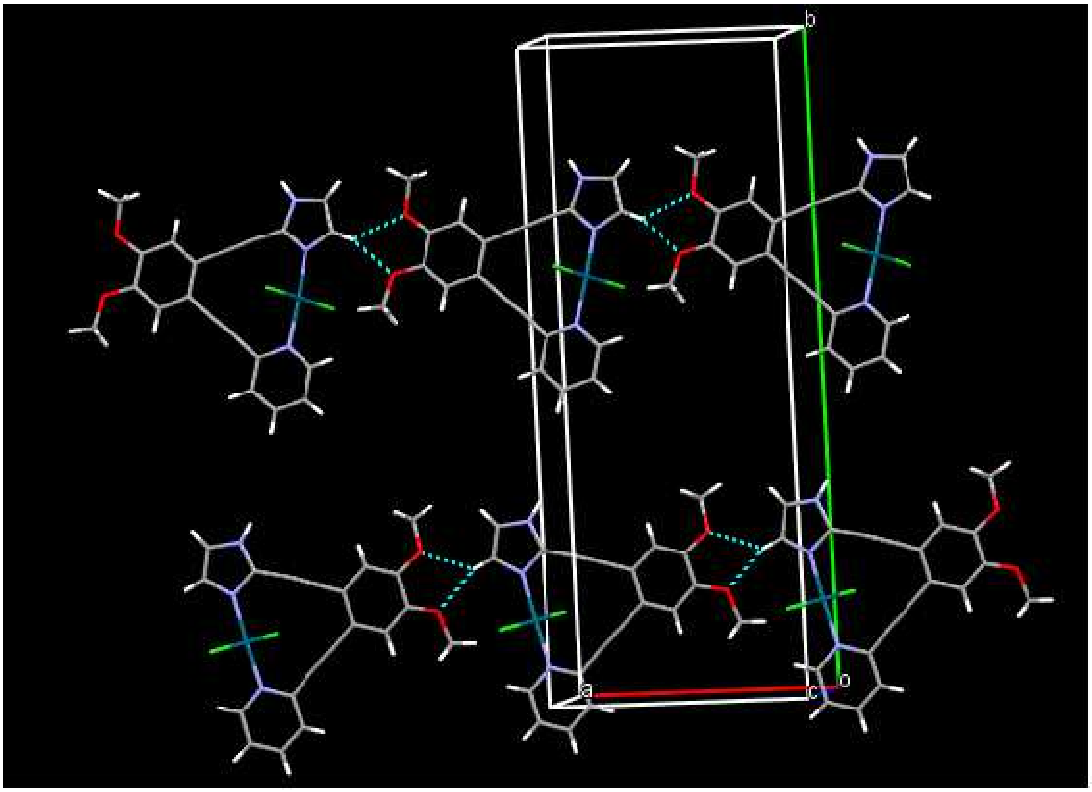

Figure 39**.** Side-by-side projection of complexes of **13.**PdCl$_2$ to form planar sheets.

There is a nonconventional C-H---O hydrogen bond that helps to stabilize adjacent complexes to form planar sheets as shown in Figure 39. The nonconventional hydrogen bond has a H17---O1 bond distance of 2.570 Å which corresponds to 94% of the sum of the van der Waals radii of 2.72 Å.

Conclusion

A novel ditopic ligand, 4-[(2-imidazylethynyl)]-5-(2-pyridylethynyl) veratrole capable of *trans*-coordination has been synthesized and well characterized. In a manner similar to 1,2-bis(2′ pyridylethynyl)benzene, this ligand also formed a trans- 1:1 complex with both silver(I) and palladium(II) cations. The 1:1 complex formation with both Pd(II) and Ag(I) was verified by elemental analysis along with NMR titration. In addition, I characterized the complex formed between the ligand and palladium(II) by single crystal X-ray analysis. The palladium(II) complex is essentially planar and the complexation accorded with my initial expectations. As part of my studies, I characterized three iodoimidazole by X-ray crystallography. Each compound exhibited halogen bonding: one of the compounds, 1-benzyl-2-iodoimidazole, exhibited a strong C-I----N halogen bond while the other two, 1-benzyl-2-iodo-1H-benzimidazole and 1-benzyl-4-iodoimidazole, showed strong C-I---π bonding in addition to other weak interactions.

EXPERIMENTAL

Chemicals

Dichloromethane, hexanes, ethylacetate, iodine, sodium carbonate, ammonium chloride (NH_4Cl), sodium bicarbonate and potassium hydroxide were purchased from Fisher Scientific Inc. Dichlorobis(triphenylphosphine)palladium(II) was purchased from Pressure Chemical Co. Tetrahydrofuran (THF), benzyl bromide, imidazole, benzimidazole, 2-iodoimidazole, 1,2-dimethoxybenzene (veratrole), potassium carbonate, silver(I) trifluoromethanesulfonate (AgOTf), anhydrous sodium sulfate (Na_2SO_4), deuterated chloroform ($CDCl_3$), N,N-dimethylformamide (DMF), deuterated DMF, acetonitrile (CH_3CN), copper iodide, anhydrous triethylamine, trifluoroacetic acid (TFA), n-butyllithium (n-BuLi) and sodium hydride (NaH) were purchased from Sigma Aldrich. 4(5)-iodoimidazole was purchased from Alfa Aesar. Trimethylsilylacetylene was purchased from Matrix Scientist. Periodic acid and 2-ethynylpyridine were purchased from GFS chemicals. 1-(trimethylsilyl ethoxy methyl) chloride (SEMCl) was purchased from TCI America. Dichlorobis(acetonitrile)palladium(II) was purchased from Strem chemicals. Ethanol was purchased from Pharmaco-Aaper. All chemicals were used as received.

Instrumentation

^1H and ^{13}C NMR spectra were recorded on Varian 400 MHz Unity INOVA spectrometer using tetramethylsilane (TMS) as the internal standard. Melting point data were obtained using an SRS Digimelt MPA 160 melting point apparatus. All elemental analyses were performed by Atlantic Microlab Inc. Column chromatography was carried out using 230-400-mesh silica gel and used as received. For single crystal X-ray determination, each single crystal was mounted on a Kryoloop using a viscous paraton hydrocarbon oil. Data were collected using a Bruker ApexII CCD diffractometer equipped with Mo Kα radiation with $\lambda = 0.71073$ Å. Data collection at 100 K was facilitated by use of a Kryoflex system with an accuracy of ±1 K. Initial data processing was carried out using the Apex II software suite.[64] Structures were solved by direct methods using SHELXS-2013 and refined against F*2* using SHELXL-2013[65] with the program X-Seed as a graphical interface**.**[66] For compound **13**, the hydrogen atom involved in intramolecular hydrogen-bonding was located by difference methods and freely refined after initial restraint with distance N-H = 0.88 Å with Uiso(H) = -1.2 Ueq(N). All other hydrogen atoms were not located in the difference maps but were placed in idealized positions and refined with a riding model. For complex **13**.$PdCl_2$, highly disordered solvent was removed from the refinement using the program PLATON SQUEEZE.[67] Two voids each corresponding to 211 Å*3* and 55 ē were identified. It is reasonable that each void corresponds to two acetonitrile molecules along with a water molecule. Crystallographic details are collected in Table 3.

Synthesis of 1-benzylimidazole, 1

The titled compound was synthesized according to the procedure by Salvio et al.[44] Thus, K_2CO_3 (2g, 14.5 mmol) and imidazole (12.5g, 36.8 mmol) were added to a solution of benzyl bromide (0.9mL, 7.57mmol) in anhydrous acetonitrile (100 mL) in a 250 mL round bottom flask. The entire mixture was refluxed for 2 h. The reaction mixture was cooled, the solid was filtered off and the solvent was removed *in vacuo*. The residue was dissolved in CH_2Cl_2 (100 mL) and the organic layer washed with saturated Na_2CO_3 solution (50 mL x 4) and dried over Na_2SO_4. The solvent was removed under reduced pressure to give **1** as a colorless oil which crystallized into white needles after 30 mins. (1.20 g, 93% yield). Mp: 69-72 °C. ^1H NMR (400 MHz, $CDCl_3$): δ 7.54 (s, 1 H), 7.32-7.35 (m, 3 H), 7.13-7.16 (m, 2 H), 7.09 (s, 1 H), 6.90 (s, 1 H), 5.11 (s, 2 H).

Synthesis of 1-benzyl-2-iodo-1H-imidazole, 2

1-benzyl-1H-imidazole (2 g, 12.64 mmol) and anhydrous THF (35 mL) were combined in a 3-necked 250 mL round bottom flask under argon. The mixture was cooled to -78 °C and stirred at this temperature for 7 mins. n-Butyllithium (1.6 M, 8 mL, 12.64 mmol, 1 equiv.) was added dropwise over 2 mins and the resultant mixture stirred at -78 °C for 45 mins. Iodine (4.81 g, 18.96 mmol, 1.5 equiv.) was crushed and added into the stirred mixture. The cooling bath was removed and the mixture stirred at room temperature for 3 h under argon. The mixture was extracted with CH_2Cl_2 (300 mL) and excess I_2 quenched with 10% Na_2SO_3 (200 mL). The organic layer was separated, washed twice with H_2O (200 mL) and twice with brine (200 mL) and then dried over Na_2SO_4. The solvent was removed *in vacuo* and the crude product purified by flash column chromatography with a 10:1 mixture of hexane and ethyl acetate as the eluent to afford **2** as a white solid (2.23 g, 62%) The solid was recrystallized from a 9:1 mixture of hexane and ethyl acetate as white needle-like crystals. $R_f = 0.27$ [Hexane/EtOAc (2:1)]. Mp: 100.5-102.9℃. ^1H NMR (400 MHz, $CDCl_3$): 7.32-7.38 (m, 3 H), 7.12-7.15 (m, 3 H), 7.01 (d, $^3J = 1.6$ Hz, 1 H), 5.10 (s, 2 H).

Synthesis of 1-benzyl-1H-benzimidazole, 3

A suspension of NaH (60% in mineral oil, 1.53 g, 37.71 mmol) in hexane (20 mL) was stirred under argon for 5 mins. After removal of the supernatant solution, anhydrous THF (20 mL) was then added. The mixture was cooled to 0 °C and a solution of benzimidazole (3.6 g, 30.47 mmol) in THF (24 mL) was added to the resulting NaH suspension and the mixture stirred at room temperature for 40 mins. The mixture was again cooled to 0 °C, followed by addition of benzyl bromide (3.8 mL, 5.47 g, 31.99 mmol). The entire mixture was stirred at 0 °C for 20 mins and then at room temperature for 15 mins. The reaction was quenched with saturated NH_4Cl (40 mL) and the solvent removed under reduced pressure. The residue was extracted with CH_2Cl_2 (2 x 40 mL), subsequently washed with H_20 (20 mL), brine (20 mL), dried over Na_2SO_4 and concentrated under reduced pressure. The crude product was purified by flash column chromatography with a mixture of 10:1 hexane and ethylacetate as the eluent. The product was isolated as an off-white solid (4.64g, 72%) which was then recrystallized from 3:2 hexane/EtOAc mixture. $R_f = 0.45$ [hexane/EtOAc 1:1)]. Mp: 116.5-117.8°C. ^{1}H NMR (400 MHz, $CDCl_3$) δ: 7.95 (s, 1H), 7.83 (d, $^3J = 8.4$ Hz, 1 H), 7.35-7.23 (m, 6 H), 7.18 (d, $^3J = 6.4$ Hz, 2 H), 5.36 (s, 2 H).

Synthesis of 1-benzyl-2-iodo-1H-benzimidazole, 4

1-benzyl-1H-benzimidazole (4 g, 19.21 mmol) and anhydrous THF (60 mL) were combined in a flask under argon. The mixture was cooled to -78 °C and stirred at this temperature for 10 mins. n-Butyllithium (1.6 M, 12 mL, 19.21 mmol, 1 equiv.) was added slowly over 2 mins. The mixture was left to stir at -78 °C for 45 mins. I_2 (7.31 g, 28.81 mmol, 1.5 equiv.) was crushed and added into the mixture. The entire mixture was stirred at room temperature for 3 h under argon. The mixture was then extracted with CH_2Cl_2 (300 mL) and excess I_2 was quenched with 10% Na_2SO_3 (200 mL). The organic layer was washed with H_2O (200 mL), brine (100 mL x 2), and dried over Na_2SO_4. The solvent was removed *in vacuo* and the crude product purified by flash column chromatography with a 10:1 mixture of hexane and ethylacetate as the eluent. The product was isolated as a white solid (3.51g, 54%). This solid was then recrystallized from (hexane/EtOAc: 3/2) to afford white crystals. $R_f = 0.81$ [Hexane/EtOAc (1:1)]. Mp: 121-122°C. ^{1}H NMR (400 MHz, $CDCl_3$) δ: 7.76 (dt, $^3J = 7.8$ Hz, $^4J = 1.2$ Hz, 1 H), 7.34-7.13 (m, 1 H), 7.35-7.23 (m, 8 H), 5.36 (s, 2 H).

Synthesis of 1-benzyl-4-iodo-1H-imidazole, 5

A suspension of NaH (60% in mineral oil, 0.401 g, 10.0 mmol) in hexane (8 mL) was stirred under argon for 5 mins. After removal of the supernatant solution, anhydrous THF (10 mL) was then added. The mixture was cooled to 0 °C and a solution of 4(5)-iodo-1H-imidazole (1.48 g, 7.64 mmol) in THF (7 mL) was added to the resulting NaH suspension. The entire mixture was stirred at room temperature for 40 mins. The mixture was again cooled to 0 °C, followed by addition of benzyl bromide (0.95 mL, 1.37 g, 7.99 mmol). The entire mixture was again stirred at 0 °C for 20 mins and at room temperature for another 20 mins. The reaction was quenched with saturated NH_4Cl (30 mL) and solvent removed *in vacuo*. The residue was extracted with CH_2Cl_2 (2 x 50 mL), and the solution was subsequently washed with H_20 (60 mL), brine (100 mL), and dried over Na_2SO_4. The solvent was removed *in vacuo* and the product obtained as a yellow oil

(2.54 g, 100 %). The crude product was isomerized by reaction with a slight excess of benzyl bromide. Thus 2.54 g of the product was dissolved in DMF (20 mL) and benzyl bromide (0.1 mL, 10 mol%) was added. The mixture was stirred at 75 °C for 24 h. The reaction was quenched with H_2O (2 mL), and dissolved in CH_2CL_2 (200 mL). DMF was removed by washing the organic layer with H_2O (7 x 200 mL). The organic layer was separated, dried over Na_2SO_4 and the solvent removed *in vacuo.* The product was recrystallized from (CH_3CN/EtOH: 1:2) to give yellow crystals. Mp: 97-102 ℃. ^1H NMR (400 MHz, $CDCl_3$) δ: 7.44 (s, 1 H), 7.34-7.38 (m, 3 H), 7.17 (dd, $^3J = 7.8$ Hz, $^4J = 2.0$ Hz, 2 H), 6.97 (s, 1 H), 5.08 (s, 2H).

Synthesis of 1-[[2-(trimethylsilyl)ethoxy]methyl]-imidazole, 6

A suspension of NaH (60% in mineral oil, 0.68 g, 16.94 mmol) in hexane (15 mL) was stirred under argon for 5 mins. After removal of the supernatant solution, anhydrous THF (14 mL) was then added. The mixture was cooled to 0 °C and a solution of imidazole (1.058 g, 15.4 mmol) in THF (6 mL) was added to the resulting NaH suspension. The mixture was then stirred at 0 °C for 5 mins and then at room temperature for 30 mins. The mixture was again cooled to 0 °C, followed by addition of 1-(trimethylsilylethoxy methyl) chloride (2.86 mL, 16.17 mmol 1.05 eq.). The entire mixture was stirred at 0 °C for 30 mins. The reaction was then quenched with saturated NH_4Cl (50 mL) and THF was removed under reduced pressure. The residue was extracted with CH_2Cl_2 (50 mL x 5), and subsequently washed with H_2O (60 mL) and brine (60 mL). The organic layer was then dried over Na_2SO_4 and the solvent removed under reduced pressure. The product was obtained as a colorless oil (3.25 g, 100%). ^1H

NMR (400 MHz, $CDCl_3$): δ 7.48 (s, 1 H), 6.94 (d, ^3J = 11.6 Hz, 1 H), 5.15 (s, 2 H), 3.35 (t, ^3J = 8.4 Hz, 2 H), 0.87 (t, ^3J = 8.4 Hz, 2 H), -0.14 (s, 9 H).

Synthesis of 1-[[2-(trimethylsilyl)ethoxy]methyl]-2-iodoimidazole, 7

1-[[2-(Trimethylsilyl)ethoxy]methyl]-imidazole (3 g, 15.46 mmol) and anhydrous THF (30 mL) were combined in a flame dried flask under argon. The mixture was cooled to -78 °C and stirred at this temperature for 10 mins. n-Butyllithium (1.6 M, 11.4 mL, 18.23 mmol, 1.2 equiv.) was added slowly over 2 mins. The mixture was stirred at -78 °C for 1 h. I_2 (4.95 g, 19.64 mmol, 1.5 equiv.) was crushed and added into the mixture, and the entire mixture was then stirred at room temperature for 3 h under argon. The mixture was extracted with CH_2Cl_2 (100 mL) and excess I_2 was quenched with 10% Na_2SO_3 (200 mL). The organic layer was separated, washed with H_2O (200 mL), brine (100 mL x 2), and dried over Na_2SO_4. The solvent was removed *in vacuo* and the crude product purified by flash column chromatography with a 10:1 mixture of ethylacetate and hexane as the eluent. The product was obtained as a yellow oil (2.75 g, 56%). R_f = 0.4 [Hexane/EtOAc (2:1)]. ^{1}H NMR (400 MHz, $CDCl_3$): δ 7.11 (d, ^3J = 1.6 Hz, 1 H), 7.068 (d, ^3J = 0.8 Hz, 1 H), 5.18 (s, 2 H), 3.48 (t, ^3J = 8.4 Hz, 2 H), 0.87 (t, ^3J = 8.4 Hz, 2 H), -0.06 (s, 9 H). ^{13}C NMR (100 MHz, $CDCl_3$): δ 133.1, 123.5, 110.9, 72.7, 66.7, 17.9, -1.2.

Synthesis of 1-[[2-(trimethylsilyl)ethoxy]methyl]-2-[2 (trimethylsilyl)ethynyl]imidazole, 8

1-[[2-(Trimethylsilyl)ethoxy]methyl]-2-iodoimidazole (2 g, 6.17 mmol) and triethylamine (15 mL) were added to a pressure flask under argon. $PdCl_2(PPh_3)_2$ (100 mg, 0.14 mmol), copper iodide (45 mg, 0.24 mmol) and trimethylsilyl acetylene (1.77 g, 2.5 mL, 18.20 mmol) were then added into the flask. Argon flow was removed and the pressure flask sealed. The mixture was heated to 60 °C for 40 h. The reaction mixture was then cooled to room temperature and the solvent was removed *in vacuo*. The residue was dissolve in CH_2Cl_2 (100 mL), washed with brine (80 mL x 2) and dried over Na_2SO_4. The solvent was again removed under reduced pressure, and the crude product purified by flash column chromatography with a mixture of 20:1 hexane and ethylacetate as the eluent. The product was obtained as a yellow oil (0.812 g, 44%). $R_f = 0.3$ [EtOAc/hexane (2:1)]. ^1H NMR (400 MHz, $CDCl_3$): δ 7.04 (d, $^3J = 3.2$ Hz, 2 H), 5.34 (s, 2 H), 3.43 (t, $^3J = 8.4$ Hz, 2 H), 0.87 (t, $^3J = 8.4$ Hz, 2 H), - 0.12 (s, 9 H), -0.06 (s, 9 H).

Synthesis of 1-{[2-(trimethylsilyl)ethoxy]methyl}-2-ethynylimidazole, 9

A solution of potassium hydroxide (0.3 g, 5.35 mmol) in water (0.5 mL) was added to a solution of compound **8** (0.812g, 2.72 mmol) in ethanol (10 mL) in a round bottom flask. The mixture was stirred at room temperature and the reaction monitored by TLC. After 2 h, the solvent was evaporated, and the residue was dissolved in CH_2Cl_2 (60 mL), washed with brine (50 mL x 2) and dried over Na_2SO_4. The solvent was remove *in vacuo* and the crude product purified by flash column chromatography with a mixture of 10:1 hexane and ethylacetate as the eluent. The product was obtained as a yellow oil (0.390 g, 65%). $R_f = 0.3$ [hexane/EtOAc (2:1)]. ^1H NMR (400 MHz, $CDCl_3$): δ 7.05 (d, $^3J = 3.2$ Hz, 2 H), 5.37 (s, 2 H), 3.50 (t, $^3J = 8.4$ Hz, 2 H), 3.32(s, 1 H), 0.87 (t, $^3J = 8.4$ Hz, 2 H), -0.06 (s, 9 H). ^{13}C NMR (100 MHz, $CDCl_3$): δ 131.1, 130.1, 120.5, 88.5, 81.5, 75.2, 72.9, 66.5, 17.6, -1.5.

Synthesis of 1,2-diiodo-4,5-dimethoxy benzene (1,2-diiodo veratrole), 10

Periodic acid (5.84 g, 25.6 mmol, 0.41 equiv.) and methanol (36 mL) were combined in a flame dried 100 mL round bottom flask. Iodine (12.86 g, 51.0 mmol, 0.8 equiv.) was then added and the mixture was stirred for 10 mins. 1,2-dimethoxybenzene (veratrole) (7.9 mL, 8.57 g, 62.0 mmol) was then added into the reaction mixture and it was heated to 70 °C for 5 h. The mixture gradually changed from an orange solution to a cloudy solution. The hot solution was poured into a 5% solution of sodium sulfite (100 mL). The solid was filtered off and washed quickly with cold methanol (30 mL x 2). The solid residue obtained, was dried overnight in the fume hood. The product (21.92 g, 91%) was then recrystallized from 2:1 mixture of hexane and ethyl acetate to give pure white crystals. Mp: 134-136 °C. ^{1}H NMR (400 MHz, $CDCl_3$): δ 7.24 (s, 2 H), 3.84 (s, 6 H). ^{13}C NMR (100 MHz, $CDCl_3$): δ 149.7, 121.8, 96.2, 56.3.

Synthesis of 4-iodo-5-(2-ethynylpyridine) veratrole, 11

1,2-diiodo veratrole (5.00 g, 12.8 mmol), $PdCl_2(PPh_3)_2$ (0.100 g, 0.14 mmol), CuI (0.092 g, 0.49 mmol), 2-ethynylpyridine (0.7 ml, 0.660 g, 6.4 mmol), THF (30 mL) and triethylamine (10 mL) were reacted under argon atmosphere at room temperature for 4 days. The mixture was diluted with ethyl acetate (200 mL) and washed with water (100 mL x 3) followed by brine (100 mL x 3). The organic layer was separated, dried over Na_2SO_4, filtered and solvent removed *in vacuo*. The crude solid was purified by flash column chromatography with a 5:1 mixture of hexane and ethylacetate as the eluent. The product was obtained as a brown oil which solidified after 2 days (1.44, 3.94 mmol, 62%). $R_f = 0.27$ [EtOAc/hexane (2:1)]. Mp: 89.5-90.1 °C. ^{1}H NMR (400 MHz, $CDCl_3$):

δ = 8.64 (d, ^{3}J= 4.8 Hz, 1 H), 7.74 (td, ^{3}J = 7.8 Hz, ^{4}J = 2.0 Hz, 1 H), 7.64 (d, ^{3}J = 7.8 Hz, 1 H), 7.28 (m, 2 H), 7.26 (s, 1 H), 3.90 (s, 3 H), 3.88 (s, 3 H). ^{13}C NMR (100 MHz, $CDCl_3$): δ = 150.5, 149.8, 149.2, 143.2, 136.8, 127.6, 123.1, 121.1, 121.0, 115.6, 92.5, 90.6, 90.2, 56.4, 56.3. 1,2-Bis(2-pyridylethynyl) veratrole was also isolated as a brown solid (0.612 g, 1.8 mmol, 26%).

Synthesis of 4-[1-(2-trimethylsilylethoxymethyl)]-1H-imidazylethynyl [5-(2pyridylethynyl)] veratrole, 12

Compound **9** (0.41 g, 1.85 mmol) and compound **11**, (1.24 g, 3.38 mmol) were reacted in triethylamine (3 mL) and THF (5 mL) with $PdCl_2(PPh_3)_2$ (100 mg, 0.14 mmol) and CuI (45 mg, 0.24 mmol) as the catalyst under argon at 60 °C for 24 h. The mixture was cooled to room temperature, diluted with CH_2Cl_2 (100 mL) and washed with brine (50 mL x 2). The organic layer was separated, dried over Na_2SO_4, and solvent removed *in vacuo*. The crude product was purified by flash column chromatography with a 1:1 mixture of hexane and ethylacetate as the eluent. The product was obtained as a red oil, which solidified after 5 days (0.3895 g, 46%). R_f = 0.30 [EtOAc/hexane (2:/1)]. Mp: 110.8-111.9 °C. ^{1}H NMR (400 MHz, $CDCl_3$): δ 8.65 (d, ^{3}J = 4.8 Hz, 1 H), 7.66 (td, ^{3}J = 7.8 Hz, ^{4}J = 2.0, Hz, 1 H), 7. 55 (d, ^{3}J = 7.8 Hz, 1 H), 7.23 (ddd, ^{3}J = 7.8 Hz, 5.0 Hz, ^{4}J = 1.2 Hz, ^{5}J = 1.2 Hz, 1 H), 7.18 (s, 1 H), 7.08 (d, ^{3}J = 1.2 Hz, 3 H), 5.52 (s, 2 H), 3.89 (s, 6 H, OCH_3), 3.49 (t, ^{3}J = 8.4Hz, 2 H), 0.76 (t, ^{3}J = 8.4 Hz, 2 H), -0.15 (s, 9 H). ^{13}C NMR (100 MHz, $CDCl_3$): δ = 150.2, 149.8, 149.7, 143.3, 136.3, 132.5, 130.7, 127.3, 123.0, 120.3, 117.7, 117.6, 114.7, 114.3, 91.7, 91.6, 88.1, 81.5, 75.6, 66.6, 56.2, 17.7, -1.4.

Synthesis of 4-[(2-imidazylethynyl)]-5-(2-pyridylethynyl) veratrole, 13

Trifluoroacetic acid (4.3 mL) was added to a solution of **12** (100 mg, 0.27 mmol) in THF (0.6 mL). The mixture was stirred at room temperature and monitored by TLC. After 7 h, trifluoroacetic acid was removed *in vacuo* and the crude product dissolved in CH_2Cl_2 (50 mL). Residual acid was neutralized by stirring the mixture in a saturated solution of $NaHCO_3$ (10 mL). The organic layer was separated, washed with brine (40 mL), and dried over Na_2SO_4. The solvent was removed under reduced pressure and the crude product was then purified by preparative-TLC with a 5:1 mixture of ethylacetate/ hexane ($R_f = 0.45$). The product was isolated as a brown solid (36 mg, 0.11 mmol, 50%) and recrystallized from a 1:1 mixture of acetonitrile and dichloromethane to afford brown crystals and the crystal structure was determined by Dr. Eric Bosch. Mp: 185.1-186.9 ^{o}C. ^{1}H NMR (400 MHz, $CDCl_3$): δ 8.58 (d, $^3J = 4.4$ Hz, 1 H), 7.74 (td, $^3J = 7.8$ Hz, $^4J = 1.6$ Hz, 1 H), 7. 55 (d, $^3J = 7.8$ Hz, 1 H), 7.30 (ddd, $^3J = 7.6$ Hz, $^4J = 4.8$ Hz, $^5J = 1.2$ Hz, 1 H), 7.15 (s, 2 H), 7.02 (d, $^3J = 2.0$ Hz, 2 H), 3.90 (s, 3 H), 3.89 (s, 3 H). ^{13}C NMR (100 MHz, $CDCl_3$): δ 150.2, 149.4, 149.2, 143.0, 137.3, 131.0, 127.2, 123.2, 120.1, 118.0, 113.5, 112.6, 91.8, 90.0, 89.0, 85.4, 56.3. Anal. Calcd. for $C_{20}H_{15}N_3O_2$: C, 72.94; H, 4.59; N, 12.76. Found: C, 72.74; H, 4.52; N, 12.63.

Synthesis of {4-[(2-imidazylethynyl)]-5-(2-pyridylethynyl) veratrole} silver trifluoroacetate

The ligand, **13** (0.0030 g, 0.0091 mmol) was dissolved in CH_3CN (2 mL), and the solution was combined with a separate solution of CF_3COOAg (0.0024 g, 0.0091 mmol) CH_3CN (0.3 mL) in a vial. The vial was loosely capped and placed in the fume hood.

After 10 days, colorless crystals were harvested (1.8 mg, 35%). ^{1}H NMR (400 MHz, DMF-d_7): δ 8.58 (dt, ^3J = 5.2 Hz, ^4J = 0.8 Hz, 1 H), 8.26 (td, ^3J = 7.8 Hz, ^4J = 1.6 Hz, 1 H), 8.05 (s, 1H), 7.79 (ddd, ^3J = 7.6 Hz, ^4J = 5.1 Hz, ^5J = 1.6 Hz, 1 H), 7.71 (s, 1 H), 7.54 (s, 1 H), 7.29 (s, 1 H), 7.19 (s, 1 H), 4.00 (s, 3H, OCH_3), 3.99 (s, 3H, OCH_3). Anal. Calcd. for $C_{22}H_{15}AgF_3N_3O_4.H_2O$: C, 46.50; H, 2.87; N, 7.13. Found: C, 46.50; H, 3.02; N, 7.39.

Synthesis of {4-[(2-imidazylethynyl)]-5-(2-pyridylethynyl) veratrole} palladium (II) dichloride

The ligand, **13** (0.0030 g, 0.0091 mmol) was dissolved in anhydrous CH_3CN (2 mL), and the solution was added to a separate solution of $PdCl_2(CH_3CN)_2$ (0.0024 g, 0.0091 mmol) in CH_3CN (0.3 mL) in a vial. The vial was capped and placed in the hood. Yellow crystals were harvested after 5 days (2.2 mg, 54 %) and the crystal structure was solver by Dr. Eric Bosch. ^{1}H NMR (400 MHz, DMF-d7): δ 8.58 (d, 1 H), 8.06 (td, ^3J = 7.8 Hz, ^4J = 1.6 Hz, 1 H), 7. 87 (d, ^3J = 7.8 Hz, 1 H), 7.62 (m, 1 H), 7.54 (m, 2H) 7.27 (t, ^3J = 1.56 Hz, 1 H), 7.24 (s, 1 H), 4.03 (s, 3H, OCH_3), 4.02 (s, 3H, OCH_3). Anal. Calcd. for $C_{20}H_{15}Cl_2N_3O_2Pd$: C, 47.41; H, 2.98; N, 8.29. Found: C, 47.26; H, 3.14; N, 8.49.

Titration of ligand,13 with silver(I) triflate

A solution of ligand, **13** (9 mg, 0.027 mmol) in DMF-d_7 (0.9 mL, 30.36 mM) was carefully transferred into a clean and dry NMR tube. A solution of CF_3SO_3Ag was then prepared in a vial by dissolving CF_3SO_3Ag (78 mg, 0.30 mmol) in DMF-d7 (0.9 mL, 337.29 mM). Thereafter, the ^{1}H NMR spectrum of the ligand was collected and then the titration begun. 10 μL aliquot of the CF_3SO_3Ag solution was added to the NMR tube containing the ligand. The mixture was vortexed to ensure homogeneity and the ^1H NMR spectrum collected at 32 scans. Injection of 10 μL of CF_3SO_3Ag into the tube and collection of ^1H NMR spectrum continued until no significant change in the chemical shift of the ligand protons were observed (150 μL was added in total).

Titration of ligand, 13 with bis(acetonitrile)palladium(II) dichloride

A solution of ligand, **13** (9 mg, 0.027 mmol) in DMF-d_7 (0.9 mL, 75.71 mM) was carefully transferred into a clean and dry NMR tube. A solution of $PdCl_2(CH_3CN)_2$ was then prepared in a vial by dissolving $PdCl_2(CH_3CN)_2$ (78 mg, 0.30 mmol) in DMF-d_7 (0.9 mL, 759.04 mM). Thereafter, the ^1H NMR spectrum of the ligand was collected and then the titration begun. 20 μL aliquot of the $PdCl_2(CH_3CN)_2$ solution was added to the NMR tube containing the ligand. The mixture was vortexed to ensure homogeneity and the ^1H NMR spectrum collected at 32 scans. Injection of 20 μL into the tube and collection of ^1H NMR spectrum continued until proton peaks associated with the ligand protons completely disappeared (100 μL was added in total).

REFERENCES

(1) Correa, A.; García Mancheño, O.; Bolm, C. *Chem. Soc. Rev.* **2008**, *37*, 1108-1117.

(2) Wilkinson, M. J.; van Leeuwen, P. W. N. M.; Reek, J. N. H. *Org. Biomol. Chem.* **2005**, *3*, 2371-2383.

(3) Paterson, B. M.; Karas, J. A.; Scanlon, D. B.; White, J. M.; Donnelly, P. S. *Inorg. Chem.* **2010**, *49*, 1884–1893.

(4) Kilpin, K. J.; Gavey, E. L.; McAdam, C. J.; Anderson, C. B.; Lind, S. J.; Keep, C. C.; Gordon, K. C.; Crowley, J. D. *Inorg. Chem.* **2011**, *50*, 6334–6346.

(5) Halcrow, M. A. *Dalt. Trans.* **2009**, *36*, 2059-2053.

(6) Lee, M. H.; Wu, J.-S.; Lee, J. W.; Jung, J. H.; Kim, J. S. *Org. Lett.* **2007**, *9*, 2501–2504.

(7) Burdette, S. C.; Frederickson, C. J.; Bu, W.; Lippard, S. J. *J. Am. Chem. Soc.* **2003**, *125*, 1778–1787.

(8) http://pubs.acs.org/page/vi/Ligand-design.html.

(9) Bosch, E.; Barnes, C. L. *Inorg. Chem.* **2001**, *40*, 3097–3100.

(10) Hu, L.; Kim, H. S.; Lee, J. Y.; Peumans, P.; Cui, Y. *ACS Nano.* **2010**, *4*, 2955–2963.

(11) Langley, D.; Giusti, G.; Mayousse, C.; Celle, C.; Bellet, D.; Simonato, J.-P. *Nanotechnology* **2013**, *24*, 452001-452013.

(12) Doudoroff, P.; Katz, M. *Sewage Ind. Waste* **1953**, *25*, 802–839.

(13) Albright, L. J.; Wentworth, J. W.; Wilson, E. M. *Water Res.* **1972**, *6*, 1589–1596.

(14) Coleman, R. L.; Cearley, J. E. *Bull. Environ. Contam. Toxicol.* **1974**, *12*, 53–61.

(15) Shafer, M. M.; Overdier, J. T.; Armstong, D. E. *Environ. Toxicol. Chem.* **1998**, *17*, 630–641.

(16) Hogstrand, C.; Galvez, F.; Wood, C. M. *Environ. Toxicol. Chem.* **1996**, *15*, 1102–1108.

(17) Eisler, R. *US Fish and Wildlife Service Report* **1988**, *85*, 1–14.

(18) Ratte, H. T. *Environ. Toxicol. Chem.* **1999**, *18*, 89–108.

(19) Thaler, A.; Cox, B.; Schneider, H. *Inorganica Chim. Acta* **2003**, *351*, 123–132.

(20) Abul Haj, M.; Aakeröy, C. B.; Desper, J. *New J. Chem.* **2012**, *1*, 204–211.

(21) Hirsch, K. A.; Venkataraman, D.; Wilson, S. R.; Moore, J. S.; Lee, S. *J. Chem. Soc., Chem. Commun.* **1995**, *44*, 2199–2200.

(22) Venkataraman, D.; Lee, S.; Moore, J. S.; Zhang, P.; Hirsch, K. A.; Gardner, G. B.; Aaron, C.; Covey, P.; Christine, L. *Chem. Mater.* 1**996**, *8*, 2030-2040.

(23) Young, A. G.; Hanton, L. R. *Coord. Chem. Rev.* **2008**, *252*, 1346–1386.

(24) Chen, C. Y.; Zeng, J. Y.; Lee, H. M. *Inorganica Chim. Acta* **2007**, *360*, 21–30.

(25) Kristiansson, O. *Acta Crystallogr. Sect. C Cryst. Struct. Commun.* **2000**, *56*, 165–167.

(26) Zhang, X.-Y.; Cheng, L.; Wang, J.; Gou, S.-H.; Fang, L. *Inorg. Chem.Comm.* 2**014**, *40*, 97-102.

(27) Beccalli, E. M.; Broggini, G.; Martinelli, M.; Sottocornola, S. *Chem Rev.* 2**007**, *205,* 5318-5365.

(28) Kielhorn, J.; Melber, C.; Keller, D.; Mangelsdorf, I. *Int. J. Hyg. Environ. Health* **2002**, *205*, 417–432.

(29) Schroeder, H. A.; Mitchener, M. *J. Nutr.* **1971**, *101*, 1431–1437.

(30) Birkholz (née Gensow), M.-N.; Freixa, Z.; van Leeuwen, P. W. N. M. *Chem. Soc. Rev.* **2009**, *38*, 1099-1118.

(31) Xiaoli Tang, L. Z. *Open J. Inorg. Chem.* **2013**, *3*, 71–75.

(32) Constable, E. C. *Adv. Inorg. Chem*. **1989**, *34*, 1–63.

(33) McWhinnie, W. R.; Miller, J. D. *Adv. Inorg. Chem. Radiochem.* **1969**, 12, 135–215.

(34) Schilt, A. *Analytical applications of 1, 10-phenanthroline and related compounds,* [1st ed.].; Pergamon Press: Oxford; New York, **1969**.

(35) Kröhnke, F. *Synthesis* **1976**, *1*, 1–24.

(36) Hu, Y. Z.; Chamchoumis, C.; Grebowicz, J. S.; Thummel, R. P. *Inorg. Chem.* **2002**, *41*, 2296–2300.

(37) Fiscus, J. E.; Shotwell, S.; Layland, R. C.; Smith, M. D.; Zur Loye, H.-C.; Bunz, U. H. F. *Chem. Commun.* **2001,** *0* 2674–2675.

(38) Kawano, T.; Shinomaru, T.; Ueda, I. *Org. Lett.* **2002**, *4*, 2545–2547.

(39) Suzaki, Y.; Shimada, K.; Chihara, E.; Saito, T.; Tsuchido, Y.; Osakada, K. *Org. Lett.* **2011**, *13*, 3774–3777.

(40) Atobe, S.; Sonoda, M.; Suzuki, Y.; Yamamoto, T.; Masuno, H.; Shinohara, H.; Ogawa, A. *Res. Chem. Intermed.* **2013**, *39*, 359–370.

(41) Clearfield, A.; Bortun, A. I.; Bortun, L. N.; Cahill, R. *Solvent Extr. Ion Exch.* **1997**, *15*, 285–304.

(42) Koskinen, L.; Jaaskelainen, S.; Oresmaa, L.; Haukka, M. *Crystengcomm.* **2012**, *14*, 3509–3514.

(43) Rowan, R.; Tallon, T.; Sheahan, A. M.; Curran, R.; McCann, M.; Kavanagh, K.; Devereux, M.; McKee, V. *Polyhedron* **2006**, *25*, 1771–1778.

(44) Salvio, R.; Cacciapaglia, R.; Mandolini, L. *J. Org. Chem.* **2011**, *76*, 5438–5443.

(45) Neildé, K.; Crozet, M.; Terme, T.; Vanelle, P. *Synthesis* **2013**, *45*, 1349–1356.

(46) Lyaskovskyy, V.; Fröhlich, R.; Würthwein, E.-U. *Synthesis* **2007**, *14*, 2135–2144.

(47) Pöverlein, C.; Jacobi, N.; Mayer, P.; Lindel, T. *Synthesis* **2007**, *4*, 3620–3626.

(48) Paul, D.; Wytko, J. A.; Koepf, M.; Weiss, J. *Inorg. Chem.* **2002**, *41*, 3699–3704.

(49) Das, J.; Mukherjee, R.; Basak, A. *J. Org. Chem.* **2014**, *79*, 3789–3798.

(50) Proulx, C.; Lubell, W. D. *Org. Lett.* **2012**, *14*, 4552–4555.

(51) Bhandari, M. R.; Yousufuddin, M.; Lovely, C. J. *Org. Lett.* **2011**, *13*, 1382–1385.

(52) Ray, A.; Mukherjee, S.; Das, J.; Bhandari, M. K.; Du, H.; Yousufuddin, M.; Lovely, C. J. *Tetrahedron Lett.* **2015**, *56*, 3518–3522.

(53) Honda, T.; Dinkova-Kostova, A. T.; David, E.; Padegimas, E. M.; Sundararajan, C.; Visnick, M.; Bumeister, R.; Christian Wigley, W. *Bioorg. Med. Chem. Lett.* 2**011**, 21, 2188-2191.

(54) Sivappa, R.; Mukherjee, S.; Dias, H. V. R.; Lovely, C. J.; Shima, H.; Kikuchi, K.; Mikami, Y.; Fromont, J.; Kobayashi, J. *Org. Biomol. Chem.* **2009**, *7*, 3215-3218.

(55) Bhandari, M. R.; Sivappa, R.; Lovely, C. J. *Org. Lett.* **2009**, *11*, 1535–1538.

(56) Bondi, A. *J. Phys. Chem.* **1964**, *68*, 441–451.

(57) Nwachukwu, C. I.; Bowling, N. P.; Bosch, E. *Acta Crystallogr. Sect. C Struct. Chem.* **2017**, *73*, 2–8.

(58) Dubowchik, G. M.; Padilla, L.; Edinger, K.; Firestone, R. A. *J. Org. Chem.* 1**996**, *61,* 4676-4684.

(59) Knapp, S.; Albaneze, J.; Schugar, H. J. J. Org. Chem. **1993**, 58, 997–998.

(60) Lacour, J.; Monchaud, D.; Mareda, J.; Favarger, F.; Bernardinelli, G. Helv. Chim. Acta **2003**, 86, 65–81.

(61) Shotwell, S.; Windscheif, P. M.; Smith, M. D.; Bunz, U. H. F. Org. Lett. **2004**, 6, 4151–4154.

(62) Vang, H. G.; Driscoll, Z. L.; Robinson, E. R.; Green, C. E.; Bosch, E.; Bowling, N. P. European J. Org. Chem. **2016**, 5, 891–895.

(63) Shotwell, S.; Ricks, H. L.; Morton, J. G. M.; Laskoski, M.; Fiscus, J.; Smith, M. D.; Shimizu, K. D.; zur Loye, H.-C.; Bunz, U. H. F. J. Organomet. Chem. **2003**, 671, 43–51.

(64) Bruker **2014**. SMART, SAINT and SADABS. Bruker AXS Inc.,Madison, Wisconsin, USA.

(65) Sheldrick, G. M. *Acta Crystallogr. Sect. C Struct. Chem.* **2015**, *71*, 3–8.

(66) Barbour, L. J. *J. Supramol. Chem.* **2001**, 1, 189-191.

(67) Spek, A. L. *Acta Crystallogr. Sect. C Struct. Chem.* **2015**, *71*, 9–18.

APPENDICES

Appendix A: Crystal data for studied compounds

Appendix A-1. Selected bond distances and angles for compounds **2**, **4**, **5**, **13** and **13.**$PdCl_2$

Compound **2**

Bong Distances (Å)

N1---I1	2.877 (2)	C1---I1	2.088 (3)
N1---C4	1.461 (4)	C7-H4	0.9500
C6---C4	1.512 (4)	C1-N2	1.357 (4)

Bond Angles (deg)

C1-I1-N2	174.42(9)	C1-N1-C3	106.4 (2)
H2-C8-C9	120.2	N2-C2-C3	110.5 (2)

Compound **4**

Bond Distances(Å)

I1---C1	2.079 (16)	N1---C8	1.459
NI---C1	1.372 (2)	C5-H5	0.95
C9---C14	1.392	C8---H8B	0.99

Bond Angles (deg)

C1-N1-C7	105.30(13)	C1-N2-C3	103.99 (14)
N1-C8-H8B	109.1	C12-C11-C10	120.19 (16)

Compound **5**

Bond Distances (Å)

I1---C2	2.0717 (18)	N1---C4	1.467 (2)
C6---C7	1.388 (30	C10---H10	0.95

Bond Angles (deg)

N2-C1-N1	112.62 (16)	N1-C3-H3	127.4
N2-C1-H1	123.7	C2-C3-H3	127.4
C3-C2-N2	111.35 (16)	N1-C4-H4B	109.0

Appendix A-1, cont.

		Compound 13	
Bond Distances (Å)			
O1---C10	1.360 (4)	C5---C6	1.440 (4)
C1---H1	0.95	C9---C10	1.393 (4)
C5---N1	1.360 (4)	N3---C16	1.331 (4)
Bond Angles (deg)			
C2-C3-H3	120.4	N3-C18-H18	110.8 (3)
C5-C6-C7	178.7 (3)	C6-C7-C8	174.4 (3)
C13-C14-C15	172.8 (3)	C14-C15-C16	172.9 (3)
		Compound **13**.$PdCl_2$	
Bond Distances			
Pd1---N1	2.018 (3)	Pd1---Cl1	2.3185 (9)
Pd1---Cl2	2.3336 (10)	Pd1-N2	2.006 (3)
Bond Angles (deg)			
N11-Pd1-Cl1	89.27 (9)	N1-Pd1-Cl2	90.42 (9)
N2-Pd1-Cl1	91.05 (9)	N2-Pd1-Cl2	89.56 (9)
N2-Pd1-N1	176.87 (12)	Cl1-Pd1-Cl2	174.40 (4)
C5-C6-C7	174.4 (4)	C6-C7-C8	175.7 (4)
C13-C14-C15	177.9 (4)	C14-C15-C16	175.9 (4)

Appendix A-2. Crystallographic data for compounds **2**, **4**, and **5**

	Compound **2**	Compound **4**	Compound **5**
Formula	$C_{10}H_9IN_2$	$C_{10}H_9IN_2$	$C_{14}H_{11}IN_2$
Formula weight	284.09	284.09	334.15
Crystal dim. (mm^3)	0.30 x 0.20 x 0.05	0.22 x 0.22 x 0.22	0.22 x 0.22 x 0.22
Crystal system,	Orthorhombic	Monoclinic	Triclinic
Crystal color	colorless	Colorless	Colorless
space group	$P2_12_12_1$	$P2_1/n$	$P\bar{1}$
a, b, c (Å)	8.7561 (5), 9.0016 (5), 12.8869 (7)	8.4574 (5), 6.1526 (3), 19.4261 (10)	6.4606 (8), 8.2346 (10), 12.3451 (14)
α, β, γ (°)	90, 90, 90	90, 96.362 (1), 90	108.064 (1), 94.174 (2), 95.366 (2)
V ($Å^3$)	1015.73 (10)	1004.61 (9)	618.05 (13)
Z	4	4	2
ρ_{calcd} (mg m^{-3})	1.858	1.796	1.878
T(K)	100	100	100
μ (mm^{-1})	3.11	3.14	2.57
Reflections/unique	13262/2228	12374/2207	8079/2777
Data/parameters/ restraints	2228/118/0	2207/118/0	2777/154/0
R_{int}	0.030	0.021	0.016
Goodness of fit	1.052	1.105	1.090
R1/wR2	0.013/0.030	0.016/0.037	0.015/0.039
R1/wR2 (all data)	0.013/0.030	0.017/0.037	0.016/0.039
Largest diff. peak/hole/$eÅ^3$	0.25/-0.27	0.73/-0.52	0.74/-0.35

Appendix A-3. Crystallographic data for compound **13** and complex **13.**$PdCl_2$

	Compound **13**	Complex **13.**$PdCl_2$
Formula	$C_{20}H_{15}N_3O_2$	$C_{20}H_{15}Cl_2N_3O_2Pd$
Formula weight	329.35	506.65
Crystal dim. (mm^3)	0.25 x 0.21 x 0.02	0.20 x 0.15 x 0.02
Crystal system	Triclinic	Monoclinic
Crystal color	Gold	Gold
Space group	*P*-1	P 21/c
a (Å)	698 (3)	11.1420 (7)
b (Å)	9.659 (4)	27.3615 (17)
c (Å)	13.379 (6)	7.4271 (5)
α (deg)	110.387 (6),	90
β (deg)	95.185 (6),	95.878 (1)
γ (deg)	92.835 (7)	90
Z	2	4
V ($Å^3$)	804.9 (6)	2252.3 (3)
ρ_{calcd} (mg m^{-3})	1.359	1.494
T (K)	100	100
μ (mm^{-1})	0.090	1.080
Reflections/unique	10259/3576	28387/5039
Data/ parameters/restraints	3576/231/1	5039/258/0
R_{int}	0.059	0.041
Goodness of fit	0.992	1.147
R1/wR2	0.065/0.166	0.045/0.100
R1/wR2 (all data)	0.128/0.209	0.051 / 0.1021

Appendix A-4. Fractional atomic coordinates and isotropic or equivalent isotropic displacement parameters (Å^2) for compound **2**

	x	*Y*	*z*	U_{iso}*/U_{eq}
I1	0.23697 (2)	0.28234 (2)	0.52915 (2)	0.01308 (5)
N1	0.1137 (3)	0.4336 (3)	0.72457 (18)	0.0140 (5)
C1	0.0779 (3)	0.3510 (3)	0.6399 (2)	0.0126 (6)
N2	−0.0686 (3)	0.3169 (3)	0.63687 (19)	0.0153 (5)
C2	−0.1294 (3)	0.3814 (3)	0.7256 (2)	0.0175 (6)
H1	−0.2337	0.3759	0.7456	0.021*
C3	−0.0203 (3)	0.4526 (3)	0.7792 (2)	0.0173 (6)
H9	−0.0329	0.5057	0.8423	0.021*
C4	0.2632 (4)	0.4913 (3)	0.7544 (2)	0.0163 (6)
H7	0.2484	0.5859	0.7923	0.020*
H8	0.3218	0.5138	0.6906	0.020*
C5	0.3573 (3)	0.3881 (3)	0.8214 (2)	0.0145 (6)
C6	0.3217 (3)	0.2395 (3)	0.8364 (2)	0.0165 (6)
H3	0.2345	0.1980	0.8035	0.020*
C7	0.4136 (3)	0.1504 (4)	0.8995 (2)	0.0210 (7)
H4	0.3885	0.0487	0.9094	0.025*
C8	0.5407 (3)	0.2094 (4)	0.9477 (2)	0.0215 (7)
H2	0.6027	0.1487	0.9909	0.026*
C9	0.5776 (4)	0.3587 (4)	0.9327 (2)	0.0222 (7)
H5	0.6647	0.4001	0.9658	0.027*
C10	0.4869 (3)	0.4463 (3)	0.8693 (2)	0.0177 (6)
H6	0.5134	0.5474	0.8583	0.021*

Appendix A-5. Atomic displacement parameters (Å^2) for compound **2**

	U^{11}	U^{22}	U^{33}	U^{12}	U^{13}	U^{23}
I1	0.01264 (8)	0.01415 (9)	0.01244 (8)	0.00140 (7)	0.00028 (7)	−0.00020 (6)
N1	0.0139 (12)	0.0132 (12)	0.0150 (12)	0.0009 (10)	−0.0017 (10)	−0.0015 (10)
C1	0.0138 (14)	0.0102 (13)	0.0138 (14)	0.0027 (11)	−0.0002 (11)	0.0008 (11)
N2	0.0134 (11)	0.0163 (14)	0.0161 (12)	0.0017 (9)	−0.0001 (9)	0.0000 (9)
C2	0.0153 (14)	0.0183 (16)	0.0189 (15)	0.0027 (12)	0.0024 (12)	−0.0005 (12)
C3	0.0206 (16)	0.0178 (15)	0.0135 (14)	0.0043 (13)	0.0023 (13)	−0.0010 (12)
C4	0.0169 (14)	0.0147 (13)	0.0172 (12)	−0.0036 (12)	−0.0032 (15)	−0.0006 (10)
C6	0.0148 (13)	0.0173 (16)	0.0174 (13)	−0.0015 (11)	−0.0003 (11)	−0.0018 (12)
C7	0.0222 (16)	0.0204 (15)	0.0203 (15)	0.0022 (13)	0.0067 (13)	0.0026 (13)
C8	0.0211 (14)	0.0277 (17)	0.0156 (14)	0.0087 (15)	−0.0008 (11)	0.0024 (14)
C9	0.0171 (15)	0.0285 (18)	0.0210 (16)	0.0039 (14)	−0.0034 (12)	−0.0039 (14)
C0	0.0169 (15)	0.0168 (15)	0.0195 (15)	−0.0010 (12)	0.0007 (13)	−0.0037 (13)

Appendix A-6. Geometric parameters (Å, º) for compound **2**

I1—C1	2.088 (3)	C5—C6	1.387 (4)
N1—C1	1.357 (4)	C5—C10	1.394 (4)
N1—C3	1.379 (3)	C6—C7	1.397 (4)
N1—C4	1.461 (4)	C6—H3	0.9500
C1—N2	1.319 (3)	C7—C8	1.381 (4)
N2—C2	1.389 (4)	C7—H4	0.9500
C2—C3	1.341 (4)	C8—C9	1.395 (5)
C2—H1	0.9500	C8—H2	0.9500
C3—H9	0.9500	C9—C10	1.386 (4)
C4—C5	1.512 (4)	C9—H5	0.9500
C4—H7	0.9900	C10—H6	0.9500
C4—H8	0.9900		
C1—N1—C3	106.4 (2)	C6—C5—C10	118.9 (3)
C1—N1—C4	127.8 (2)	C6—C5—C4	123.4 (3)
C3—N1—C4	125.8 (2)	C10—C5—C4	117.7 (3)
N2—C1—N1	112.1 (2)	C5—C6—C7	120.4 (3)
N2—C1—I1	124.0 (2)	C5—C6—H3	119.8
N1—C1—I1	123.9 (2)	C7—C6—H3	119.8
C1—N2—C2	104.5 (2)	C8—C7—C6	120.3 (3)
C3—C2—N2	110.5 (3)	C8—C7—H4	119.8
C3—C2—H1	124.7	C6—C7—H4	119.8
N2—C2—H1	124.7	C7—C8—C9	119.7 (3)
C2—C3—N1	106.5 (3)	C7—C8—H2	120.2
C2—C3—H9	126.8	C9—C8—H2	120.2
N1—C3—H9	126.8	C10—C9—C8	119.8 (3)
N1—C4—C5	114.8 (2)	C10—C9—H5	120.1
N1—C4—H7	108.6	C8—C9—H5	120.1
C5—C4—H7	108.6	C9—C10—C5	120.9 (3)
N1—C4—H8	108.6	C9—C10—H6	119.5
C5—C4—H8	108.6	C5—C10—H6	119.5
H7—C4—H8	107.5		
C3—N1—C1—N2	0.2 (3)	C3—N1—C4—C5	90.2 (3)
C4—N1—C1—N2	179.7 (2)	N1—C4—C5—C6	13.0 (4)
C3—N1—C1—I1	−178.7 (2)	N1—C4—C5—C10	−167.7 (2)
C4—N1—C1—I1	0.9 (4)	C10—C5—C6—C7	0.8 (4)
N1—C1—N2—C2	−0.3 (3)	C4—C5—C6—C7	−179.9 (3)
I1—C1—N2—C2	178.5 (2)	C5—C6—C7—C8	0.0 (4)
C1—N2—C2—C3	0.3 (3)	C6—C7—C8—C9	−0.3 (4)
N2—C2—C3—N1	−0.2 (3)	C7—C8—C9—C10	−0.2 (4)
C1—N1—C3—C2	0.1 (3)	C8—C9—C10—C5	1.1 (4)
C4—N1—C3—C2	−179.5 (3)	C6—C5—C10—C9	−1.4 (4)
C1—N1—C4—C5	−89.3 (3)	C4—C5—C10—C9	179.3 (3)

Appendix A-7. Fractional atomic coordinates and isotropic or equivalent isotropic displacement parameters (Å^2) for compound **4**

	x	y	z	U_{iso}*/U_{eq}
I1	0.78435 (2)	0.28882 (2)	0.99037 (2)	0.02415 (5)
N1	0.62017 (18)	0.7607 (3)	0.84311 (8)	0.0184 (3)
C1	0.6885 (2)	0.6133 (3)	0.80429 (9)	0.0193 (4)
H1	0.6911	0.6269	0.7557	0.023*
N2	0.75130 (18)	0.4480 (3)	0.84125 (8)	0.0202 (3)
C2	0.7195 (2)	0.4950 (3)	0.90773 (9)	0.0176 (4)
C3	0.6390 (2)	0.6861 (3)	0.91019 (9)	0.0202 (4)
H3	0.6035	0.7533	0.9497	0.024*
C4	0.5408 (2)	0.9614 (3)	0.81736 (10)	0.0234 (4)
H4A	0.5420	0.9692	0.7665	0.028*
H4B	0.6011	1.0876	0.8381	0.028*
C5	0.3709 (2)	0.9758 (3)	0.83403 (9)	0.0180 (4)
C6	0.2651 (2)	0.8056 (3)	0.81699 (10)	0.0212 (4)
H6	0.3005	0.6781	0.7958	0.025*
C7	0.1081 (2)	0.8218 (3)	0.83096 (10)	0.0256 (4)
H7	0.0365	0.7048	0.8197	0.031*
C8	0.0554 (2)	1.0088 (4)	0.86130 (10)	0.0265 (4)
H8	−0.0523	1.0201	0.8705	0.032*
C9	0.1594 (3)	1.1779 (3)	0.87815 (11)	0.0277 (4)
H9	0.1231	1.3058	0.8988	0.033*
C10	0.3176 (2)	1.1619 (3)	0.86495 (10)	0.0240 (4)
H10	0.3891	1.2783	0.8771	0.029*

Appendix A-8. Atomic displacement parameters (Å^2) for compound **4**

	U^{11}	U^{22}	U^{33}	U^{12}	U^{13}	U^{23}
I1	0.02821 (8)	0.02566 (8)	0.01895 (7)	0.00504 (5)	0.00421 (5)	0.00451 (5)
N1	0.0185 (8)	0.0183 (8)	0.0193 (8)	0.0004 (6)	0.0055 (6)	0.0031 (6)
C1	0.0177 (9)	0.0255 (10)	0.0152 (8)	0.0006 (7)	0.0038 (7)	−0.0016 (7)
N2	0.0198 (8)	0.0235 (8)	0.0177 (7)	0.0025 (6)	0.0045 (6)	−0.0027 (6)
C2	0.0171 (8)	0.0191 (9)	0.0167 (8)	0.0005 (7)	0.0027 (7)	0.0004 (7)
C3	0.0248 (10)	0.0203 (10)	0.0167 (9)	0.0003 (7)	0.0075 (7)	0.0000 (7)
C4	0.0248 (10)	0.0186 (9)	0.0281 (10)	0.0021 (8)	0.0089 (8)	0.0080 (8)
C5	0.0211 (9)	0.0178 (9)	0.0151 (8)	0.0028 (7)	0.0022 (7)	0.0043 (7)
C6	0.0259 (10)	0.0184 (9)	0.0190 (9)	0.0042 (7)	0.0009 (7)	−0.0028 (7)
C7	0.0212 (10)	0.0305 (12)	0.0236 (10)	−0.0015 (8)	−0.0045 (8)	−0.0048 (8)
C8	0.0195 (9)	0.0380 (12)	0.0216 (9)	0.0078 (8)	0.0004 (7)	−0.0019 (8)
C9	0.0314 (11)	0.0263 (11)	0.0257 (10)	0.0106 (9)	0.0050 (8)	−0.0037 (8)
C10	0.0279 (10)	0.0185 (10)	0.0254 (10)	0.0007 (8)	0.0015 (8)	−0.0010 (8)

Appendix A-9. Geometric parameters (Å, º) for compound **4**

I1—C2	2.0717 (18)	C5—C10	1.391 (3)
N1—C1	1.349 (2)	C5—C6	1.393 (3)
N1—C3	1.374 (2)	C6—C7	1.388 (3)
N1—C4	1.467 (2)	C6—H6	0.9500
C1—N2	1.322 (2)	C7—C8	1.388 (3)
C1—H1	0.9500	C7—H7	0.9500
N2—C2	1.379 (2)	C8—C9	1.378 (3)
C2—C3	1.362 (3)	C8—H8	0.9500
C3—H3	0.9500	C9—C10	1.394 (3)
C4—C5	1.510 (3)	C9—H9	0.9500
C4—H4A	0.9900	C10—H10	0.9500
C4—H4B	0.9900		
C1—N1—C3	107.09 (15)	C10—C5—C6	119.40 (17)
C1—N1—C4	125.67 (16)	C10—C5—C4	120.18 (18)
C3—N1—C4	127.24 (16)	C6—C5—C4	120.39 (17)
N2—C1—N1	112.62 (16)	C7—C6—C5	120.18 (18)
N2—C1—H1	123.7	C7—C6—H6	119.9
N1—C1—H1	123.7	C5—C6—H6	119.9
C1—N2—C2	103.82 (15)	C8—C7—C6	120.08 (19)
C3—C2—N2	111.35 (16)	C8—C7—H7	120.0
C3—C2—I1	126.28 (13)	C6—C7—H7	120.0
N2—C2—I1	122.34 (13)	C9—C8—C7	120.02 (19)
C2—C3—N1	105.11 (16)	C9—C8—H8	120.0
C2—C3—H3	127.4	C7—C8—H8	120.0
N1—C3—H3	127.4	C8—C9—C10	120.24 (19)
N1—C4—C5	112.76 (15)	C8—C9—H9	119.9
N1—C4—H4A	109.0	C10—C9—H9	119.9
C5—C4—H4A	109.0	C5—C10—C9	120.08 (19)
N1—C4—H4B	109.0	C5—C10—H10	120.0
C5—C4—H4B	109.0	C9—C10—H10	120.0
H4A—C4—H4B	107.8		
C3—N1—C1—N2	−0.3 (2)	N1—C4—C5—C10	129.69 (19)
C4—N1—C1—N2	179.94 (17)	N1—C4—C5—C6	−52.0 (2)
N1—C1—N2—C2	0.3 (2)	C10—C5—C6—C7	−0.2 (3)
C1—N2—C2—C3	−0.1 (2)	C4—C5—C6—C7	−178.49 (18)
C1—N2—C2—I1	178.38 (13)	C5—C6—C7—C8	0.7 (3)
N2—C2—C3—N1	0.0 (2)	C6—C7—C8—C9	−0.6 (3)
I1—C2—C3—N1	−178.47 (13)	C7—C8—C9—C10	−0.1 (3)
C1—N1—C3—C2	0.2 (2)	C6—C5—C10—C9	−0.5 (3)
C4—N1—C3—C2	179.96 (17)	C4—C5—C10—C9	177.82 (18)
C1—N1—C4—C5	123.20 (19)	C8—C9—C10—C5	0.7 (3)
C3—N1—C4—C5	−56.5 (3)		

Appendix A-10. Hydrogen-bond geometry (Å, º) for compound **4**

Donor—H···Acceptor	Donor-H	H···Acceptor	Donor···Acceptor	Angle
C4—H4*B*···N2	0.99	2.55	3.488 (3)	158
C4—H4*B*···N2	0.99	2.55	3.488 (3)	158
C4—H4*B*···N2	0.99	2.55	3.488 (3)	158
C4—H4*B*···N2	0.99	2.55	3.488 (3)	158

Appendix A-11. Fractional atomic coordinates and isotropic or equivalent isotropic displacement parameters ($Å^2$) for compound **5**

	x	*y*	*z*	$U_{iso}*/U_{eq}$
I1	0.36505 (2)	0.21176 (2)	−0.00445 (2)	0.01647 (5)
N1	0.6779 (2)	0.27787 (17)	0.20512 (12)	0.0120 (3)
C1	0.4707 (3)	0.2345 (2)	0.16333 (14)	0.0128 (3)
N2	0.3471 (2)	0.20232 (18)	0.23569 (12)	0.0150 (3)
C2	0.4817 (3)	0.2263 (2)	0.33480 (14)	0.0139 (3)
C3	0.4394 (3)	0.2054 (2)	0.43956 (15)	0.0182 (3)
H3	0.3012	0.1724	0.4531	0.022*
C4	0.6071 (3)	0.2349 (2)	0.52297 (15)	0.0194 (4)
H4	0.5828	0.2201	0.5945	0.023*
C5	0.8118 (3)	0.2859 (2)	0.50456 (15)	0.0175 (3)
H5	0.9221	0.3057	0.5641	0.021*
C6	0.8566 (3)	0.3081 (2)	0.40127 (15)	0.0151 (3)
H6	0.9943	0.3438	0.3885	0.018*
C7	0.6875 (3)	0.2749 (2)	0.31748 (14)	0.0122 (3)
C8	0.8525 (3)	0.3389 (2)	0.15353 (14)	0.0132 (3)
H8B	0.8223	0.2938	0.0691	0.016*
H8A	0.9799	0.2929	0.1749	0.016*
C9	0.8940 (3)	0.5343 (2)	0.19092 (13)	0.0117 (3)
C10	1.0811 (3)	0.6095 (2)	0.16685 (15)	0.0158 (3)
H10	1.1789	0.5383	0.1290	0.019*
C11	1.1250 (3)	0.7877 (2)	0.19790 (15)	0.0177 (3)
H11	1.2523	0.8376	0.1811	0.021*
C12	0.9832 (3)	0.8928 (2)	0.25341 (15)	0.0160 (3)
H12	1.0129	1.0144	0.2742	0.019*
C13	0.7972 (3)	0.8192 (2)	0.27853 (14)	0.0150 (3)
H13	0.7006	0.8907	0.3173	0.018*
C14	0.7526 (3)	0.6401 (2)	0.24673 (14)	0.0136 (3)
H14	0.6250	0.5904	0.2633	0.016*

Appendix A-12. Atomic displacement parameters (Å^2) for compound **5**

	U^{11}	U^{22}	U^{33}	U^{12}	U^{13}	U^{23}
I1	0.01853 (7)	0.01995 (7)	0.01172 (6)	0.00853 (4)	0.00073 (4)	0.00460 (4)
N1	0.0124 (6)	0.0118 (6)	0.0118 (6)	0.0009 (5)	0.0018 (5)	0.0038 (5)
C1	0.0145 (8)	0.0118 (7)	0.0120 (7)	0.0031 (6)	0.0003 (6)	0.0036 (6)
N2	0.0129 (7)	0.0168 (7)	0.0161 (7)	0.0012 (5)	0.0005 (5)	0.0069 (6)
C2	0.0138 (8)	0.0130 (7)	0.0157 (8)	0.0018 (6)	0.0016 (6)	0.0058 (6)
C3	0.0155 (8)	0.0236 (9)	0.0182 (8)	0.0018 (7)	0.0050 (7)	0.0099 (7)
C4	0.0229 (9)	0.0238 (9)	0.0144 (8)	0.0035 (7)	0.0036 (7)	0.0098 (7)
C5	0.0193 (9)	0.0179 (8)	0.0144 (8)	0.0025 (7)	−0.0026 (7)	0.0048 (6)
C6	0.0133 (8)	0.0136 (7)	0.0170 (8)	0.0005 (6)	0.0001 (6)	0.0038 (6)
C7	0.0158 (8)	0.0099 (7)	0.0113 (7)	0.0021 (6)	0.0025 (6)	0.0035 (6)
C8	0.0121 (7)	0.0135 (7)	0.0148 (8)	0.0016 (6)	0.0046 (6)	0.0049 (6)
C9	0.0130 (7)	0.0128 (7)	0.0102 (7)	0.0022 (6)	0.0003 (6)	0.0051 (6)
C10	0.0142 (8)	0.0165 (8)	0.0174 (8)	0.0040 (6)	0.0051 (6)	0.0049 (6)
C11	0.0155 (8)	0.0190 (8)	0.0194 (8)	−0.0008 (6)	0.0040 (7)	0.0078 (7)
C12	0.0199 (8)	0.0129 (7)	0.0151 (8)	0.0010 (6)	0.0011 (6)	0.0048 (6)
C13	0.0161 (8)	0.0142 (8)	0.0150 (8)	0.0045 (6)	0.0028 (6)	0.0043 (6)
C14	0.0122 (7)	0.0159 (8)	0.0141 (8)	0.0021 (6)	0.0029 (6)	0.0063 (6)

Appendix A-13. Geometric parameters (Å, º) for compound **5**

I1—C1	2.0787 (16)	C6—H6	0.9500
N1—C1	1.372 (2)	C8—C9	1.522 (2)
N1—C7	1.392 (2)	C8—H8B	0.9900
N1—C8	1.459 (2)	C8—H8A	0.9900
C1—N2	1.310 (2)	C9—C14	1.392 (2)
N2—C2	1.398 (2)	C9—C10	1.399 (2)
C2—C3	1.399 (2)	C10—C11	1.392 (2)
C2—C7	1.403 (2)	C10—H10	0.9500
C3—C4	1.388 (3)	C11—C12	1.389 (2)
C3—H3	0.9500	C11—H11	0.9500
C4—C5	1.406 (3)	C12—C13	1.394 (2)
C4—H4	0.9500	C12—H12	0.9500
C5—C6	1.390 (2)	C13—C14	1.399 (2)
C5—H5	0.9500	C13—H13	0.9500
C6—C7	1.393 (2)	C14—H14	0.9500
C1—N1—C7	105.30 (13)	N1—C8—C9	112.67 (13)
C1—N1—C8	129.42 (14)	N1—C8—H8B	109.1
C7—N1—C8	124.77 (14)	C9—C8—H8B	109.1
N2—C1—N1	114.90 (14)	N1—C8—H8A	109.1

Appendix A-13, cont.

N2—C1—I1	122.95 (12)	C9—C8—H8A	109.1
N1—C1—I1	122.10 (12)	H8B—C8—H8A	107.8
C1—N2—C2	103.99 (14)	C14—C9—C10	119.12 (15)
N2—C2—C3	130.02 (16)	C14—C9—C8	122.54 (14)
N2—C2—C7	110.06 (14)	C10—C9—C8	118.33 (14)
C3—C2—C7	119.90 (16)	C11—C10—C9	120.50 (16)
C4—C3—C2	117.39 (16)	C11—C10—H10	119.8
C4—C3—H3	121.3	C9—C10—H10	119.8
C2—C3—H3	121.3	C12—C11—C10	120.19 (16)
C3—C4—C5	121.86 (16)	C12—C11—H11	119.9
C3—C4—H4	119.1	C10—C11—H11	119.9
C5—C4—H4	119.1	C11—C12—C13	119.71 (15)
C6—C5—C4	121.53 (16)	C11—C12—H12	120.1
C6—C5—H5	119.2	C13—C12—H12	120.1
C4—C5—H5	119.2	C12—C13—C14	120.09 (16)
C5—C6—C7	116.04 (16)	C12—C13—H13	120.0
C5—C6—H6	122.0	C14—C13—H13	120.0
C7—C6—H6	122.0	C9—C14—C13	120.39 (15)
N1—C7—C6	131.00 (15)	C9—C14—H14	119.8
N1—C7—C2	105.74 (14)	C13—C14—H14	119.8
C6—C7—C2	123.26 (15)		
C7—N1—C1—N2	−0.68 (19)	C5—C6—C7—C2	1.7 (2)
C8—N1—C1—N2	−172.65 (15)	N2—C2—C7—N1	−0.90 (18)
C7—N1—C1—I1	−178.20 (11)	C3—C2—C7—N1	177.77 (15)
C8—N1—C1—I1	9.8 (2)	N2—C2—C7—C6	179.92 (15)
N1—C1—N2—C2	0.12 (19)	C3—C2—C7—C6	−1.4 (3)
I1—C1—N2—C2	177.62 (11)	C1—N1—C8—C9	93.38 (19)
C1—N2—C2—C3	−178.00 (18)	C7—N1—C8—C9	−77.17 (19)
C1—N2—C2—C7	0.49 (18)	N1—C8—C9—C14	−13.4 (2)
N2—C2—C3—C4	178.48 (17)	N1—C8—C9—C10	167.25 (14)
C7—C2—C3—C4	0.1 (3)	C14—C9—C10—C11	−0.2 (2)
C2—C3—C4—C5	0.8 (3)	C8—C9—C10—C11	179.10 (15)
C3—C4—C5—C6	−0.5 (3)	C9—C10—C11—C12	0.1 (3)
C4—C5—C6—C7	−0.7 (3)	C10—C11—C12—C13	0.4 (3)
C1—N1—C7—C6	−179.98 (17)	C11—C12—C13—C14	−0.8 (3)
C8—N1—C7—C6	−7.5 (3)	C10—C9—C14—C13	−0.1 (2)
C1—N1—C7—C2	0.92 (17)	C8—C9—C14—C13	−179.45 (15)
C8—N1—C7—C2	173.37 (14)	C12—C13—C14—C9	0.6 (3)
C5—C6—C7—N1	−177.29 (16)		

Appendix A-14. Fractional atomic coordinates and isotropic or equivalent isotropic displacement parameters (Å2) for compound **13**

	x	y	z	Uiso*/Ueq
O1	0.2589 (3)	0.3212 (2)	0.57357 (15)	0.0311 (5)
N1	0.2368 (4)	0.4800 (3)	−0.00272 (19)	0.0288 (6)
C1	0.2531 (4)	0.4554 (3)	−0.1062 (2)	0.0313 (7)
H1	0.2271	0.5334	−0.1321	0.038*
O2	0.2716 (3)	0.6019 (2)	0.68566 (14)	0.0305 (5)
N2	0.1769 (4)	0.7836 (3)	0.11557 (19)	0.0289 (6)
H2N	0.180 (5)	0.6857 (12)	0.084 (2)	0.035*
C2	0.3049 (5)	0.3244 (4)	−0.1777 (2)	0.0334 (7)
H2	0.3145	0.3129	−0.2506	0.040*
N3	0.1808 (4)	1.0086 (3)	0.24033 (19)	0.0338 (6)
C3	0.3424 (4)	0.2110 (3)	−0.1412 (2)	0.0329 (7)
H3	0.3781	0.1192	−0.1886	0.039*
C4	0.3277 (4)	0.2320 (3)	−0.0337 (2)	0.0299 (7)
H4	0.3534	0.1549	−0.0068	0.036*
C5	0.2748 (4)	0.3675 (3)	0.0333 (2)	0.0282 (7)
C6	0.2560 (4)	0.3968 (3)	0.1450 (2)	0.0282 (7)
C7	0.2432 (4)	0.4237 (3)	0.2385 (2)	0.0282 (7)
C8	0.2401 (4)	0.4691 (3)	0.3528 (2)	0.0263 (7)
C9	0.2468 (4)	0.3660 (3)	0.4053 (2)	0.0275 (7)
H9	0.2467	0.2633	0.3646	0.033*
C10	0.2536 (4)	0.4134 (3)	0.5166 (2)	0.0269 (7)
C11	0.2575 (4)	0.5652 (3)	0.5766 (2)	0.0276 (7)
C12	0.2451 (4)	0.6673 (3)	0.5254 (2)	0.0265 (6)
H12	0.2417	0.7695	0.5665	0.032*
C13	0.2375 (4)	0.6206 (3)	0.4130 (2)	0.0260 (6)
C14	0.2227 (4)	0.7229 (3)	0.3575 (2)	0.0293 (7)
C15	0.2086 (5)	0.7954 (3)	0.3007 (2)	0.0303 (7)
C16	0.1876 (4)	0.8645 (3)	0.2224 (2)	0.0290 (7)
C17	0.1612 (5)	0.8807 (3)	0.0632 (2)	0.0319 (7)
H17	0.1506	0.8575	−0.0123	0.038*
C18	0.1636 (5)	1.0164 (3)	0.1386 (2)	0.0344 (7)
H18	0.1546	1.1055	0.1241	0.041*
C19	0.2497 (5)	0.1666 (3)	0.5147 (2)	0.0356 (8)
H19A	0.1282	0.1367	0.4630	0.053*
H19B	0.2459	0.1122	0.5642	0.053*
H19C	0.3687	0.1443	0.4763	0.053*
C20	0.2961 (5)	0.7562 (3)	0.7483 (2)	0.0352 (8)
H20A	0.4098	0.8032	0.7273	0.053*
H20B	0.3219	0.7695	0.8245	0.053*
H20C	0.1732	0.8020	0.7363	0.053*

Appendix A-15. Atomic displacement parameters (Å2) for compound **13**

	U11	U22	U33	U12	U13	U23
O1	0.0398 (12)	0.0368 (13)	0.0222 (11)	0.0042 (9)	0.0041 (9)	0.0169 (9)
N1	0.0287 (14)	0.0386 (15)	0.0223 (13)	0.0015 (11)	0.0031 (10)	0.0150 (11)
C1	0.0338 (17)	0.0390 (18)	0.0254 (16)	0.0009 (13)	−0.0010 (13)	0.0182 (14)
O2	0.0386 (12)	0.0415 (13)	0.0139 (10)	0.0049 (9)	0.0036 (8)	0.0126 (9)
N2	0.0334 (14)	0.0337 (14)	0.0213 (13)	0.0055 (11)	0.0041 (10)	0.0113 (11)
C2	0.0358 (17)	0.049 (2)	0.0186 (15)	0.0000 (14)	0.0008 (13)	0.0162 (14)
N3	0.0461 (16)	0.0340 (15)	0.0245 (13)	0.0027 (12)	0.0029 (11)	0.0147 (11)
C3	0.0356 (18)	0.0367 (18)	0.0245 (16)	0.0032 (13)	0.0062 (13)	0.0079 (13)
C4	0.0320 (16)	0.0369 (18)	0.0242 (16)	−0.0003 (13)	0.0027 (12)	0.0159 (13)
C5	0.0294 (16)	0.0372 (18)	0.0208 (15)	0.0017 (13)	0.0028 (12)	0.0140 (13)
C6	0.0330 (17)	0.0298 (16)	0.0248 (16)	0.0031 (12)	0.0032 (12)	0.0137 (13)
C7	0.0322 (16)	0.0327 (17)	0.0232 (16)	0.0050 (13)	0.0049 (12)	0.0134 (13)
C8	0.0246 (15)	0.0385 (18)	0.0193 (15)	0.0042 (12)	0.0049 (11)	0.0138 (13)
C9	0.0266 (16)	0.0381 (18)	0.0204 (15)	0.0043 (12)	0.0024 (12)	0.0136 (13)
C10	0.0249 (15)	0.0383 (18)	0.0224 (15)	0.0037 (12)	0.0036 (11)	0.0164 (13)
C11	0.0287 (16)	0.0408 (18)	0.0157 (14)	0.0028 (13)	0.0037 (11)	0.0127 (13)
C12	0.0264 (15)	0.0352 (17)	0.0205 (15)	0.0047 (12)	0.0035 (12)	0.0126 (13)
C13	0.0243 (15)	0.0354 (17)	0.0222 (15)	0.0051 (12)	0.0036 (11)	0.0146 (13)
C14	0.0303 (16)	0.0360 (17)	0.0214 (15)	0.0024 (13)	0.0039 (12)	0.0097 (13)
C15	0.0358 (17)	0.0353 (17)	0.0212 (15)	0.0047 (13)	0.0004 (12)	0.0121 (13)
C16	0.0280 (16)	0.0404 (18)	0.0212 (15)	0.0020 (13)	0.0028 (12)	0.0142 (13)
C17	0.0388 (18)	0.0356 (18)	0.0262 (16)	0.0047 (14)	0.0039 (13)	0.0171 (14)
C18	0.0435 (19)	0.0376 (18)	0.0293 (17)	0.0018 (14)	0.0008 (14)	0.0216 (14)
C19	0.047 (2)	0.0377 (19)	0.0287 (17)	0.0044 (15)	0.0056 (14)	0.0191 (14)
C20	0.0452 (19)	0.0411 (19)	0.0199 (15)	0.0069 (15)	0.0057 (13)	0.0107 (13)

Appendix A-16. Geometric parameters (Å, °) for compound **13**

O1—C10	1.359 (3)	C7—C8	1.438 (4)
O1—C19	1.420 (3)	C8—C9	1.405 (4)
N1—C1	1.336 (4)	C8—C13	1.405 (4)
N1—C5	1.360 (4)	C9—C10	1.393 (4)
C1—C2	1.377 (4)	C9—H9	0.9500
C1—H1	0.9500	C10—C11	1.402 (4)
O2—C11	1.370 (3)	C11—C12	1.384 (4)
O2—C20	1.425 (3)	C12—C13	1.407 (4)
N2—C17	1.356 (4)	C12—H12	0.9500
N2—C16	1.362 (4)	C13—C14	1.430 (4)
N2—H2N	0.892 (10)	C14—C15	1.200 (4)
C2—C3	1.371 (4)	C15—C16	1.426 (4)
C2—H2	0.9500	C17—C18	1.346 (4)
N3—C16	1.331 (4)	C17—H17	0.9500
N3—C18	1.383 (4)	C18—H18	0.9500
C3—C4	1.394 (4)	C19—H19A	0.9800
C3—H3	0.9500	C19—H19B	0.9800
C4—C5	1.388 (4)	C19—H19C	0.9800
C4—H4	0.9500	C20—H20A	0.9800
C5—C6	1.439 (4)	C20—H20B	0.9800
C6—C7	1.199 (4)	C20—H20C	0.9800
C10—O1—C19	117.3 (2)	O2—C11—C12	124.0 (3)
C1—N1—C5	117.2 (2)	O2—C11—C10	115.6 (2)
N1—C1—C2	124.3 (3)	C12—C11—C10	120.4 (3)
N1—C1—H1	117.8	C11—C12—C13	120.4 (3)
C2—C1—H1	117.8	C11—C12—H12	119.8
C11—O2—C20	116.4 (2)	C13—C12—H12	119.8
C17—N2—C16	106.8 (3)	C8—C13—C12	119.5 (3)
C17—N2—H2N	125 (2)	C8—C13—C14	118.7 (2)
C16—N2—H2N	128 (2)	C12—C13—C14	121.8 (3)
C3—C2—C1	118.3 (3)	C15—C14—C13	172.8 (3)
C3—C2—H2	120.8	C14—C15—C16	172.9 (3)
C1—C2—H2	120.8	N3—C16—N2	111.7 (3)
C16—N3—C18	103.9 (2)	N3—C16—C15	127.1 (3)
C2—C3—C4	119.3 (3)	N2—C16—C15	121.2 (3)
C2—C3—H3	120.4	C18—C17—N2	106.8 (3)
C4—C3—H3	120.4	C18—C17—H17	126.6
C5—C4—C3	118.9 (3)	N2—C17—H17	126.6
C5—C4—H4	120.6	C17—C18—N3	110.8 (3)
C3—C4—H4	120.6	C17—C18—H18	124.6
N1—C5—C4	122.0 (3)	N3—C18—H18	124.6
N1—C5—C6	116.0 (2)	O1—C19—H19A	109.5
C4—C5—C6	121.9 (3)	O1—C19—H19B	109.5
C7—C6—C5	178.7 (3)	H19A—C19—H19B	109.5
C6—C7—C8	174.4 (3)	O1—C19—H19C	109.5
C9—C8—C13	119.7 (3)	H19A—C19—H19C	109.5
C9—C8—C7	121.4 (3)	H19B—C19—H19C	109.5
C13—C8—C7	118.9 (2)	O2—C20—H20A	109.5
C10—C9—C8	120.3 (3)	O2—C20—H20B	109.5

Appendix A-16, cont.

C10—C9—H9	119.8	H20A—C20—H20B	109.5
C8—C9—H9	119.8	O2—C20—H20C	109.5
O1—C10—C9	124.1 (3)	H20A—C20—H20C	109.5
O1—C10—C11	116.1 (2)	H20B—C20—H20C	109.5
C9—C10—C11	119.7 (3)		
C5—N1—C1—C2	0.2 (4)	O1—C10—C11—C12	−177.6 (3)
N1—C1—C2—C3	0.1 (5)	C9—C10—C11—C12	3.1 (4)
C1—C2—C3—C4	−0.2 (4)	O2—C11—C12—C13	178.0 (2)
C2—C3—C4—C5	0.1 (4)	C10—C11—C12—C13	−2.9 (4)
C1—N1—C5—C4	−0.2 (4)	C9—C8—C13—C12	1.0 (4)
C1—N1—C5—C6	−179.9 (2)	C7—C8—C13—C12	−176.7 (3)
C3—C4—C5—N1	0.1 (4)	C9—C8—C13—C14	−177.6 (3)
C3—C4—C5—C6	179.8 (3)	C7—C8—C13—C14	4.7 (4)
C13—C8—C9—C10	−0.8 (4)	C11—C12—C13—C8	0.8 (4)
C7—C8—C9—C10	176.8 (3)	C11—C12—C13—C14	179.4 (3)
C19—O1—C10—C9	−2.3 (4)	C18—N3—C16—N2	0.4 (3)
C19—O1—C10—C11	178.4 (2)	C18—N3—C16—C15	178.8 (3)
C8—C9—C10—O1	179.5 (2)	C17—N2—C16—N3	−0.5 (3)
C8—C9—C10—C11	−1.2 (4)	C17—N2—C16—C15	−178.9 (3)
C20—O2—C11—C12	−6.8 (4)	C16—N2—C17—C18	0.3 (3)
C20—O2—C11—C10	173.9 (2)	N2—C17—C18—N3	0.0 (3)
O1—C10—C11—O2	1.7 (4)	C16—N3—C18—C17	−0.3 (3)
C9—C10—C11—O2	−177.7 (2)		

Appendix A-17. Hydrogen-bond geometry (Å, °) for compound **13**

D—H···A	Donor—H	H···Acceptor	Donor···Acceptor	Angle
C2—H2···O1	0.95	2.38	3.303 (4)	164
C9—H9···N3	0.95	2.43	3.369 (4)	168
N2—H2N···N1	0.89 (1)	2.00 (1)	2.874 (4)	167 (3)
C2—H2···O1	0.95	2.38	3.303 (4)	164
N2—H2N···N1	0.89 (1)	2.00 (1)	2.874 (4)	167 (3)
C2—H2···O1	0.95	2.38	3.303 (4)	164
C9—H9···N3	0.95	2.43	3.369 (4)	168
C2—H2···O1	0.95	2.38	3.303 (4)	164
C9—H9···N3	0.95	2.43	3.369 (4)	168
C9—H9···N3	0.95	2.43	3.369 (4)	168
N2—H2N···N1	0.89 (1)	2.00 (1)	2.874 (4)	167 (3)

Appendix A-18. Fractional atomic coordinates and isotropic or equivalent isotropic displacement parameters (Å2) for compound **13.**$PdCl_2$

	x	y	z	Uiso*/Ueq
Pd1	1.07271 (2)	0.12824 (2)	0.77120 (4)	0.01568 (9)
Cl1	1.22830 (8)	0.11273 (3)	0.59441 (13)	0.0248 (2)
O1	0.4002 (2)	0.15228 (10)	0.1247 (4)	0.0245 (6)
N1	1.0259 (3)	0.05703 (10)	0.7525 (4)	0.0168 (6)
C1	1.1005 (3)	0.02246 (14)	0.8281 (5)	0.0219 (8)
H1	1.1753	0.0323	0.8903	0.026*
Cl2	0.92913 (9)	0.14172 (3)	0.97352 (12)	0.0240 (2)
O2	0.4587 (2)	0.24354 (9)	0.1387 (4)	0.0229 (6)
N2	1.1124 (3)	0.19978 (10)	0.7785 (4)	0.0155 (6)
C2	1.0730 (4)	−0.02644 (14)	0.8193 (5)	0.0242 (8)
H2	1.1286	−0.0499	0.8725	0.029*
N3	1.0819 (3)	0.27840 (11)	0.7249 (4)	0.0201 (6)
H3N	1.044 (4)	0.3051 (17)	0.688 (6)	0.024*
C3	0.9644 (4)	−0.04087 (14)	0.7330 (5)	0.0239 (8)
H3	0.9426	−0.0745	0.7286	0.029*
C4	0.8879 (3)	−0.00653 (13)	0.6531 (5)	0.0216 (8)
H4	0.8130	−0.0162	0.5907	0.026*
C5	0.9191 (3)	0.04264 (13)	0.6629 (5)	0.0183 (7)
C6	0.8428 (3)	0.07952 (14)	0.5712 (5)	0.0221 (8)
C7	0.7765 (3)	0.10708 (13)	0.4845 (5)	0.0197 (7)
C8	0.6988 (3)	0.14240 (14)	0.3920 (5)	0.0207 (7)
C9	0.5875 (3)	0.12801 (14)	0.2987 (5)	0.0211 (7)
H9	0.5657	0.0944	0.2937	0.025*
C10	0.5099 (3)	0.16253 (14)	0.2143 (5)	0.0212 (7)
C11	0.5423 (3)	0.21242 (14)	0.2216 (5)	0.0201 (7)
C12	0.6514 (3)	0.22678 (14)	0.3100 (5)	0.0205 (7)
H12	0.6734	0.2603	0.3125	0.025*
C13	0.7299 (3)	0.19195 (14)	0.3965 (5)	0.0201 (7)
C14	0.8387 (3)	0.20787 (13)	0.4989 (5)	0.0207 (7)
C15	0.9284 (3)	0.22085 (13)	0.5898 (5)	0.0199 (7)
C16	1.0367 (3)	0.23264 (13)	0.6953 (5)	0.0172 (7)
C17	1.2094 (3)	0.22510 (13)	0.8628 (5)	0.0188 (7)
H17	1.2773	0.2110	0.9317	0.023*
C18	1.1912 (3)	0.27419 (14)	0.8301 (5)	0.0249 (8)
H18	1.2436	0.3001	0.8716	0.030*
C19	0.3534 (4)	0.10390 (15)	0.1406 (6)	0.0307 (9)
H19A	0.4050	0.0806	0.0845	0.046*
H19B	0.2713	0.1023	0.0793	0.046*
H19C	0.3520	0.0957	0.2688	0.046*
C20	0.4758 (3)	0.29462 (13)	0.1773 (5)	0.0225 (8)
H20A	0.4834	0.2997	0.3086	0.034*

Appendix A-19. Atomic displacement parameters (Å2) for compound **13.**$PdCl_2$

	U11	U22	U33	U12	U13	U23
Pd1	0.01706 (14)	0.01209 (14)	0.01776 (14)	0.00119 (10)	0.00103 (10)	0.00135 (10)
Cl1	0.0264 (5)	0.0169 (4)	0.0333 (5)	−0.0036 (3)	0.0126 (4)	−0.0031 (4)
O1	0.0202 (13)	0.0233 (14)	0.0282 (15)	−0.0014 (10)	−0.0065 (11)	0.0019 (11)
N1	0.0203 (14)	0.0135 (13)	0.0167 (14)	0.0012 (11)	0.0019 (11)	0.0003 (11)
C1	0.0227 (18)	0.0255 (19)	0.0178 (17)	0.0034 (15)	0.0029 (14)	0.0024 (15)
Cl2	0.0384 (5)	0.0126 (4)	0.0225 (4)	−0.0037 (3)	0.0098 (4)	0.0003 (3)
O2	0.0194 (13)	0.0225 (13)	0.0256 (14)	0.0027 (10)	−0.0031 (11)	0.0041 (11)
N2	0.0169 (14)	0.0141 (14)	0.0152 (14)	0.0006 (11)	0.0009 (11)	0.0004 (11)
C2	0.034 (2)	0.0172 (18)	0.0222 (19)	0.0045 (15)	0.0084 (16)	0.0035 (14)
N3	0.0261 (16)	0.0145 (15)	0.0203 (16)	0.0003 (12)	0.0048 (13)	0.0014 (12)
C3	0.032 (2)	0.0204 (18)	0.0204 (18)	0.0014 (15)	0.0074 (16)	0.0004 (14)
C4	0.0257 (19)	0.0204 (18)	0.0195 (18)	−0.0059 (15)	0.0056 (15)	−0.0022 (14)
C5	0.0193 (17)	0.0208 (18)	0.0156 (16)	0.0032 (14)	0.0050 (13)	0.0018 (14)
C6	0.0183 (17)	0.0230 (19)	0.0253 (19)	0.0008 (14)	0.0038 (15)	−0.0006 (15)
C7	0.0199 (17)	0.0179 (17)	0.0215 (18)	−0.0001 (14)	0.0031 (14)	0.0000 (14)
C8	0.0184 (17)	0.0290 (19)	0.0147 (17)	0.0060 (15)	0.0011 (13)	0.0010 (14)
C9	0.0211 (18)	0.0214 (18)	0.0208 (18)	0.0018 (14)	0.0016 (14)	−0.0019 (14)
C10	0.0177 (17)	0.0285 (19)	0.0171 (17)	0.0009 (14)	0.0006 (14)	−0.0016 (14)
C11	0.0176 (17)	0.0262 (19)	0.0166 (17)	0.0034 (14)	0.0020 (13)	0.0032 (14)
C12	0.0174 (17)	0.0239 (19)	0.0208 (18)	0.0025 (14)	0.0039 (14)	0.0046 (14)
C13	0.0152 (17)	0.0256 (19)	0.0193 (18)	0.0027 (14)	0.0014 (14)	0.0019 (14)
C14	0.0199 (18)	0.0202 (18)	0.0224 (18)	0.0049 (14)	0.0041 (15)	0.0036 (14)
C15	0.0196 (18)	0.0218 (18)	0.0189 (18)	0.0035 (14)	0.0047 (14)	0.0012 (14)
C16	0.0174 (17)	0.0161 (16)	0.0181 (17)	0.0012 (13)	0.0022 (14)	−0.0007 (13)
C17	0.0156 (17)	0.0243 (18)	0.0164 (17)	−0.0014 (14)	0.0009 (13)	−0.0004 (14)
C18	0.0250 (19)	0.026 (2)	0.025 (2)	−0.0101 (15)	0.0060 (16)	−0.0067 (15)
C20	0.0226 (19)	0.0214 (18)	0.0236 (19)	0.0036 (14)	0.0026 (15)	0.0049 (15)

Appendix A-20. Geometric parameters (Å, °) for compound **13.**PdCl$_2$

Pd1—N2	2.006 (3)	C5—C6	1.444 (5)
Pd1—N1	2.018 (3)	C6—C7	1.197 (5)
Pd1—Cl1	2.3185 (9)	C7—C8	1.426 (5)
Pd1—Cl2	2.3336 (10)	C8—C13	1.399 (5)
O1—C10	1.360 (4)	C8—C9	1.413 (5)
O1—C19	1.432 (5)	C9—C10	1.386 (5)
N1—C1	1.343 (5)	C9—H9	0.9500
N1—C5	1.361 (5)	C10—C11	1.411 (5)
C1—C2	1.373 (5)	C11—C12	1.378 (5)
C1—H1	0.9500	C12—C13	1.404 (5)
O2—C11	1.362 (4)	C12—H12	0.9500
O2—C20	1.436 (4)	C13—C14	1.431 (5)
N2—C16	1.340 (4)	C14—C15	1.201 (5)
N2—C17	1.379 (4)	C15—C16	1.407 (5)
C2—C3	1.368 (6)	C17—C18	1.376 (5)
C2—H2	0.9500	C17—H17	0.9500
N3—C16	1.359 (5)	C18—H18	0.9500
N3—C18	1.383 (5)	C19—H19A	0.9800
N3—H3N	0.87 (5)	C19—H19B	0.9800
C3—C4	1.363 (5)	C19—H19C	0.9800
C3—H3	0.9500	C20—H20A	0.9800
C4—C5	1.390 (5)	C20—H20B	0.9800
C4—H4	0.9500	C20—H20C	0.9800
N2—Pd1—N1	176.87 (12)	C10—C9—H9	119.8
N2—Pd1—Cl1	91.05 (9)	C8—C9—H9	119.8
N1—Pd1—Cl1	89.27 (9)	O1—C10—C9	124.6 (3)
N2—Pd1—Cl2	89.56 (9)	O1—C10—C11	115.6 (3)
N1—Pd1—Cl2	90.42 (9)	C9—C10—C11	119.8 (3)
Cl1—Pd1—Cl2	174.40 (4)	O2—C11—C12	124.5 (3)
C10—O1—C19	117.8 (3)	O2—C11—C10	115.3 (3)
C1—N1—C5	118.2 (3)	C12—C11—C10	120.2 (3)
C1—N1—Pd1	120.4 (3)	C11—C12—C13	120.2 (3)
C5—N1—Pd1	121.3 (2)	C11—C12—H12	119.9
N1—C1—C2	122.8 (4)	C13—C12—H12	119.9
N1—C1—H1	118.6	C8—C13—C12	120.3 (3)
C2—C1—H1	118.6	C8—C13—C14	120.1 (3)
C11—O2—C20	116.6 (3)	C12—C13—C14	119.4 (3)
C16—N2—C17	107.4 (3)	C15—C14—C13	177.9 (4)
C16—N2—Pd1	121.1 (2)	C14—C15—C16	175.9 (4)
C17—N2—Pd1	131.5 (2)	N2—C16—N3	109.8 (3)
C3—C2—C1	119.1 (4)	N2—C16—C15	124.5 (3)
C3—C2—H2	120.5	N3—C16—C15	125.7 (3)
C1—C2—H2	120.5	C18—C17—N2	108.4 (3)

Appendix A-20, cont.

C16—N3—C18	107.8 (3)	C18—C17—H17	125.8
C16—N3—H3N	124 (3)	N2—C17—H17	125.8
C18—N3—H3N	128 (3)	C17—C18—N3	106.6 (3)
C4—C3—C2	119.3 (4)	C17—C18—H18	126.7
C4—C3—H3	120.4	N3—C18—H18	126.7
C2—C3—H3	120.4	O1—C19—H19A	109.5
C3—C4—C5	120.2 (4)	O1—C19—H19B	109.5
C3—C4—H4	119.9	H19A—C19—H19B	109.5
C5—C4—H4	119.9	O1—C19—H19C	109.5
N1—C5—C4	120.5 (3)	H19A—C19—H19C	109.5
N1—C5—C6	118.1 (3)	H19B—C19—H19C	109.5
C4—C5—C6	121.3 (3)	O2—C20—H20A	109.5
C7—C6—C5	174.4 (4)	O2—C20—H20B	109.5
C6—C7—C8	175.7 (4)	H20A—C20—H20B	109.5
C13—C8—C9	119.0 (3)	O2—C20—H20C	109.5
C13—C8—C7	120.5 (3)	H20A—C20—H20C	109.5
C9—C8—C7	120.4 (3)	H20B—C20—H20C	109.5
C10—C9—C8	120.5 (3)		
C5—N1—C1—C2	−0.4 (5)	O1—C10—C11—C12	179.7 (3)
Pd1—N1—C1—C2	−180.0 (3)	C9—C10—C11—C12	0.9 (6)
N1—C1—C2—C3	−1.2 (6)	O2—C11—C12—C13	177.9 (3)
C1—C2—C3—C4	2.0 (6)	C10—C11—C12—C13	−1.2 (6)
C2—C3—C4—C5	−1.3 (6)	C9—C8—C13—C12	0.3 (5)
C1—N1—C5—C4	1.1 (5)	C7—C8—C13—C12	−178.0 (3)
Pd1—N1—C5—C4	−179.3 (3)	C9—C8—C13—C14	176.3 (3)
C1—N1—C5—C6	−175.8 (3)	C7—C8—C13—C14	−2.0 (5)
Pd1—N1—C5—C6	3.8 (4)	C11—C12—C13—C8	0.7 (6)
C3—C4—C5—N1	−0.2 (5)	C11—C12—C13—C14	−175.4 (3)
C3—C4—C5—C6	176.6 (3)	C17—N2—C16—N3	−0.4 (4)
C13—C8—C9—C10	−0.6 (5)	Pd1—N2—C16—N3	178.0 (2)
C7—C8—C9—C10	177.7 (3)	C17—N2—C16—C15	178.1 (3)
C19—O1—C10—C9	9.7 (5)	Pd1—N2—C16—C15	−3.5 (5)
C19—O1—C10—C11	−169.0 (3)	C18—N3—C16—N2	0.5 (4)
C8—C9—C10—O1	−178.6 (3)	C18—N3—C16—C15	−178.0 (3)
C8—C9—C10—C11	0.1 (6)	C16—N2—C17—C18	0.2 (4)
C20—O2—C11—C12	−12.7 (5)	Pd1—N2—C17—C18	−178.0 (3)
C20—O2—C11—C10	166.5 (3)	N2—C17—C18—N3	0.0 (4)
O1—C10—C11—O2	0.4 (5)	C16—N3—C18—C17	−0.3 (4)
C9—C10—C11—O2	−178.4 (3)		

Appendix A-21. Hydrogen-bond geometry (Å, °) for **13.**$PdCl_2$

D—H···A	Donor—H	H···Acceptor	Donor···Acceptor	Angle
C2—H2···Cl2	0.95	2.86	3.510 (4)	127
N3—H3N···Cl2	0.87 (5)	2.43 (5)	3.242 (3)	156 (4)
C17—H17···O1	0.95	2.47	3.380 (4)	160
C17—H17···O2	0.95	2.57	3.317 (4)	136
C18—H18···Cl1	0.95	2.92	3.665 (4)	137
C19—H19C···Cl1	0.98	2.94	3.785 (5)	145
C20—H20B···Cl1	0.98	2.83	3.750 (4)	156

Appendix B: CheckCIF-reports for all studied compounds.

Appendix B-1. CheckCIF reports for compound **2**

Bond precision: C-C = 0.0041 A Wavelength=0.71073

Cell:	a=8.7561(5)	b=9.0016(5)	c=12.8869(7)
	alpha=90	beta=90	gamma=90

Temperature: 100 K

	Calculated	Reported
Volume	1015.73(10)	1015.73(10)
Space group	P 21 21 21	P 21 21 21
Hall group	P 2ac 2ab	P 2ac 2ab
Moiety formula	C10 H9 I N2	C10 H9 I N2
Sum formula	C10 H9 I N2	C10 H9 I N2
Mr	284.09	284.09
Dx,g cm-3	1.858	1.858
Z	4	4
Mu (mm-1)	3.107	3.107
F000	544.0	544.0
F000'	542.26	
h,k,lmax	11,11,16	11,11,16
Nref	2229[1303]	2228
Tmin,Tmax	0.479,0.856	0.622,0.746
Tmin'	0.390	

Correction method= # Reported T Limits: Tmin=0.622 Tmax=0.746
AbsCorr = MULTI-SCAN

Data completeness= 1.71/1.00 Theta(max)= 27.087

R(reflections)= 0.0129(2202) wR2(reflections)= 0.0300(2228)

S = 1.051 Npar= 118

The following ALERTS were generated. Each ALERT has the format
test-name_ALERT_alert-type_alert-level.
Click on the hyperlinks for more details of the test.

Alert level G

PLAT431_ALERT_2_G Short Inter HL..A Contact I1 .. N2 .. 2.88 Ang.
PLAT978_ALERT_2_G Number C-C Bonds with Positive Residual Density. 8 Note

---

0 **ALERT level A** = Most likely a serious problem - resolve or explain
0 **ALERT level B** = A potentially serious problem, consider carefully
0 **ALERT level C** = Check. Ensure it is not caused by an omission or oversight
2 **ALERT level G** = General information/check it is not something unexpected

0 ALERT type 1 CIF construction/syntax error, inconsistent or missing data
2 ALERT type 2 Indicator that the structure model may be wrong or deficient
0 ALERT type 3 Indicator that the structure quality may be low
0 ALERT type 4 Improvement, methodology, query or suggestion
0 ALERT type 5 Informative message, check

Datablock I - ellipsoid plot

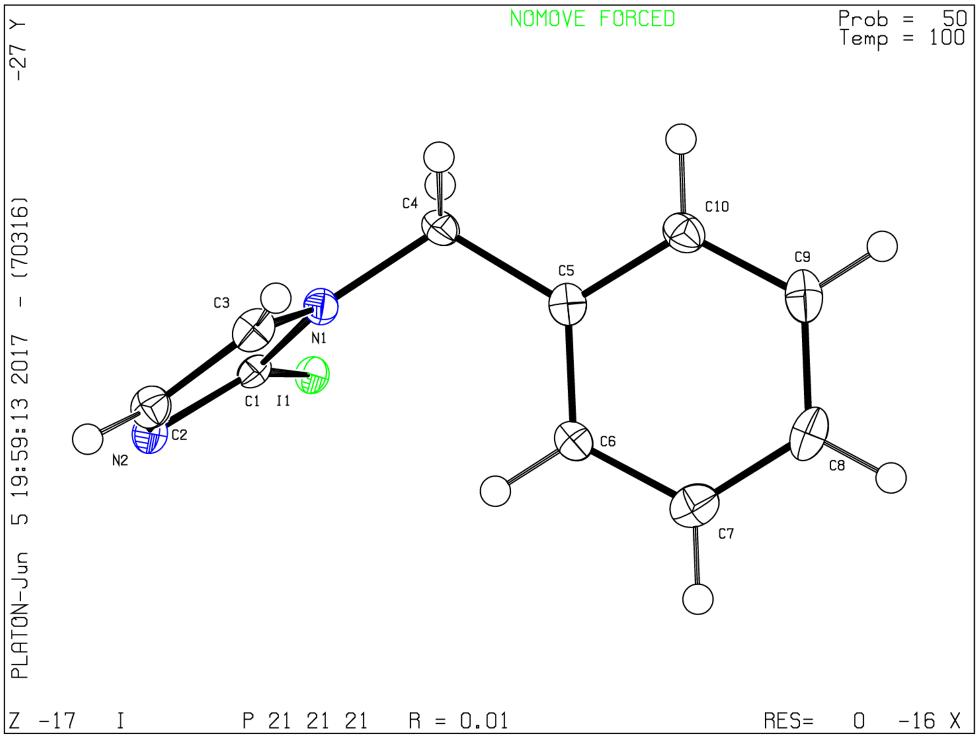

Appendix B-2. CheckCIF reports for compound **4**

Bond precision: C-C = 0.0026 A Wavelength=0.71073

Cell:	a=6.4606(8)	b=8.2346(10)	c=12.3451(14)
	alpha=108.064(1)	beta=94.174(2)	gamma=95.366(2)

Temperature: 100 K

	Calculated	Reported
Volume	618.05(13)	618.05(13)
Space group	P -1	P -1
Hall group	-P 1	-P 1
Moiety formula	C14 H11 I N2	C14 H11 I N2
Sum formula	C14 H11 I N2	C14 H11 I N2
Mr	334.15	334.15
Dx,g cm-3	1.796	1.796
Z	2	2
Mu (mm-1)	2.568	2.568
F000	324.0	324.0
F000'	323.15	
h,k,lmax	8,10,15	8,10,15
Nref	2782	2777
Tmin,Tmax	0.604,0.598	0.588,0.746
Tmin'	0.592	

Correction method= # Reported T Limits: Tmin=0.588 Tmax=0.746
AbsCorr = MULTI-SCAN

Data completeness= 0.998 Theta(max)= 27.292

R(reflections)= 0.0154(2725) wR2(reflections)= 0.0389(2777)

S = 1.090 Npar= 154

The following ALERTS were generated. Each ALERT has the format
test-name_ALERT_alert-type_alert-level.

● **Alert level C**

PLAT094_ALERT_2_C Ratio of Maximum / Minimum Residual Density .... 2.12 Report

● **Alert level G**

PLAT432_ALERT_2_G Short Inter X...Y Contact I1 .. C13 .. 3.39 Ang.
PLAT912_ALERT_4_G Missing # of FCF Reflections Above STh/L= 0.600 6 Note
PLAT978_ALERT_2_G Number C-C Bonds with Positive Residual Density. 12 Note

0 **ALERT level A** = Most likely a serious problem - resolve or explain

0 **ALERT level B** = A potentially serious problem, consider carefully
1 **ALERT level C** = Check. Ensure it is not caused by an omission or oversight
3 **ALERT level G** = General information/check it is not something unexpected

0 ALERT type 1 CIF construction/syntax error, inconsistent or missing data
3 ALERT type 2 Indicator that the structure model may be wrong or deficient
0 ALERT type 3 Indicator that the structure quality may be low
1 ALERT type 4 Improvement, methodology, query or suggestion
0 ALERT type 5 Informative message, check

Datablock I - ellipsoid plot

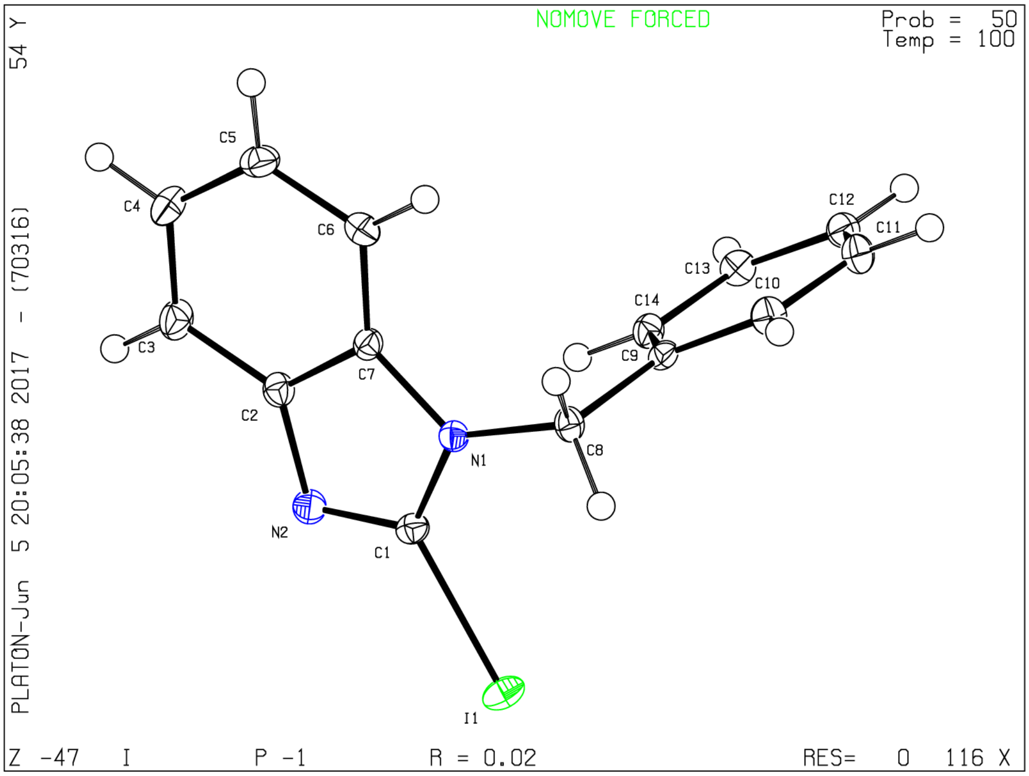

Appendix B-3. CheckCIF reports for compound **5**

Bond precision: C-C = 0.0028 A Wavelength=0.71073

Cell:	a=8.4574(5)	b=6.1526(3)	c=19.4261(10)
	alpha=90	beta=96.362(1)	gamma=90

Temperature: 100 K

	Calculated	Reported
Volume	1004.61(9)	1004.61(9)
Space group	P 21/n	P 21/n
Hall group	-P 2yn	-P 2yn
Moiety formula	C10 H9 I N2	C10 H9 I N2
Sum formula	C10 H9 I N2	C10 H9 I N2
Mr	284.09	284.09
Dx,g cm-3	1.878	1.878
Z	4	4
Mu (mm-1)	3.141	3.141
F000	544.0	544.0
F000'	542.26	
h,k,lmax	10,7,24	10,7,24
Nref	2208	2207
Tmin,Tmax	0.506,0.501	0.594,0.746
Tmin'	0.496	

Correction method= # Reported T Limits: Tmin=0.594 Tmax=0.746
AbsCorr = MULTI-SCAN

Data completeness= 1.000 Theta(max)= 27.108

R(reflections)= 0.0161(2114) wR2(reflections)= 0.0367(2207)

S = 1.106 Npar= 118

The following ALERTS were generated. Each ALERT has the format
test-name_ALERT_alert-type_alert-level.
Click on the hyperlinks for more details of the test.

Alert level G

PLAT912_ALERT_4_G Missing # of FCF Reflections Above STh/L= 0.600 2 Note

PLAT978_ALERT_2_G Number C-C Bonds with Positive Residual Density. 9 Note

---

0 **ALERT level A** = Most likely a serious problem - resolve or explain
0 **ALERT level B** = A potentially serious problem, consider carefully
0 **ALERT level C** = Check. Ensure it is not caused by an omission or oversight
2 **ALERT level G** = General information/check it is not something unexpected

0 ALERT type 1 CIF construction/syntax error, inconsistent or missing data
1 ALERT type 2 Indicator that the structure model may be wrong or deficient
0 ALERT type 3 Indicator that the structure quality may be low
1 ALERT type 4 Improvement, methodology, query or suggestion
0 ALERT type 5 Informative message, check

Datablock I - ellipsoid plot

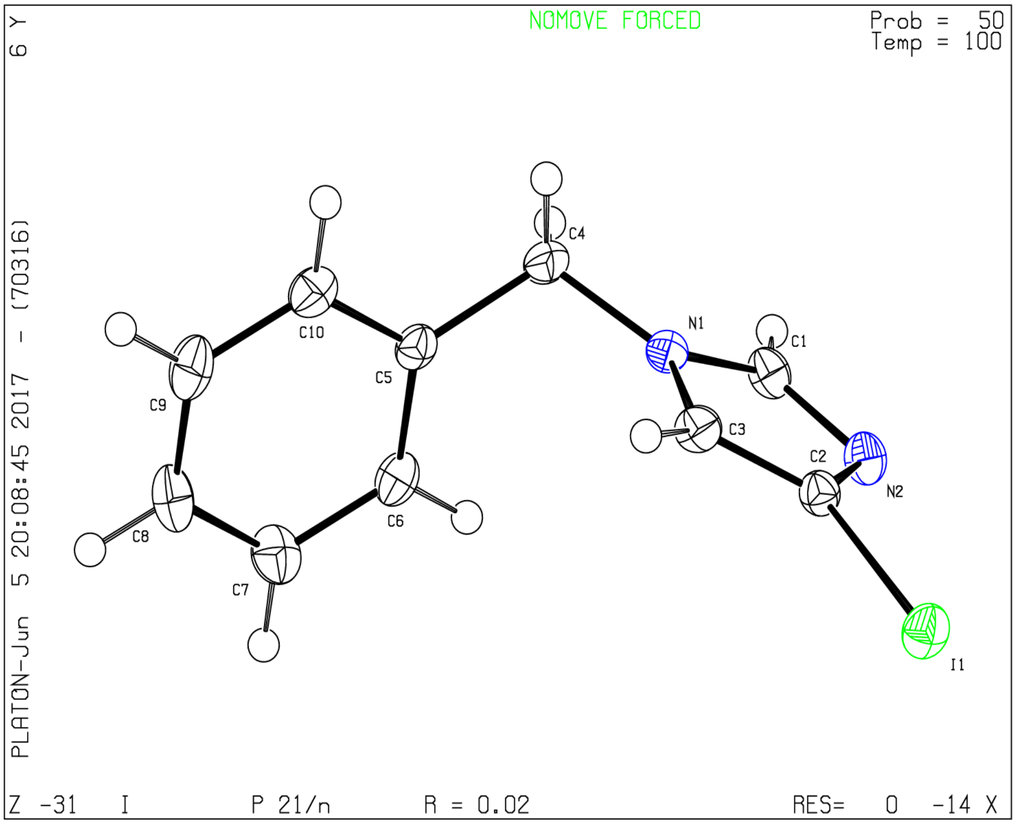

Appendix B-4. CheckCIF reports for compound **13**

Bond precision: C-C = 0.0041 A Wavelength=0.71073

Cell:	a=6.698(3)	b=9.659(4)	c=13.379(6)
	alpha=110.387(6)	beta=95.185(6)	gamma=92.835(7)

Temperature: 100 K

	Calculated	Reported
Volume	805.0(6)	804.9(6)
Space group	P -1	P -1
Hall group	-P 1	-P 1
Moiety formula	C20 H15 N3 O2	C20 H15 N3 O2
Sum formula	C20 H15 N3 O2	C20 H15 N3 O2
Mr	329.35	329.35
Dx,g cm-3	1.359	1.359
Z	2	2
Mu (mm-1)	0.090	0.090
F000	344.0	344.0
F000'	344.14	
h,k,lmax	8,12,17	8,12,17
Nref	3588	3576
Tmin,Tmax	0.978,0.998	0.640,0.746
Tmin'	0.978	

Correction method= # Reported T Limits: Tmin=0.640 Tmax=0.746
AbsCorr = MULTI-SCAN

Data completeness= 0.997 Theta(max)= 27.142

R(reflections)= 0.0650(1869) wR2(reflections)= 0.2086(3576)

S = 0.992 Npar= 231

The following ALERTS were generated. Each ALERT has the format
test-name_ALERT_alert-type_alert-level.
Click on the hyperlinks for more details of the test.

Alert level C

PLAT340_ALERT_3_C Low Bond Precision on C-C Bonds .... 0.00406 Ang.
PLAT906_ALERT_3_C Large K value in the Analysis of Variance ...... 3.078 Check
PLAT911_ALERT_3_C Missing # FCF Refl Between THmin & STh/L= 0.600 3 Report
PLAT978_ALERT_2_C Number C-C Bonds with Positive Residual Density. 0 Note

---

Alert level G

PLAT002_ALERT_2_G Number of Distance or Angle Restraints on AtSite 2 Note

PLAT072_ALERT_2_G SHELXL First Parameter in WGHT Unusually Large 0.11 Report
PLAT172_ALERT_4_G The CIF-Embedded .res File Contains DFIX Records 1 Report
PLAT371_ALERT_2_G Long C(sp2)-C(sp1) Bond C5 - C6 .. 1.44 Ang.
And 3 other PLAT371 Alerts
More ...
PLAT860_ALERT_3_G Number of Least-Squares Restraints .... 1 Note
PLAT912_ALERT_4_G Missing # of FCF Reflections Above STh/L= 0.600 9 Note

---

0 **ALERT level A** = Most likely a serious problem - resolve or explain
0 **ALERT level B** = A potentially serious problem, consider carefully
4 **ALERT level C** = Check. Ensure it is not caused by an omission or oversight
9 **ALERT level G** = General information/check it is not something unexpected

0 ALERT type 1 CIF construction/syntax error, inconsistent or missing data
7 ALERT type 2 Indicator that the structure model may be wrong or deficient
4 ALERT type 3 Indicator that the structure quality may be low
2 ALERT type 4 Improvement, methodology, query or suggestion
0 ALERT type 5 Informative message, check

Datablock I - ellipsoid plot

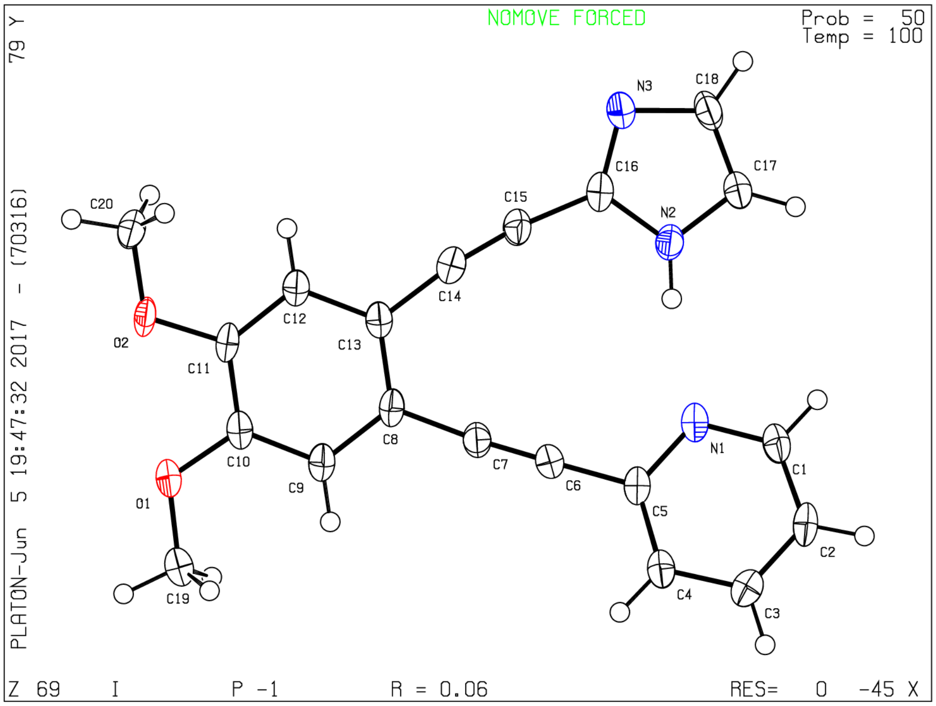

Appendix B-5. CheckCIF reports for compound **13.**$PdCl_2$

Bond precision: C-C = 0.0051 A Wavelength=0.71073

Cell:	a=11.1420(7)	b=27.3615(17)	c=7.4271(5)
	alpha=90	beta=95.878(1)	gamma=90

Temperature: 100 K

	Calculated	Reported
Volume	2252.3(3)	2252.3(3)
Space group	P 21/c	P 21/c
Hall group	-P 2ybc	-P 2ybc
Moiety formula	C20 H15 Cl2 N3 O2 Pd [+ solvent]	?
Sum formula	C20 H15 Cl2 N3 O2 Pd [+ solvent]	C20 H15 Cl2 N3 O2 Pd
Mr	506.65	506.65
Dx,g cm-3	1.494	1.494
Z	4	4
Mu (mm-1)	1.080	1.080
F000	1008.0	1008.0
F000'	1005.50	
h,k,lmax	14,35,9	14,35,9
Nref	5041	5039
Tmin,Tmax	0.823,0.979	0.640,0.746
Tmin'	0.806	

Correction method= # Reported T Limits: Tmin=0.640 Tmax=0.746
AbsCorr = MULTI-SCAN

Data completeness= 1.000 Theta(max)= 27.240

R(reflections)= 0.0448(4570) wR2(reflections)= 0.1021(5039)

S = 1.147 Npar= 258

The following ALERTS were generated. Each ALERT has the format
test-name_ALERT_alert-type_alert-level.
Click on the hyperlinks for more details of the test.

Alert level C

PLAT048_ALERT_1_C MoietyFormula Not Given (or Incomplete) .... Please Check

PLAT480_ALERT_4_C Long H...A H-Bond Reported H2 .. CL2 .. 2.86 Ang.

And 2 other PLAT480 Alerts

More ...

PLAT906_ALERT_3_C Large K value in the Analysis of Variance ...... 3.328 Check

Alert level G

PLAT083_ALERT_2_G SHELXL Second Parameter in WGHT Unusually Large 6.20 Why ?

PLAT232_ALERT_2_G Hirshfeld Test Diff (M-X) Pd1 -- Cl2 .. 12.2 s.u.
PLAT371_ALERT_2_G Long C(sp2)-C(sp1) Bond C5 - C6 .. 1.44 Ang.
And 2 other PLAT371 Alerts
More ...
PLAT605_ALERT_4_G Largest Solvent Accessible VOID in the Structure 209 A**3
PLAT802_ALERT_4_G CIF Input Record(s) with more than 80 Characters 1 Info
PLAT869_ALERT_4_G ALERTS Related to the use of SQUEEZE Suppressed ! Info
PLAT912_ALERT_4_G Missing # of FCF Reflections Above STh/L= 0.600 3 Note
PLAT978_ALERT_2_G Number C-C Bonds with Positive Residual Density. 6 Note

---

0 **ALERT level A** = Most likely a serious problem - resolve or explain
0 **ALERT level B** = A potentially serious problem, consider carefully
5 **ALERT level C** = Check. Ensure it is not caused by an omission or oversight
10 **ALERT level G** = General information/check it is not something unexpected

1 ALERT type 1 CIF construction/syntax error, inconsistent or missing data
6 ALERT type 2 Indicator that the structure model may be wrong or deficient
1 ALERT type 3 Indicator that the structure quality may be low
7 ALERT type 4 Improvement, methodology, query or suggestion
0 ALERT type 5 Informative message, check

PLATON version of 27/03/2017; check.def file version of 24/03/2017

Datablock I - ellipsoid plot